



**DOTTORATO DI RICERCA IN INGEGNERIA CIVILE PER
L'AMBIENTE ED IL TERRITORIO**
XII Ciclo - Nuova Serie (2011-2013)
DIPARTIMENTO DI INGEGNERIA CIVILE, UNIVERSITÀ DEGLI STUDI DI SALERNO

NUMERICAL MODELING OF TRACERS IN GRAVEL-BED RIVERS

**MODELLAZIONE NUMERICA DI TRACCIANTI
IN FIUMI A LETTO GHIAIOSO**

ING. ANNA PELOSI

Relatore:
PROF. ING. PIERLUIGI FURCOLO

Coordinatore
PROF. ING. VINCENZO BELGIORNO

Correlatori:
PROF. ING. FABIO ROSSI
PROF. GARY PARKER

On the book cover: Tracer stones (painted particles) in motion during a flume experiment at St. Anthony Falls Laboratory (SAFL) –University of Minnesota. Courtesy of Dr. Miguel Wong and Prof. Gary Parker.

NUMERICAL MODELING OF TRACERS IN GRAVEL-BED RIVERS

Copyright © 2014 Università degli Studi di Salerno – via Ponte don Melillo, 1 – 84084 Fisciano (SA), Italy – web: www.unisa.it

Proprietà letteraria, tutti i diritti riservati. La struttura ed il contenuto del presente volume non possono essere riprodotti, neppure parzialmente, salvo espressa autorizzazione. Non ne è altresì consentita la memorizzazione su qualsiasi supporto (magnetico, magnetico-ottico, ottico, cartaceo, etc.).

Benché l'autore abbia curato con la massima attenzione la preparazione del presente volume, Egli declina ogni responsabilità per possibili errori ed omissioni, nonché per eventuali danni dall'uso delle informazione ivi contenute.

Finito di stampare il 14/02/2014

*Dedicated to my parents, Emilia and Maurizio, for their unconditional Love and
to Gianluca because, wherever life is bringing us, I will be always grateful
for the time spent together.*

TABLE OF CONTENTS

TABLE OF CONTENTS	i
LIST OF FIGURES	iii
LIST OF TABLES.....	vii
ABSTRACT	ix
ACKNOLEGMENTS	xi
About the author	xii
1 Introduction	1
1.1 Objectives of the Thesis	3
1.2 Structure of the thesis	4
2 Morphodynamics of river bed variation	7
2.1 The Exner Equation of Sediment Continuity	7
2.1.1 Parker-Paola-Leclair (PPL) Framework for Exner equation of sediment continuity.....	11
2.2 Bedload transport relations	14
3 Morphodynamics of river bed variation with variable bedload step length.....	17
3.1 Introduction.....	18
3.2 Methods	19
3.2.1 Theoretical framework	19
3.2.2 Numerical model.....	22
3.3 Results	28
3.4 Discussion and concluding remarks	36
4 On advection and diffusion of river pebble tracers	39
4.1 Streamwise advection slowdown of tracers	39
4.2 Particles diffusion	41
5 Exner Based Master Equation for transport and dispersion of river pebble tracers. Part 1. Derivation, asymptotic forms, and quantification of nonlocal vertical dispersion.....	43
5.1 Introduction.....	44
5.2 Master Equation for the standard CTRW model	47
5.3 Problems associated with application of the CRTW ME to bedload tracers	50

5.4	PPL Framework for Exner equation of sediment continuity: some more comments.....	50
5.5	Exner-based Master Equations for rivers carrying bedload.....	52
5.6	Vertical and streamwise dispersal of tracers within an equilibrium bed	54
5.7	Asymptotic fractional formulations	56
5.8	Simplified model for vertical dispersion: thin-versus heavy- tailed probability densities for elevation from which a particle jumps	59
5.9	Discussion and concluding remarks	67
6	Exner Based Master Equation for transport and dispersion of river pebble tracers. Part 2. Implementation for coevolving vertical and streamwise dispersion	69
6.1	Introduction	70
6.2	Flume experiments by Wong et al. (2007)	72
6.3	Structure functions of PDFs for particle step length, bed fluctuation and jump elevation	75
6.3.1	Particle step length	75
6.3.2	Bed fluctuations	76
6.3.3	Jump elevation	80
6.4	Numerical results for EBME-N: vertical and streamwise dispersion of river pebble tracers	84
6.5	Discussion.....	95
6.6	Concluding remarks	96
7	Conclusions.....	99
	References	103

LIST OF FIGURES

Figure 1.1 Gravel-bed rivers: a) Elbow River, Alberta, Canada at low flow (Parker, 2004); b) Schematization of sediment transport (Copyright © 2006 Pearson Prentice Hall inc).....	1
Figure 2.1 Control volume for the derivation of the Exner equation of sediment mass conservation (Parker, 2004)	8
Figure 2.2 Particle step length	9
Figure 2.3 Active layer concept	10
Figure 2.4 Variation in probability of Entrainment as in Parker et al. (2000): (a) actual variation; (b) approximation given by active layer formulation.....	11
Figure 2.5 Definition diagram for the Parker-Paola-Leclair framework for sediment and sediment tracer conservation.....	12
Figure 3.1 Discretization of the domain	28
Figure 3.2 Bed profile evolution for the case $\hat{E}_r = 2$: a) flux form; b) entrainment form for $\varepsilon = \bar{\tau}/L_d = 0.01$, c) entrainment form for $\varepsilon = 0.5$ and d) entrainment form for $\varepsilon = 1.$, using the thin-tailed exponential step length function of Equation (3.8). Increasing ε , the differences between the results from the two forms increase because of the non-locality of particle movement: from upward concave transient profiles to downward concave ones.	29
Figure 3.3 Aggradation case: variation in time of the concavity parameter δ in the case of the flux formulation and in the cases of the entrainment formulation for different values of ε ranging from 0.01 to 1. The result for the flux form overlaps with the result for the entrainment form with $\varepsilon = 0.01$	30
Figure 3.4 Slope profile evolution for the case $\hat{E}_r = 2$: a) flux form; b) entrainment form for $\varepsilon = \bar{\tau}/L_d = 0.01$, c) entrainment form for $\varepsilon = 0.5$ and d) entrainment form for $\varepsilon = 1.$, using the thin-tailed exponential step length function of Equation (3.8).	31
Figure 3.5 Bed profile evolution for the case $\hat{E}_r = 1/2$: a) flux form; b) entrainment form for $\varepsilon = \bar{\tau}/L_d = 0.01$, c) entrainment form for $\varepsilon = 0.5$ and d) entrainment form for $\varepsilon = 1.$, using the thin-tailed exponential step	

length function of Equation (3.8). Increasing ε , the differences between the results from the two forms increase because of the non-locality of particle movement: from upward concave transient profiles to downward concave ones.32

Figure 3.6 Degradation case: variation in time of the concavity parameter δ in the case of the flux formulation and in the cases of the entrainment formulation for different values of ε ranging from 0.01 to 1. The result for the flux form overlaps with the result for the entrainment form with $\varepsilon = 0.01$33

Figure 3.7 Slope profile evolution for the case $\hat{E}_r = 1/2$: a) flux form; b) entrainment form for $\varepsilon = \bar{r}/L_d = 0.01$, c) entrainment form for $\varepsilon = 0.5$ and d) entrainment form for $\varepsilon = 1.$, using the thin-tailed exponential step length function of Equation (3.8).34

Figure 3.8 Bed profile evolution for the case $\hat{E}_r = 2$. i) $\varepsilon = 0.015$: a) Thin-tailed exponential step length PDF; b) heavy-tailed Pareto step length PDF ($\alpha = 1.5, r_0 = 1.5\text{m}$). ii) $\varepsilon = 1$ a) Thin-tailed exponential step length PDF; b) heavy-tailed Pareto step length PDF ($\alpha = 1.5, r_0 = 100\text{m}$).35

Figure 3.9 Variation in time of the concavity parameter δ for the case of the thin-tailed exponential distribution for step length, and the case of heavy-tailed Pareto distribution for step length. The parameter $\varepsilon = \bar{r}/L_d$ takes the value 0.015 in a) and 1.0 in b).36

Figure 4.1 Observed and simulated slowdown of recovered tracers (with relative errors bands) – from Ferguson and Hoey (2002)40

Figure 4.2 Conceptual representation of a particle trajectory consisting of three distinct ranges of scale: (i) local; (ii) intermediate; (iii) global. Nikora et al. hypothesized ballistic diffusion regime for the local range, normal or anomalous diffusion regime for the intermediate range and subdiffusion regime for the global range – from Nikora et al. (2002)42

Figure 5.1 Thin-tailed (Gaussian) and heavy-tailed PDFs for p_j^* . The heavy-tailed distribution corresponds to a Lévy α -stable distribution with $\alpha = 1.1$61

Figure 5.2 Evolution in time of distribution of tracer fraction f^* for the case of a thin-tailed (i.e. Gaussian) form for the PDF p_j^* describing the probability that an entrained particle jumps from elevation y^* . Here $P_e = 1$, resulting in a symmetric pattern.62

Figure 5.3 Evolution in time of distribution of tracer fraction f^* for the case of a heavy-tailed (i.e. α -stable) form for the PDF p_j^* describing the

probability that an entrained particle jumps from elevation y^* . Here $P_e = 1$, resulting in a symmetric pattern.....	62
Figure 5.4 Evolution in time of the variance of the vertical standard deviation σ_y^* for the thin- and heavy- tailed case for p_j , with $P_e = 1$. Also plotted is the line $\sigma_y^* \sim (t^*)^{1/2}$ corresponding to normal diffusion.	63
Figure 5.5 Evolution in time of the distribution of tracer fraction f_{sw}^* , for the case of vertically varying P_e corresponding to a fluctuating water-sediment interface (river bed). Here a thin-tailed (i.e. Gaussian) form for the PDF p_j^* describing the probability that an entrained particle jumps from elevation y^* is used.	65
Figure 5.6 Evolution in time of the distribution of tracer fraction f_{sw}^* , for the case of vertically varying P_e corresponding to a fluctuating water-sediment interface (river bed). Here a heavy-tailed form for the PDF p_j^* describing the probability that an entrained particle jumps from elevation y^* is used.	65
Figure 5.7 Evolution in time of the mean elevation \bar{y}^* of tracer particle distribution for the thin- and heavy- tailed cases. Here a vertically varying form P_e corresponding to a fluctuating water-sediment interface (river bed) is used.	66
Figure 5.8 Evolution in time of the variance of the vertical standard deviation σ_y^* of the tracer distribution for the thin- and heavy- tailed cases. Also plotted is the line $\sigma_y^* \sim (t^*)^{1/2}$ corresponding to normal diffusion. Here a vertically varying form P_e corresponding to a fluctuating water-sediment interface (river bed) is used.	66
Figure 6.1 Examples of time series of bed elevation fluctuations obtained with ultrasonic transducer probes. Simultaneous recording at five indicated streamwise positions along the flume. (a) Run 10. (b) Run 8. (Wong et al., 2007)	74
Figure 6.2 Exponential PDF for particle step length p_s based on Run 8.	76
Figure 6.3 Empirical probability density function for bed elevation p_e , as well as with the Gaussian fit given in Wong et al. (2007) and the α -stable distribution fit. a) Run 10 and b) Run 8.....	78
Figure 6.4 Tails of the empirical distributions for p_e , as well as the Gaussian fit and the α -stable fit. a) Run 10 and b) Run 8	79
Figure 6.5 Schematic time series of bed fluctuations. The yellow (red) arrows indicates the crossing of bed at levels y_1 (y_2).	80

Figure 6.6 Empirical distribution for p_j , along with a Gaussian fit for p_j , a fit using the α -stable PDF for p_j and Gaussian distribution for p_e given by Wong et al. (2007). a) Run 10 and b) Run 8.....	82
Figure 6.7 Tails of the distributions of Figure 6.6 plotted in a log-log graph. a) Run 10 and b) Run 8.	83
Figure 6.8 Contour map of f_{sw} at $t=0$ hr. The inset provides an expanded view of the initial condition.	85
Figure 6.9 Contour map of f_{sw} at $t = 6$ hr.....	85
Figure 6.10 Contour map of f_{sw} at $t = 30$ hr	86
Figure 6.11 Contour map of f_{sw} at $t = 60$ hr.....	86
Figure 6.12 Contour map of f_{sw} at $t = 120$ hr	87
Figure 6.13 Contour map of f_{sw} at $t = 180$ hr	87
Figure 6.14 Contour map of f_{sw} at $t = 240$ hr	88
Figure 6.15 Contour map of f_{sw} at $t = 300$ hr	88
Figure 6.16 Contour map of f_{sw} at $t = 360$ hr	89
Figure 6.17 Mean streamwise travel distance versus time.	91
Figure 6.18 Mean streamwise speed of advection versus time.	91
Figure 6.19 Standard deviation of streamwise travel distance versus time. The solid blue line denotes the calculational results, and the dashed black line corresponds to normal diffusion.	92
Figure 6.20 Mean vertical travel distance versus time.....	93
Figure 6.21 Mean vertical speed of advection versus time.....	93
Figure 6.22 Standard deviation of vertical travel distance versus time. The solid red line denotes the calculational results, and the dashed black line corresponds to normal diffusion.	94

LIST OF TABLES

Table 6.1 Water discharge Q_w , sediment feed rate Q_f and Shields number τ^* for each run	73
Table 6.2 Parameters of the Gaussian distribution for bed fluctuations by Wong et al. (2007).	77
Table 6.3 Parameters of the α -stable distribution fitted to the measured bed fluctuations of Wong et al. (2007).	77
Table 6.4a Fitted values of the parameters of the PDFs for p_j	80
Table 6.4b Fitted values of the parameters of the PDFs for p_j	81

ABSTRACT

The erosion, transport and deposition of pebbles in rivers have often been studied by considering the motion of tracer particles. There are reports of bedload tracing programs in field and laboratory since the late 1930s. The theoretical basis for the study of the dispersal of sediment tracer particles was delineated for the first time in 1950 by Einstein, who formulated the problem in terms of a standard 1D random walk in which each particle moves in a series of steps punctuated by waiting times. Subsequent to Einstein's original work on tracers, the study of random walks has been extended to the case of continuous time random walks (CTRW). CTRW, accompanied by appropriate probability distribution functions (PDFs) for walker step length and waiting time, yields asymptotically the standard advection-diffusion equation (ADE) for thin-tailed PDFs, and the fractional advection-diffusion equation (fADE) for heavy-tailed PDFs, the latter allowing the possibilities of subdiffusion or superdiffusion of particles, which is often referred as non-local behavior or anomalous diffusion.

In latest years, considerable emphasis has been placed on non-locality associated with heavy-tailed PDFs for particle step length. This appears to be in part motivated by the desire to construct fractional advective-diffusive equations for pebble tracer dispersion corresponding to the now-classical fADE model. Regardless of the thin tail of the PDF, the degree of non-locality nevertheless increases with increasing mean step length. In the thesis, we firstly consider the general case of 1D morphodynamics of an erodible bed subject to bedload transport analysing the effects of non-locality mediated by both heavy- and thin-tailed PDFs for particle step length on transient aggradational-degradational bed profiles.

Then, we focus on tracers. (i) We show that the CTRW Master Equation is inappropriate for river pebbles moving as bed material load and (ii) by using the Parker-Paola-Leclair (PPL) framework for the Exner equation of sediment conservation, which captures the vertical structure of bed elevation variation as particles erode and deposit, we develop a new ME for tracer transport and dispersion for alluvial morphodynamics.

The new ME is derived from the Exner equation of sediment continuity and it yields asymptotic forms for ADE and fADE that differ significantly from CTRW. It allows a) vertical dispersion, as well as streamwise advection-diffusion, and b) mean waiting time to vary in the vertical. We also show that vertical dispersion is nonlocal (subdiffusive), but cannot be expressed with fractional derivatives. Vertical dispersion is the likely reason for the slowdown of streamwise advection of tracer pebbles observed in the field, which is the key result of our modeling when co-evolution of vertical and streamwise dispersion are considered.

ACKNOLEGMENTS

I would like to express deep gratitude to Prof. Gary Parker for having adopted me as his graduated student. I'm sincerely grateful for the constant support, motivation and lessons that he gave me during my stay at the University of Illinois at Urbana-Champaign. Without him, none of this would have been possible. Having the chance to work with him was a remarkable honor and pleasure.

I would like to acknowledge Prof. Pierluigi Furcolo and Prof. Fabio Rossi for all their insight, help and care. I'll be always indebted for the opportunity to conduct my scientific research abroad and for believing in me.

Then, my acknowledgments are due to University of Salerno, for having funded my research; I would also like to thank the professors and researchers of the Department of Civil and Environmental Engineering (DICIV) and, specifically, all the professors and researchers at LIDAM (Laboratory of Environmental and Maritime Hydraulics), for having contributed to my improvements and growth.

On a personal note, I wish to thank all the friends, housemates, officemates and colleagues who I met on my way. They were (and are) a source of courage, innovation and inspiration and thanks to them I can feel the entire world my home.

Then, a thought to my parents and my family for their precious examples of life and endless guidance, to my cousins, who are like siblings for me and to my grandmothers, who I would have liked to have still with me in these days.

Finally, my last, special and heartfelt thanks belongs to Gianluca for his time, patience and affection in one (and half) of the most unforgettable, happiest and hardest year of my existence. He was my everything, my haven, my strength and my weakness. He deeply contributed to *make me* the person I am today and his friendship and love have an inestimable value for me.

ABOUT THE AUTHOR

Anna Pelosi, was born in Salerno on July 18th, 1986. She earned her BS in Civil and Environmental Engineering (2007) and her MS in Environmental Engineering (2010) from the University of Salerno (Italy) with a Master Thesis in hydrology (“Assessment of the orographic effect in the regional analysis of maxima rainfall in Campania region”). She enrolled in the ph.D program in Civil and Environmental Engineering at the University of Salerno (Italy) in March 2011 with Prof. Pierluigi Furcolo and Prof. Fabio Rossi as advisers. During the program, she was a visiting scholar at the University of Illinois at Urbana-Champaign (USA) with Prof. Gary Parker as adviser from March 2012 to December 2013. Her research interests range from hydrology, stochastic processes, flood risk and assessment to sediment transport and river morphodynamics.

1 INTRODUCTION

Gravel-bed rivers have a surface median sediment size that is in the range of gravel or coarser material ($2 < D_{50} < 256$ mm). The particles that make up the bed are transported as bedload during floods. Their movement, as schematized in Figure 1.1b, consists of (i) rolling, (ii) sliding or (iii) saltation within a thin layer near the stream bed (Wong et al., 2007; Ganti et al., 2010).

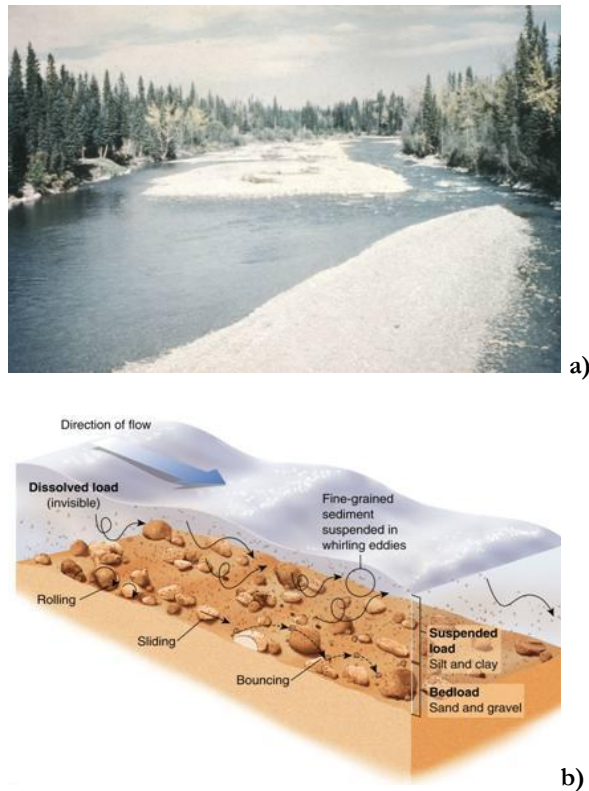


Figure 1.1 Gravel-bed rivers: a) Elbow River, Alberta, Canada at low flow (Parker, 2004); b) Schematization of sediment transport (Copyright © 2006 Pearson Prentice Hall inc)

Reliable and accurate estimates of the bedload transport rate are essential to evaluate the morphodynamic evolution of this kind of rivers (Parker, 2004). In particular, sediment movement in gravel-bed rivers can be measured by direct sampling of the transport rate or by using tracer gravels, which can give insight into many different aspects of gravel transport such as entrainment rates, downstream dispersion (to determine grain displacement lengths and virtual velocities), downstream sediment sorting, vertical mixing, burial, and preferential storage in bars or other locations (Ferguson and Hoey, 2002; Wilcock, 1997).

The working hypothesis is that tracers vertical and streamwise displacement history may serve as good indicator of the bedload transport response of a stream to given water discharge and sediment supply conditions (DeVries, 2000; Parker, 2004; Wong et al, 2007).

There are reports of bedload tracing programs in field and laboratory since the late 1930s. Einstein (1937) was the first to use tracers in a flume, while Takayama (1965) and Leopold et al. (1966) were pioneers in using painted tracers in the field (Hassan and Ergenzinger, 2005). Since then, the techniques have improved, guaranteeing higher recovery rates, and pebble tracers have found increased use in field (for a close examination and summary about tracer techniques, recovery rates and field programs, refer to Hassan and Ergenzinger, 2005). Also in laboratory, the interest in tracers dispersion has increased in recent years (e.g. Ganti et al., 2010; Martin et al., 2012) because of a rediscovered concern about stochasticity in particle motion. Tracers are well suited to the stochastic and spatially variable nature of bedload transport because they are based on a predetermined bed sample composed of individual grains (Wilcock, 1997). They in fact provide a way of characterizing not only mean parameters pertaining to transport, but also the stochasticity of particle motion itself. This stochasticity was first elaborated by Einstein (1937). Einstein based his analysis on experimental observations of painted tracer particles. He noted that: *“The results demonstrated clearly that even under the same experimental conditions stones having essentially identical characteristics were transported to widely varying distances [...]. Consequently, it seemed reasonable to approach the subject of particle movement as a probability problem”* (Ganti et al. 2010).

Einstein (1937) considered the particle motion as a stochastic sequence of discrete steps interrupted by periods of rest. He quantified the problem in terms of the statistics of step length (distance that a particle travels once entrained before depositing) and resting period (waiting

time). Both step length and waiting time are stochastic variables and the shape of their probabilities densities affect advection and diffusion of river tracer pebbles (and, in general, sediment particles) in a way that, only recently, has been described by applying the ideas deriving from the standard formulation for Continuous Time Random Walk (CTRW).

CTRW, accompanied by appropriate probability distribution functions (PDFs) for walker step length and waiting time, yields asymptotically the standard advection-diffusion equation (ADE) for thin-tailed PDFs, and the fractional advection-diffusion equation (fADE) for heavy-tailed PDFs, the latter allowing the possibilities of subdiffusion or superdiffusion of particles, which is often referred as non-local behavior or anomalous diffusion (e.g. Schumer et al., 2009).

1.1 OBJECTIVES OF THE THESIS

In latest years, considerable emphasis has been placed on non-locality associated with heavy-tailed PDFs for particle step length (e.g. Schumer et al., 2009; Bradley et al. 2010; Ganti et al. 2010). This appears to be in part motivated by the desire to construct fractional advective-diffusive equations for pebble tracer dispersion corresponding to the now-classical fADE model (e.g. Schumer et al., 2009).

In the thesis, we firstly consider the 1D morphodynamics of an erodible bed subject to bedload transport and we focus on the case of non-locality mediated by both heavy- and thin-tailed PDFs for particle step length. Regardless of the thin tail of the PDF, the degree of non-locality nevertheless increases with increasing mean step length.

The first objective of the thesis is therefore analysing the effects of this non-locality on transient aggradational/degradational bed profiles and trying to give an explanation to anomalously flat aggradational long profiles that have been observed in some short laboratory flume experiments and, until now, modelled by considering fADE.

The second objective is strictly related to pebble tracer dispersion: we show that the CTRW Master Equation is inappropriate for river pebbles moving as bed material load. We want to develop a new Master Equation, for tracer transport and dispersion for alluvial morphodynamics, which is based on the Exner equation of sediment mass conservation as well as on the existence of a mean bed elevation

averaged over fluctuation, which precludes the possibility of streamwise subdiffusion mediated by a waiting time PDF with no mean. The new so called Exner-Based Master Equation (EBME) yields asymptotic forms for ADE and fADE that differ significantly from CTRW. It allows a) vertical dispersion, as well as streamwise advection-diffusion, and b) mean waiting time to vary in the vertical. The possibility to look at the vertical exchanges is needed to describe the advective slowdown of tracer particles described by Ferguson and Hoey (2002).

Then, the third objective is to construct a simplified model for showing the role of vertical dispersion on tracers motion. The vertical dispersion is another example of non-local behaviour, which cannot be expressed with fractional derivatives.

The last objective is to show some numerical solutions of the proposed EBME for streamwise and vertical transport and dispersion of tracers.

1.2 STRUCTURE OF THE THESIS

The thesis is organized in six chapters and here briefly the content of each chapter is presented.

In Chapter 2, some basic and well-known notions are reported: different formulations of the Exner equation of sediment mass conservation are stated, with specific interest only in bedload transport which characterizes grave-bed streams. For completeness, some general definition for bedload transport relations are given as well.

In Chapter 3, we consider the 1D morphodynamics of an erodible bed subject to bedload transport. We show all the results concerning the first objective of the thesis, looking at the effects of non-locality due to variable step length on bed evolution.

In Chapter 4, we introduce the tracers problem providing some experimental and theoretical findings on advection and diffusion of river pebble tracers.

In Chapter 5, we set the pebble tracer dispersion in the CTRW framework and we define a generalized (Exner-based) Master Equation for the case of bedload transport (moving as bed material load) in rivers, so as to include PDFs of particle step length and particle waiting time, as well as vertical exchange of particles, according to the above mentioned second objective. Then, we illustrate the key aspect of vertical dispersion

by means of a numerical solution of the simplified version of EBME, in which streamwise variation is neglected.

In Chapter 6, using existing experimental data by Wong et al. (2007), we try to extract new information from time series of bed elevation about the structure functions of the parameters of the model EBME-N and then we report some numerical results for the case of vertical and streamwise transport and dispersion of tracers.

2 MORPHODYNAMICS OF RIVER BED VARIATION

The field of morphodynamics consists of the class of problems for which the flow over a bed interacts strongly with the shape of the bed, both of which evolve in time (Parker, 2004).

The flow field determines the sediment transport rate by means of sediment transport relations and the sediment transport rate controls the morphodynamics of the bed surface (e.g., slope, bedforms) by means of the equation of sediment mass conservation. If changes in flow field (or, directly, in sediment transport rate) occur, then, the morphodynamics of bed changes. This alteration induces a changed flow field, which, again, changes the bed until an equilibrium condition is reached.

Felix Exner was the first researcher to state a morphodynamic problem in quantitative terms, that's why, in spite of the term "morphodynamics" itself evolved many decades afterward, he deserves credit as the founder of morphodynamics. In particular, in the early part of the 20th Century he derived one version of the various statements of conservation of bed sediment (Exner, 1920; 1925) that are now referred to as "Exner equations" (Parker, 2004). The equation was brought to the attention of the English-speaking world via the book by Leliavsky (1955), as pointed out by Paola and Voller (2005).

In the current Chapter, some different formulations of the Exner equation of sediment mass conservation are presented, with specific interest only in bedload transport which characterizes grave-bed streams. For the sake of completeness, some general definition for bedload transport relations are given as well.

2.1 THE EXNER EQUATION OF SEDIMENT CONTINUITY

The Exner equation of sediment conservation, when combined with a hydrodynamic model and a sediment transport model (i.e. bedload transport relations), is a central tool to evaluate the bed evolution (e.g.

aggradation and degradation) in the field of morphodynamics of the Earth's surface.

It's 1D derivation can be easily shown considering mass conservation within a control volume with a unit width (Figure 2.1).

Let q [L^2T^{-1}] denote the volume sediment transport rate per unit width, λ_p [1] denote bed porosity (i.e., fraction of bed volume that is pores rather than sediment) and ρ_s [ML^{-3}] the material density of sediment: the mass sediment transport rate per unit width is then $\rho_s q$ [$ML^{-1}T^{-1}$].

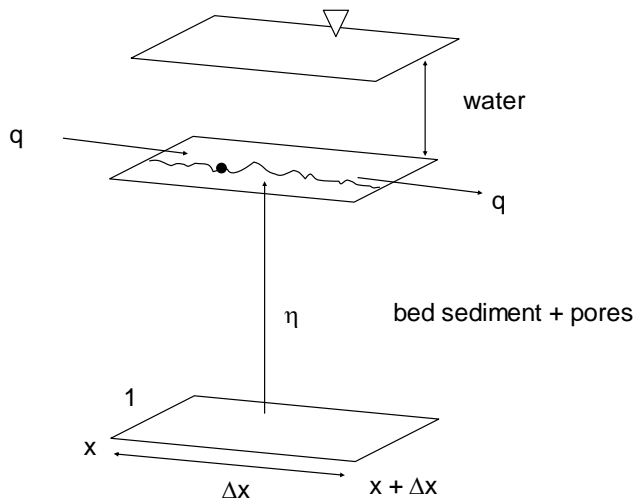


Figure 2.1 Control volume for the derivation of the Exner equation of sediment mass conservation (Parker, 2004)

Sediment mass conservation within the control volume requires that the variation in time of the sediment mass within the control volume is given by the difference between the sediment mass inflow rate and the sediment mass outflow rate:

$$\frac{\partial}{\partial t} [\rho_s (1 - \lambda_p) \eta] \Delta x \cdot 1 = \rho_s [q|_x - q|_{x+\Delta x}] \cdot 1 \quad (2.1)$$

where η [L] denotes the bed elevation, t [T] denotes the time, x [L] denotes the streamwise distance.

From Equation 2.1, the 1D Exner equation of sediment conservation in its (classical) flux form (or equivalently in the 2D case, divergence formulation) can be written as:

$$(1-\lambda_p) \frac{\partial \eta(x,t)}{\partial t} = - \frac{\partial q(x,t)}{\partial x} \quad (2.2)$$

There is, however, a completely equivalent entrainment form of sediment conservation (e.g. Tsujimoto, 1978, Parker et al. 2000, Ganti et al. 2010; Pelosi and Parker, 2013):

$$(1-\lambda_p) \frac{\partial \eta(x,t)}{\partial t} = D(x,t) - E(x,t) \quad (2.3)$$

where $E [LT^{-1}]$ denotes the volume rate of entrainment of bed particles into bedload per unit area per unit time and $D [LT^{-1}]$ denotes the volume rate of deposition of bedload material onto the bed per unit area per unit time.

The deposition rate can be related to the entrainment rate by means of the probability density of the step length $p_s(r) [L^{-1}]$, that is the probability density of the distance that an entrained particle moves before being re-deposited.

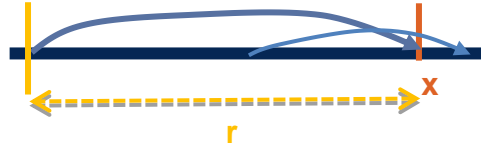


Figure 2.2 Particle step length

Assuming that, once entrained, a particle undergoes a step with length r before depositing (Figure 2.2), and that this step length has the probability density $p_s(r)$ (pdf of step length), the volume deposition rate D can be specified as follows in terms of entrainment rate upstream and travel distance (e.g. Parker et al., 2000; Ganti et al. 2010),

$$D(x) = \int_0^{\infty} E(x-r) p_s(r) dr \quad (2.4)$$

so that the entrainment form of sediment mass conservation can be written as:

$$\frac{\partial \eta}{\partial t} = -E(x) + \int_0^{\infty} E(x-r)p_s(r)dr \quad (2.5)$$

As has been shown by Tsujimoto (1978), the two forms (2.2) and (2.3), are in principle completely equivalent in so far as the following equation precisely describes the bedload transport rate:

$$q(x) = \int_0^{\infty} E(x-r) \int_r^{\infty} p_s(r')dr'dr \quad (2.6)$$

Cases in which the two forms are not equivalent will be shown in Chapter 3, which is about the morphodynamics of bed river variation with variable step length.

Many other different formulations for the Exner equation have been developed during the years in order to address more complex problems (Paola and Voller, 2005), such as modeling (i) the bed evolution and stratigraphy in rivers containing a mixture of grain sizes over a wide range (Hirano, 1971; Parker et al., 2000; Bloom et al., 2004; Parker, 2008) or (ii) the evolution of tracers particle moving as bedload into a stream (Parker et al., 2000; Ganti et al., 2010). The major advance in this regard was made by Hirano (1971), who introduced the concept of “active layer” (Figure 2.3).

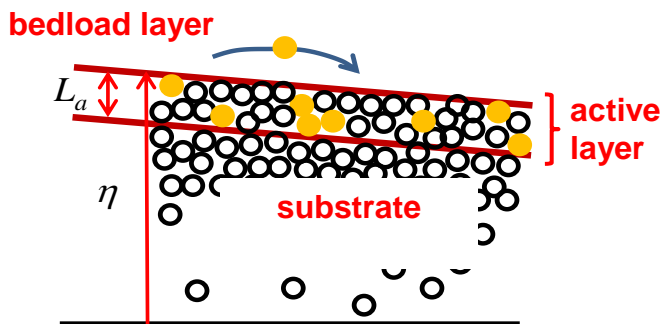


Figure 2.3 Active layer concept

According to his indication, the bed can be ideally divided into two parts: (i) a superficial well-mixed layer (i.e., the active layer) of thickness L_a , which exchanges actively (and equally) with the bedload layer and (ii) a deeper layer (i.e., the substrate), which exchanges with the bedload only in case of bed aggradation/degradation.

The thickness of the active layer is supposed to be a function of D_{90} , the diameter such that 90 percent of the bed sediment is finer (Parker, 2008). Considering a well-mixed active layer means giving to the particles contained in it, the same probability of entrainment into bedload, which sharply vanishes into the substrate (Figure 2.4b).

The reality is that the deeper the particle is buried, the lower is its probability of being entrained into bedload, i.e., the probability of exposure of a grain decreases with depth as shown in Figure 2.4a (Parker et al., 2000).

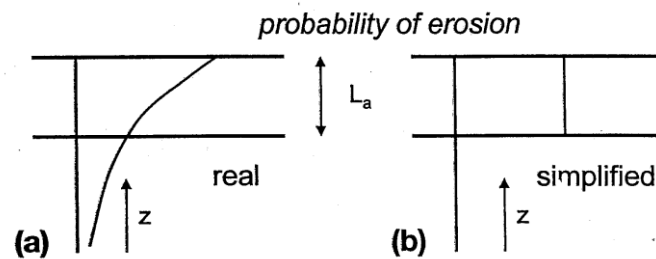


Figure 2.4 Variation in probability of Entrainment as in Parker et al. (2000): (a) actual variation; (b) approximation given by active layer formulation

Parker et al. (2000), however, specified a general probabilistic formulation of the Exner equation of sediment continuity with no discrete layers. It is able to capture vertical exchange of sediment particles (and specifically tracer particles, as later) with no need of the relatively heavy-handed assumption of an active layer. Here we refer to this framework as PPL (Parker-Paola-Leclair).

2.1.1 Parker-Paola-Leclair (PPL) Framework for Exner equation of sediment continuity

Let z [L] denote a coordinate oriented upward normal to the local mean bed and $P_e(x, z, t)$ [1] denote the probability that a point at elevation z is in the sediment bed (rather than the water above it; Figure 2.5). Thus $P_e(x, z, t)$ approaches unity when $z \rightarrow -\infty$ (deep in the deposit) and zero when $z \rightarrow \infty$ (in the water column). Because of its definition, P_e also

indicates the probability that the bed surface elevation is higher than z , hence the probability density $p_e [L^{-1}]$ that instantaneous bed elevation is at level z is:

$$p_e(z) = -\frac{\partial P_e}{\partial z}, \quad \int_{-\infty}^{\infty} p_e(z) dz = 1 \quad (2.7a,b)$$

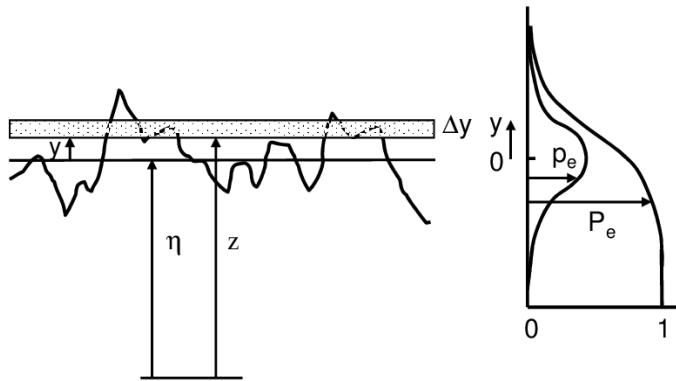


Figure 2.5 Definition diagram for the Parker-Paola-Leclair framework for sediment and sediment tracer conservation.

A new vertical coordinate system can now be introduced in terms of the variable $y [L]$, representing the deviation from the mean bed elevation η :

$$y = z - \eta(x, t) \quad (2.8)$$

Consequently, P_e becomes function of y and (2.7a) takes the form:

$$p_e(y) = -\frac{\partial P_e}{\partial y} \quad (2.9)$$

Now let $p_{jO}(y) [L^{-1}]$ be the probability density that a particle that is entrained into bedload comes from level y , and $p_{jI}(y) [L^{-1}]$ be the probability density that a particle that is deposited is emplaced in the bed at level y . As shown in Figure 2.5, the volume of sediment per unit length and width contained in a strip with height dy is given as $(1-\lambda_p)P_e dy$, and the entrainment and deposition rates within this strip are given as $(1-\lambda_p)p_{jO} E dy$ and $(1-\lambda_p)p_{jI} E dy$. A formulation of mass balance in correspondence with (2.3), then, yields the PPL elevation-specific form of the Exner equation of mass balance:

$$\frac{\partial P_e}{\partial t} = -E(x, t)p_{JO}(y) + p_{JI}(y) \int_0^\infty E(x-r, t)p_s(r)dr \quad (2.10)$$

Thus particles can jump out from any elevation y with probability p_{JO} , and jump back into the bed at any elevation y with probability p_{JI} , after having been entrained at any distance r upstream from any level y . The above equation involves a simplification, in that it assumes that the elevation of deposition is uncorrelated with step length.

In general, P_e is a function of x , y and t , where y is according to (2.8) the elevation relative to the mean bed. Thus $P_e = P_e(x, z-\eta(t), t)$. Note that P_e can vary in time in two ways; the structure of P_e itself can vary in time, and the value of P_e can change at a given elevation due to bed aggradation. The chain rule applied to equations (2.8) and (2.9) yields:

$$\begin{aligned} \frac{\partial P_e[x, y(t), t]}{\partial t} &= \frac{\partial P_e(x, y, t)}{\partial t} - \frac{\partial P_e(x, y, t)}{\partial y} \frac{\partial \eta}{\partial t} = \\ &= \frac{\partial P_e}{\partial t} + p_e(y) \frac{\partial \eta}{\partial t} \end{aligned} \quad (2.11)$$

which substituted in (2.10) gives:

$$\frac{\partial P_e}{\partial t} + p_e \frac{\partial \eta}{\partial t} = -E(x, t)p_{JO}(y) + p_{JI}(y) \int_0^\infty E(x-r, t)p_s(r)dr \quad (2.12)$$

In the following, we make the simplification that the probability density that a particle is jumps into the bed at level y is equal to the probability density that a particle jumps out from level y :

$$p_{JI}(y) = p_{JO}(y) = p_J(y) \quad (2.13)$$

so that (2.12) becomes

$$\frac{\partial P_e}{\partial t} + p_e \frac{\partial \eta}{\partial t} = -E(x, t)p_J(y) + p_J(y) \int_0^\infty E(x-r, t)p_s(r)dr \quad (2.14)$$

This assumption must be valid for a bed that is in macroscopic equilibrium (constant η), and is a first-order approximation for a bed that is only slowly aggrading or degrading (in which case bed elevation is driven by slow spatiotemporal variation in E).

It is shown in Blom and Parker (2004) that integrating (2.12) in y recovers the Exner equation (2.5).

Equation (2.14) is, in and of itself, a fairly trivial extension of the Exner formulation. Its true value becomes apparent when applied to bedload tracers. The PPL framework is applied to this case in Chapter 4. Here, we just wanted to present the general framework and to show together the main different formulations of the Exner equation of sediment continuity, which will be recalled in the following sections.

2.2 BEDLOAD TRANSPORT RELATIONS

Bedload transport relations allow to relate the sediment transport rate q with the flow field. In particular, having defined (i) a dimensionless sediment transport rate q^* (i.e., Einstein number) as follows

$$q^* = \frac{q}{\sqrt{RgD_p} D_p} \quad (2.15)$$

where D_p [L] is the particle diameter, R [1] the submerged specific gravity of the sediment and g [LT^{-2}] the acceleration of gravity and (ii) a dimensionless shear stress (i.e., Shields number):

$$\tau^* = \frac{\tau_b}{\rho R g D_p} \quad (2.16)$$

where τ_b [$ML^{-1}T^{-2}$] is the shear stress and ρ [ML^{-3}] is water density, a common approach is empirically relating q^* with either the Shields stress τ^* or the excess of the Shields stress τ^* above some appropriately defined critical Shields stress τ_c^* .

$$q^* = f(\tau^*) \quad \text{or} \quad q^* = f(\tau^* - \tau_c^*) \quad (2.17a,b)$$

Famous empirical bedload relations are the ones by Meyer-Peter and Müller (1948), Einstein (1950), Ashida & Michiue (1972), Wong and Parker (2006) and so on. In the following, as later specified, the relation by Wong and Parker (2006) is used for our numerical model of bed evolution with variable step length (cfr. Section 3.2.2) because it is well-suited for gravel-bed rivers.

The volume bedload transport rate per unit width q at equilibrium can also be written as:

$$q = E \cdot \bar{r} \quad (2.18)$$

Einstein (1950), where \bar{r} [L] is mean particle step length. The relation (2.18) is used to define the entrainment rate E in our numerical model of bed evolution with variable step length (Section 3.2.2).

3 MORPHODYNAMICS OF RIVER BED VARIATION WITH VARIABLE BEDLOAD STEP LENGTH

Here we consider the 1D morphodynamics of an erodible bed subject to bedload transport. Fluvial bed elevation variation is typically modeled by the Exner equation which, in its classical form, expresses mass conservation in terms of the divergence of the bedload sediment flux. An entrainment form of the Exner equation can be written as an alternative description of the same bedload processes, by introducing the notions of an entrainment rate into bedload and of a particle step length, and assuming a certain probability distribution for the step length. This entrainment form implies some degree of non-locality which is absent from the standard flux form, so that these two expressions, which are different ways to look at same conservation principle (i.e. sediment continuity), may no longer become equivalent in cases when channel complexity and flow conditions allow for long particle saltation steps (including, but not limited to the case where particle step length has a heavy tailed distribution) or when the domain of interest is not long compared to the step length (e.g. laboratory scales, or saltation over relatively smooth surfaces). We perform a systematic analysis of the effects of the non-locality in the entrainment form of Exner equation on transient aggradational/degradational bed profiles by using the flux form as a benchmark. As expected, the two forms converge to the same results as the step length converges to zero, in which case non-locality is negligible. As step length increases relative to domain length, the mode of aggradation changes from an upward-concave form to a rotational, and then eventually a downward-concave form. Corresponding behavior is found for the case of degradation. These results may explain anomalously flat aggradational long profiles that have been observed in some short laboratory flume experiments.

The Chapter is a version of a recent paper (Pelosi and Parker, 2013), published on *ESurfD* journal, and under revision for the publication on *ESurf* journal.

3.1 INTRODUCTION

The Exner equation, in its classical formulation, relates the bed evolution to the divergence of the bedload sediment flux (q), which is assumed to be a local function of the flow and the topography. However, certain sediment dynamics, such as (i) particle diffusion in river bedload (e.g. Nikora et al., 2002; Bradley et al., 2010; Ganti et al. 2010; Martin et al., 2012), (ii) bed sediment transport along bedrock channels (Stark et al., 2009) and (iii) particle displacements on hillslopes (Foufoula-Georgiou et al., 2010) may show non-local behaviour that is not easily captured by the classical form of the Exner equation.

The non-locality of interest here is embedded in the step length r of a bedload particle, i.e. the distance that a particle, once entrained into motion, travels before depositing. The existence of a finite step length r implies a non-local connection between point x (where a particle is deposited) and point $x - r$ (where it was entrained). The degree of non-locality can be characterized in terms of the probability density (PDF) of step lengths $p_s(r)$. This PDF can be hypothesized to be thin-tailed (e.g. exponential) or heavy-tailed (e.g. power).

In recent years, considerable emphasis has been placed on non-locality associated with heavy-tailed PDFs for step length (e.g. Schumer et al., 2009; Bradley et al. 2010; Ganti et al. 2010). This appears to be in part motivated by the desire to construct fractional advective-diffusive equations for pebble tracer dispersion corresponding to the now-classical fADE model (e.g. Schumer et al., 2009).

Experiments conducted under the simplest possible conditions (including steady, uniform flow, single-sized sediment and the absence of bedforms) yield thin-tailed, and more specifically exponential distributions for step length PDF (Nakagawa and Tsujimoto, 1980; Hill et al., 2010). Ganti et al. (2010), however showed that were a) the bed to consist of a range of sizes, b) the PDF of size distribution to obey a gamma distribution and c) the PDF of for step length of each grain size to be exponential, the resulting PDF for step length would be heavy-tailed. Hassan et al. (2013) analysed 64 sets of field data on pebble tracer dispersion in mountain rivers (which by nature contain a range of sizes). They found that all but 5 cases either showed thin-tailed PDFs, or could be rescaled as thin-tailed PDFs. Their results, combined with those of Ganti et al. (2010), however, do suggest that the gradual incorporation of

the many factors in nature that lead to complexity can also lead to non-local behaviour mediated by heavy-tailed PDFs.

Here, however, we focus on the case of non-locality mediated by thin-tailed (exponential) PDFs for step length. Regardless of the thin tail of the PDF, the degree of non-locality nevertheless increases with increasing mean step length \bar{r} . This non-locality may become dominant when \bar{r} approaches the same order of magnitude as the domain length L_d under consideration. We show that patterns of bed aggradation and degradation are strongly dependent on the ratio \bar{r}/L_d , a parameter that may be surprisingly large in some small-scale experiments. Our results may explain anomalously flat aggradational long profiles that have been observed in some short laboratory flume experiments, without relying on either of the fractional partial differential equations or heavy-tailed distributions invoked or implied by Voller and Paola (2010). We use our framework to explore the consequences of heavy-tailed PDFs for step lengths as well.

3.2 METHODS

3.2.1 Theoretical framework

The current Section recalls part of Section 2.1, to which it's possible to refer for more details.

1D river bed elevation variation is classically described, as pointed out in Chapter 2, by the 1D Exner equation of sediment conservation in flux form:

$$\frac{\partial \eta(x, t)}{\partial t} = - \frac{\partial q(x, t)}{\partial x} \quad (3.1)$$

where η [L] denotes the bed elevation, t [T] denotes the time, x [L] denotes the streamwise distance and q [L^2T^{-1}] is the volume bedload transport rate per unit width. (Here, the porosity of the bed sediment is set = 0 and bedload only is considered, both for the sake of simplicity). There is, however, a completely equivalent entrainment form of sediment conservation (e.g. Tsujimoto, 1978):

$$\frac{\partial \eta(\mathbf{x}, t)}{\partial t} = D(\mathbf{x}, t) - E(\mathbf{x}, t) \quad (3.2)$$

where E [LT^{-1}] denotes the volume rate of entrainment of bed particles into bedload per unit area per unit time and D [LT^{-1}] denotes the volume rate of deposition of bedload material onto the bed per unit area per unit time.

The deposition rate can be related to the entrainment rate by means of the probability density of the step length $p_s(r)$ [L^{-1}]:

$$D(\mathbf{x}) = \int_0^\infty E(\mathbf{x} - \mathbf{r}) p_s(\mathbf{r}) d\mathbf{r} \quad (3.3)$$

so that the entrainment form of sediment mass conservation can be written as:

$$\frac{\partial \eta}{\partial t} = -E(\mathbf{x}) + \int_0^\infty E(\mathbf{x} - \mathbf{r}) p_s(\mathbf{r}) d\mathbf{r} \quad (3.4)$$

As has been shown by Tsujimoto (1978), the two forms (3.1) and (3.4), are in principle completely equivalent in so far as the following equation precisely describes the bedload transport rate:

$$q(\mathbf{x}) = \int_0^\infty E(\mathbf{x} - \mathbf{r}) \int_r^\infty p_s(\mathbf{r}') d\mathbf{r}' d\mathbf{r} \quad (3.5)$$

Yet in any given implementation, they are rarely equivalent. More specifically, in most implementations of the flux form (3.1), q is taken to be a local function of the flow (e.g. bed shear stress), whereas in most implementations of the entrainment form (3.4), E is taken to be a local function of the flow (again, e.g. bed shear stress). The presence of the spatial convolution term in the entrainment form of (3.3) and (3.4) ensures non-locality in the entrainment form as compared to the flux form. This non-locality is present regardless of whether the PDF of step length $p_s(r)$ is thin-tailed or heavy-tailed, and vanishes only when $p_s(r)$ becomes proportional to $\delta(r)$, where δ denotes the Dirac function.

Here we explore the consequences of non-locality, and compare the local and nonlocal forms (3.1) and (3.4) for Exner over a range of conditions. To do this, we assume that the PDF $p_s(r)$ has a mean step length, and consider the dimensionless parameter ϵ :

$$\varepsilon = \frac{\bar{r}}{L_d} \quad (3.6)$$

where \bar{r} [L] denotes the mean particle step length and L_d [L] denotes the length of the domain of interest (e.g. flume length or length of river reach). The flux and entrainment forms become strictly equivalent only under the constraint:

$$\varepsilon = \frac{\bar{r}}{L_d} \ll 1 \quad (3.7)$$

Here we demonstrate that this equivalence for $\varepsilon \ll 1$ breaks down with increasing ε . This is because a finite mean step length \bar{r} in and of itself implies non-locality, regardless of whether or not the probabilistic distribution of particle step length $p_s(r)$ is thin- or heavy-tailed. A further degree of non-locality can be introduced by adopting a heavy-tailed distribution for $p_s(r)$.

The standard thin-tailed form for the particle step length probability density function is the exponential distribution (e.g. Nakagawa and Tsujimoto, 1980; Hill et al., 2010):

$$p_s(r) = \frac{1}{\bar{r}} \exp\left(-\frac{r}{\bar{r}}\right) \quad (3.8)$$

The heavy-tailed Pareto distribution with a shift, which ensures that the maximum value of the distribution is realized at $r = 0$, can be considered as an alternative:

$$p_s(r) = \frac{\alpha r_0^\alpha}{(r + r_0)^{\alpha+1}}, \begin{cases} r_0 > 0 \\ \alpha > 0 \end{cases} \quad (3.9)$$

where α is the shape parameter and r_0 [L] is the scale parameter. The mean value \bar{r} of the distribution of Equation (3.9) can be written as:

$$\bar{r} = \frac{\alpha r_0}{\alpha - 1} - r_0, \begin{cases} r_0 > 0 \\ \alpha > 0 \end{cases} \quad (3.10)$$

3.2.2 Numerical model

Here we solve the flux and entrainment formulations under parallel conditions, the only exception being the formulation for step length. To simplify the problem and focus on this point, we approximate the flow as obeying the normal (steady, uniform) approximation. Momentum conservation then dictates that bed shear stress τ_b [$\text{ML}^{-1}\text{T}^{-2}$] can be represented as proportional to the product of depth H [L] and slope S [1]:

$$\tau_b = \rho u_*^2 = \rho g H S, \quad S = -\frac{\partial \eta}{\partial x} \quad (3.11\text{a,b})$$

where u_* [LT^{-1}] is the shear velocity.

The dimensionless Shields number governing particle mobility defined as

$$\tau^* = \frac{\tau_b}{\rho R g D_p} \quad (3.12)$$

where ρ [ML^{-3}] is water density, D_p [L] is characteristic bed particle size (here taken to be uniform for simplicity) and R denotes the submerged specific gravity of the sediment (~ 1.65 for quartz).

The flow can be computed by introducing the Manning-Strickler resistance relation:

$$\frac{U}{u_*} = \alpha_r \left(\frac{H}{k_c} \right)^{1/6} \quad (3.13)$$

where U [LT^{-1}] is the depth-averaged flow velocity, α_r is a dimensionless coefficient between 8 and 9 (Chaudhry, 1993), and k_c denotes a composite roughness height. In absence of bedforms, k_c is equivalent to the roughness height k_s which is proportional to grain size D_c by means of a dimensionless coefficient with typical values between 2 and 5 (Parker, 2004). Here, α_r is set equal to 8.1, as suggested by Parker (1991) for gravel-bed streams, while k_c , in absence of bedforms, is taken to be 2.5 times the grain size D_c (Parker, 2004).

The equation for water conservation for quasi-steady flow is:

$$Q_w = UBH \quad (3.14)$$

where Q_w [L^3T^{-1}] is the water discharge and B [L] denotes the channel width.

Combining Equations (3.11) - (3.14), we relate the dimensionless Shields number to the flow properties:

$$\tau^* = \left[\frac{(k_c)^{1/3} Q_w^2}{\alpha_r^2 g B^2} \right]^{3/10} \frac{S^{7/10}}{RD_p} \quad (3.15)$$

The basis for our morphodynamic calculations is the form of Meyer-Peter and Müller (1948), as modified by Wong and Parker (2006). It takes the form:

$$q = \gamma \sqrt{RgD_p} D_p (\tau^* - \tau_c^*)^{3/2} \quad (3.16)$$

where g [LT^{-2}] denotes the gravitational acceleration. The parameter τ_c^* denotes the threshold Shields number and γ is a coefficient of proportionality; these parameters take the respective values 0.0495 and 3.97 (as specified by Wong and Parker, 2006).

The volume bedload transport rate per unit width q at equilibrium can also be written as:

$$q = E \cdot \bar{r} \quad (3.17)$$

(Einstein, 1950), so that the entrainment rate takes the form:

$$E = \frac{\gamma}{\beta} \sqrt{RgD_p} (\tau^* - \tau_c^*)^{3/2}, \quad \beta = \frac{\bar{r}}{D_p} \quad (3.18)$$

Here β is a dimensionless parameter. Einstein (1950), suggested, based on a simple flume-like configuration, that \bar{r}/D_p takes a value on the order of $100 \sim 1000$, so that a step length is about $100 \sim 1000$ grain sizes. This order of magnitude has been confirmed by the experiments of Nakagawa and Tsujimoto (1980), Wong et al. (2007) and Hill et al. (2010).

In systems with higher degrees of complexity, however, β is likely to vary over a wide range. Combinations of multiple grain sizes, bedforms, scour and fill and partially exposed bedrock are likely to give rise to connected pathways along which particles may travel for an extended distance, so giving rise to larger values of \bar{r} (e.g. Parker, 2008). In order to capture this effect in a simplified 1D model, we allow the ratio \bar{r} , and thus

$\beta = \bar{r} / D_p$ to vary freely, so that the ratio \bar{r} / L_d of step length to domain length can vary from 0 (in which case the flux and entrainment formulations become equivalent) to unity (in which a particle starting at the upstream end of the domain reaches the downstream end in a single step)..

Linking Equations (3.16) - (3.18), the following relation arises at equilibrium conditions:

$$\frac{q}{\sqrt{RgD_p D_p}} = \beta \frac{E}{\sqrt{RgD_p}} \quad (3.19)$$

Our formulation is such that increased step length is adjusted against reduced entrainment, so that the equilibrium bedload transport rate is the same whether the flux or entrainment formulation is used. A difference, however, arises under disequilibrium conditions, in which case Equation (3.16) is solved in conjunction with Equation (3.1) in the flux case, and Equation (3.18) is solved in conjunction with Equation (3.4) in the entrainment case. This allows us to capture the difference between the two formulations in a comparable way.

The flux formulation, Equation (3.1) corresponds to a nonlinear diffusion equation, i.e.

$$\frac{\partial \eta(x, t)}{\partial t} = \frac{\partial}{\partial x} \left(v \frac{\partial \eta}{\partial x} \right) \quad (3.20)$$

where according to Equations (3.11), (3.15) and (3.16), the kinematic diffusivity v is a function of bed slope $S = -\partial \eta / \partial x$:

$$v = \frac{\sqrt{RgD_p D_p}}{S} \gamma \left\{ \left[\frac{(k_c)^{1/3} Q_w^2}{\alpha_r^2 g B^2} \right]^{3/10} \frac{S^{7/10}}{RD_p} - \tau_c^* \right\}^{3/2} \quad (3.21)$$

The governing equation is second order in x , and thus requires two boundary conditions. Here we require that the bed elevation at the downstream end is zero, and that the sediment transport rate at the upstream end is given as a constant, specified feed rate:

$$\eta|_{x=L_d} = 0, \quad q|_{x=0} = q_f \quad (3.22a,b)$$

The entrainment formulation of Equation (3.4), however, is only first order in x , in so far as the entrainment rate E is a specified function of bed slope $S = -\partial\eta/\partial x$ according to Equations (3.4) and (3.24). Thus there can be only one boundary condition in x ; here we use Equation (3.22a) for this, so that both the flux and entrainment formulations satisfy the condition of vanishing bed elevation (corresponding to set base level) at the downstream end.

Although no boundary condition can be set at the upstream end for the entrainment formulation, it is still possible to choose conditions so that the sediment transport rate at the upstream equals the feed value under equilibrium conditions.

To do this, we assume that the entrainment rate everywhere upstream of $x = 0$ equals a specified value E_f , specified as follows:

$$E_f = \frac{q_f}{\bar{r}} \quad (3.23)$$

The deposition rate $D(x)$ of Equation (3.3) can then be re-written in terms of the sum of particles that originate within the domain ($x - r \geq 0$) and those that originate upstream of the domain ($x - r < 0$):

$$\begin{aligned} D(x) &= \int_0^\infty E(x-r)p_s(r)dr = \int_0^x E(x-r)p_s(r)dr + \int_x^\infty E(x-r)p_s(r)dr = \\ &= \int_0^x E(x-r)p_s(r)dr + E_f p_{ls}(x) \end{aligned} \quad (3.24)$$

where

$$p_{ls}(x) = \int_x^\infty p_s(r)dr \quad (3.25)$$

is the probability [L^{-1}], that a particle travels at least a distance x .

The entrainment form of sediment mass conservation thus takes the ultimate form:

$$\frac{\partial\eta}{\partial t} = -E(x) + \int_0^x E(x-r)p_s(r)dr + E_f p_{ls}(x) \quad (3.26)$$

For the numerical computation, we non-dimensionalize Equations (1) and (26). We assume that the computation begins from some equilibrium initial condition with spatially constant slope S_{in} , bedload transport rate and entrainment rate $q_{in} = \bar{r} E_{in}$. At $t = 0$, however, the supply of

sediment is impulsively altered, causing subsequent bed aggradation or degradation, but with an altered sediment feed rate for $t > 0$. We normalize against initial equilibrium conditions using the following definitions:

$$\hat{\eta} = \frac{\eta}{L_d \cdot S_{in}}, \quad \hat{x} = \frac{x}{L_d}, \quad \hat{r} = \frac{r}{L_d} \quad (3.27a,b,c)$$

$$\hat{t} = \frac{E_{in} \cdot \varepsilon}{L_d \cdot S_{in}} t, \quad \hat{s} = \frac{S}{S_{in}} \quad (3.27d,e)$$

In addition, we non-dimensionalize the entrainment rate (for the entrainment formulation) and the bedload transport rate (for the flux formulation) as

$$\hat{E} = \frac{E}{E_{in}}, \quad \hat{q} = \varepsilon \cdot \hat{E} \quad (3.27f)$$

Then, the non-dimensional flux and entrainment forms of the sediment mass conservation, Equations (3.1) and (3.26) take the respective forms:

$$\frac{\partial \hat{\eta}}{\partial \hat{t}} = -\frac{1}{\varepsilon} \frac{\partial \hat{q}}{\partial \hat{x}} = -\frac{\partial \hat{E}}{\partial \hat{x}} \quad (3.28)$$

$$\frac{\partial \hat{\eta}}{\partial \hat{t}} = -\frac{1}{\varepsilon} \hat{E}(x) + \frac{1}{\varepsilon} \int_0^{\hat{x}} \hat{E}(\hat{x} - \hat{r}) \tilde{p}_s \left(\frac{\hat{r}}{\varepsilon} \right) d\hat{r} + \frac{1}{\varepsilon} \int_{\hat{x}}^{\infty} \tilde{p}_s \left(\frac{\hat{r}}{\varepsilon} \right) d\hat{r} \quad (3.29)$$

where

$$\tilde{p}_s \left(\frac{\hat{r}}{\varepsilon} \right) = \frac{1}{\varepsilon} \exp \left(-\frac{\hat{r}}{\varepsilon} \right) \quad (3.30)$$

is the dimensionless step length PDF for the exponential distribution, and

$$\tilde{p}_s \left(\frac{\hat{r}}{\varepsilon} \right) = \frac{\alpha \hat{r}_0^\alpha}{(\hat{r} + \hat{r}_0)^{\alpha+1}} \quad (3.31)$$

is the corresponding form for the Pareto distribution, where \hat{r}_0 is the dimensionless scale parameter equal to r_0/L_d .

These are the upstream conditions, for the entrainment formulation

$$\hat{E}(\mathbf{x}, t)\Big|_{\hat{x} \leq 0} = \hat{E}_f \quad (3.32a)$$

and for the flux formulation

$$\hat{q}(\mathbf{x}, t)\Big|_{\hat{x} \leq 0} = \varepsilon \hat{E}_f \quad (3.32b)$$

The downstream boundary condition is the same for both

$$\hat{\eta}(\mathbf{x}, t)\Big|_{\hat{x}=1} = 0 \quad (3.32c)$$

Here \hat{E}_f is an imposed upstream entrainment rate, and $\varepsilon \hat{E}_f$ is an imposed upstream bedload feed rate, chosen to be different from the initial equilibrium values so that the bed is forced to aggrade (or degrade) toward a new equilibrium state.

Manipulating the relations (3.15) and (3.18), with the definitions of Equations (3.27), \hat{E} , can be at any given time as:

$$\hat{E} = \left(\frac{\tau_{in}^* \hat{s}^{7/10} - \tau_c^*}{\tau_{in}^* - \tau_c^*} \right)^{3/2} \quad (3.33)$$

where τ_{in}^* is the dimensionless Shields number, calculated from (3.15) with the initial flow and bed conditions and \hat{s} is the local dimensionless slope.

The key parameter of interest here in describing the difference between the entrainment and flux formulations is ε . In the case $\varepsilon \ll 1$, both formulations become identical. We show below, however, that as ε increases, the response to change in sediment supply differs between the two cases.

We discretize the relation between dimensionless slope and dimensionless bed elevation as follows:

$$\hat{s} = \begin{cases} \frac{\hat{\eta}_1 - \hat{\eta}_2}{\Delta \hat{x}}, i = 1 \\ \frac{\hat{\eta}_{i-1} - \hat{\eta}_{i+1}}{2\Delta \hat{x}}, i = 2 \dots M \\ \frac{\hat{\eta}_M - \hat{\eta}_{M+1}}{\Delta \hat{x}}, i = M + 1 \end{cases} \quad (3.34)$$

The discretization of the domain is schematized in Figure 3.1: a central finite-difference scheme is used to solve Equations (3.28) and (3.29).

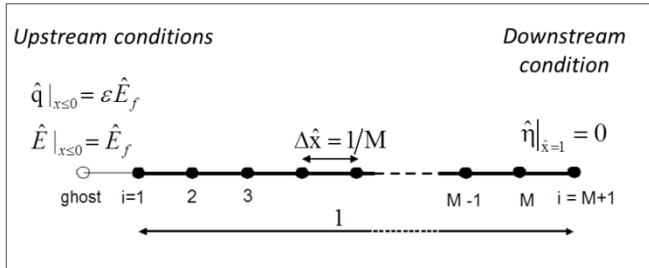


Figure 3.1 Discretization of the domain

3.3 RESULTS

Here we compare the results for aggradation and degradation for the entrainment formulation with varying values of ε against those for the flux formulation. In Figure 3.2, bed elevation profiles are shown, having set as an upstream boundary condition $\hat{E}_f = 2$, so forcing the bed to aggrade. Case (a) is the solution for the flux form of Equation (3.28), while cases (b), (c) and (d) are the solutions for the entrainment form of Equation (3.29), solved, respectively for $\varepsilon = 0.01, 0.5$, and 1.

As expected, the solutions of Equation (3.28) and Equation (3.29) collapse to the same results in the case of $\varepsilon = 0.01$, i.e. when the mean particle step length is short compared to the length of the domain. Thus under this condition the local (flux) form, essentially coincides with the non-local form. For higher values of ε , however, the differences between the results increase because the entrainment form is able to capture the non-local feature of the particle movement. For the flux form and the case $\varepsilon = 0.01$, the aggradational profile is strongly upward concave, with bed slop declining downstream. The transient aggradational bed profiles tend to assume a nearly linear profile, and thus the bed rotates upward, for values of ε close to 0.5. For higher values a downward-concave form profile is realized.

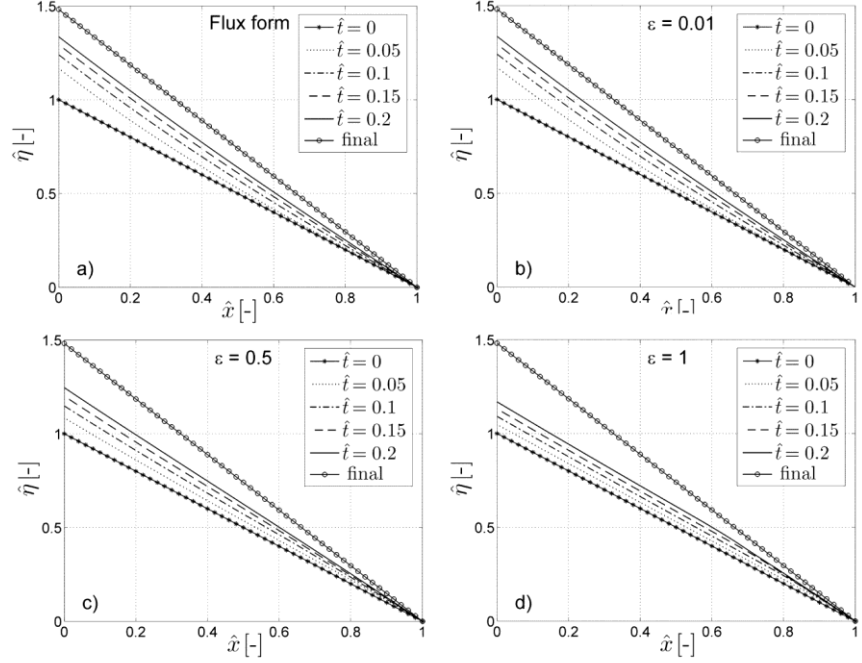


Figure 3.2 Bed profile evolution for the case $\hat{E}_f = 2$: a) flux form; b) entrainment form for $\varepsilon = \bar{\Gamma}/L_d = 0.01$, c) entrainment form for $\varepsilon = 0.5$ and d) entrainment form for $\varepsilon = 1$, using the thin-tailed exponential step length function of Equation (3.8). Increasing ε , the differences between the results from the two forms increase because of the non-locality of particle movement: from upward concave transient profiles to downward concave ones.

To highlight and quantify this change in shape, we introduce a concavity parameter δ , which measures the deviation, in the centre of the profile, at $\hat{x} = 0.5$ relative to the constant initial slope:

$$\delta = \frac{0.5 \cdot \hat{\eta}|_{\hat{x}=0} - \hat{\eta}|_{\hat{x}=0.5}}{\hat{\eta}|_{\hat{x}=0}} \quad (3.35)$$

where $\hat{\eta}|_{\hat{x}=0}$ denotes the dimensionless bed elevation at $\hat{x} = 0$ and $\hat{\eta}|_{\hat{x}=0.5}$ denotes the same quantity in the center of the profile ($\hat{x} = 0.5$). Positive δ indicates upward concavity, while negative δ indicates

downward concavity. In Figure 3.3, the variation in time of δ is shown for the flux case, and different values of ε for the entrainment case. It is seen that δ is positive for smaller ε and but becomes negative for ε greater than 0.5. The results for the flux form overlap with the form for $\varepsilon = 0.01$.

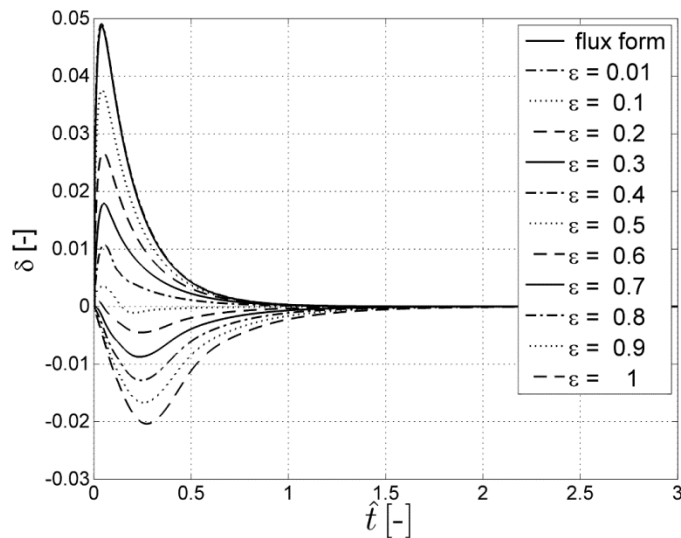


Figure 3.3 Aggradation case: variation in time of the concavity parameter δ in the case of the flux formulation and in the cases of the entrainment formulation for different values of ε ranging from 0.01 to 1. The result for the flux form overlaps with the result for the entrainment form with $\varepsilon = 0.01$.

In Figure 3.4, the slope evolution is plotted: the typical upward concave shape for the flux case and $\varepsilon = 0.01$ is due to the preferential proximal deposition of sediment, which causes the sediment load, and thus the Shields number τ^* to decrease downstream (Parker, 2004). Thus, according to Equation (3.15), a downstream decreasing slope is realized (Figure 3.4a,b). On the other hand, a downward concave shape for $\varepsilon = 1$ is characterized by an increasing slope downstream (Figure 3.4d). This corresponds to bedload particles that can jump from the upstream end of the domain to the downstream end in one step.

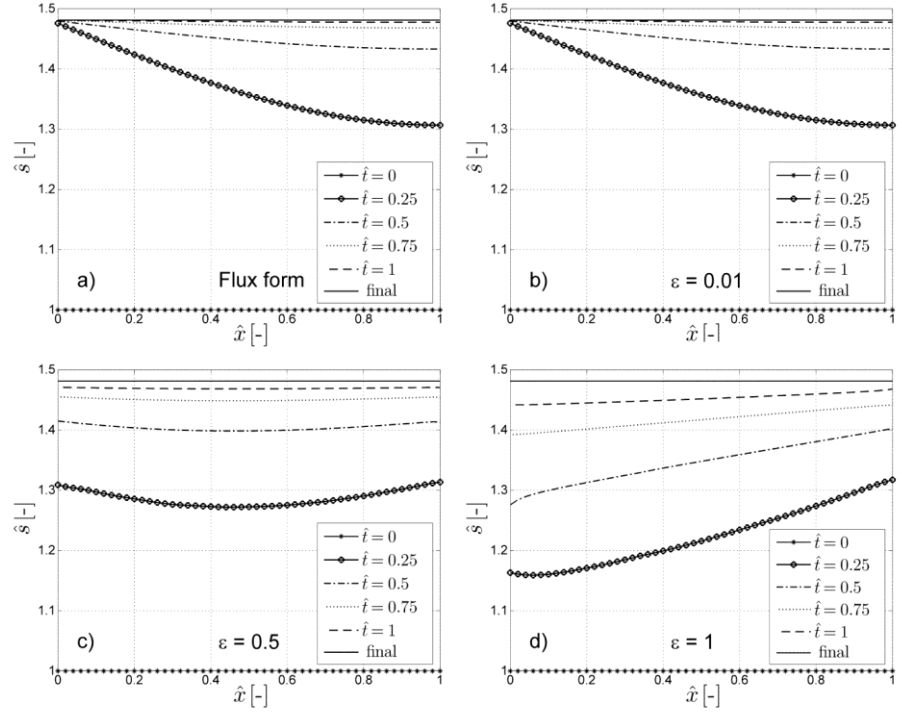


Figure 3.4 Slope profile evolution for the case $\hat{E}_f = 2$: a) flux form; b) entrainment form for $\varepsilon = \bar{\Gamma}/L_d = 0.01$, c) entrainment form for $\varepsilon = 0.5$ and d) entrainment form for $\varepsilon = 1$, using the thin-tailed exponential step length function of Equation (3.8).

For completeness, the case of degradation, due to an imposed entrainment and feed rate upstream $\hat{E}_f = 1/2$, is described by Figure 3.5, Figure 3.6 and Figure 3.7. The results show a congruent behavior with the aggradation case. In Figure 3.5, for $\varepsilon = 0.01$ and $\hat{E}_f = 1/2$, it is seen that the two profiles more or less agree.

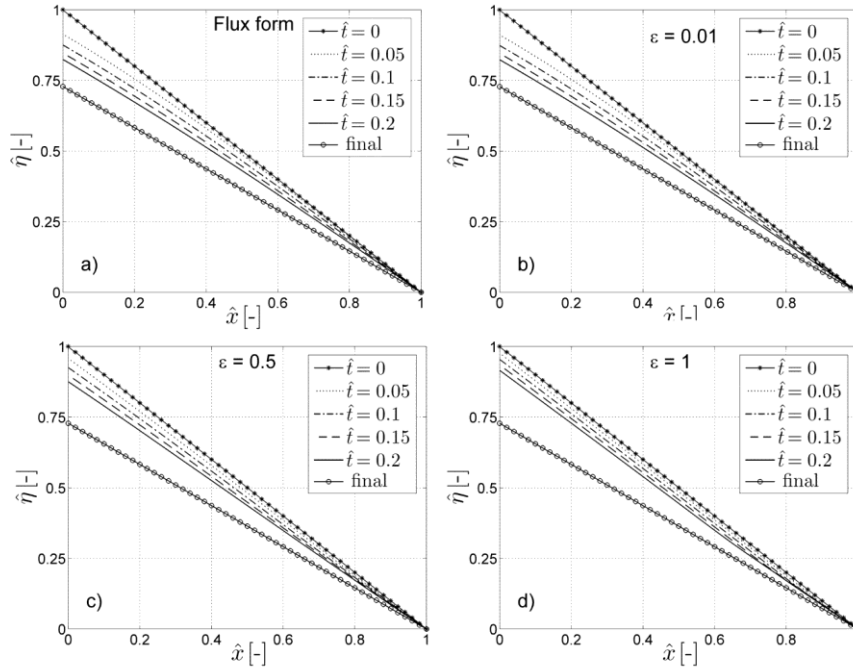


Figure 3.5 Bed profile evolution for the case $\hat{E}_r = 1/2$: a) flux form; b) entrainment form for $\varepsilon = \bar{\tau}/L_d = 0.01$, c) entrainment form for $\varepsilon = 0.5$ and d) entrainment form for $\varepsilon = 1$, using the thin-tailed exponential step length function of Equation (3.8). Increasing ε , the differences between the results from the two forms increase because of the non-locality of particle movement: from upward concave transient profiles to downward concave ones.

In Figure 3.6, the concavity parameters δ also more or less agree for this case. When ε increases to 1, the concavity of the transient degradational profiles changes from downward to upward.

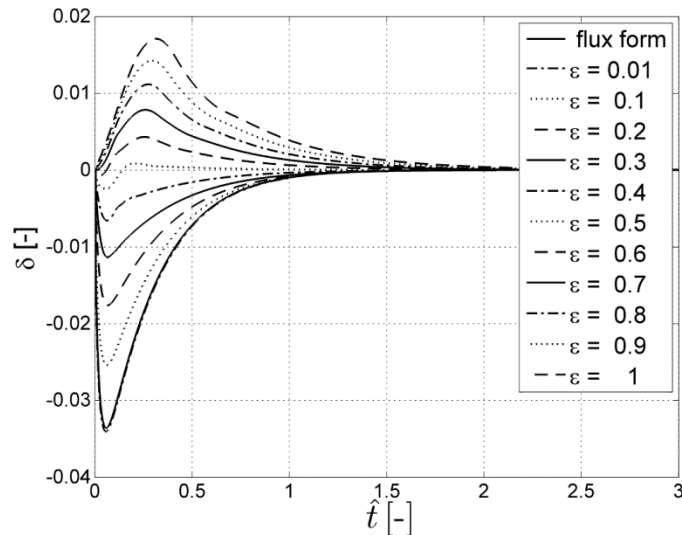


Figure 3.6 Degradation case: variation in time of the concavity parameter δ in the case of the flux formulation and in the cases of the entrainment formulation for different values of ε ranging from 0.01 to 1. The result for the flux form overlaps with the result for the entrainment form with $\varepsilon = 0.01$.

In Figure 3.7, slope changes from increasing downstream to decreasing upstream. When $\varepsilon = 0.5$, it is shown in Figure 3.7 that the transient profile tend to keep a straight shape, and the evolution of the bed is essentially rotational about the downstream end.

Summarizing i) the flux model and the entrainment model yield essentially the same results for $\varepsilon = 0.01$; ii) for $\varepsilon = 0.5$, nearly rotational aggradation and degradation are obtained; and iii) for $\varepsilon = 1$, the pattern of concavity is reversed compared to the flux case.

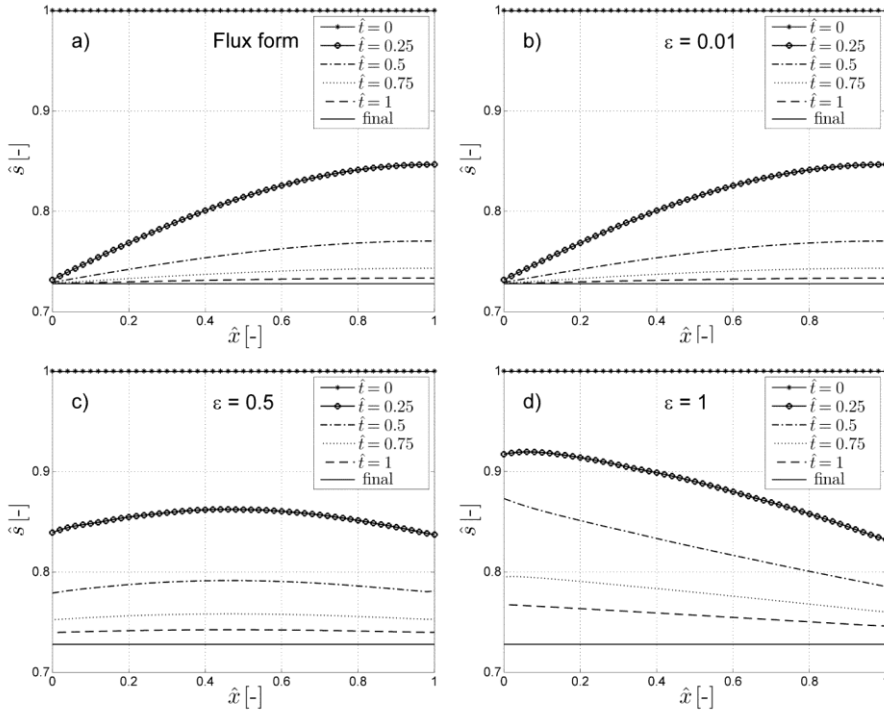


Figure 3.7 Slope profile evolution for the case $\hat{E}_f = 1/2$: a) flux form; b) entrainment form for $\varepsilon = \bar{\Gamma}/L_d = 0.01$, c) entrainment form for $\varepsilon = 0.5$ and d) entrainment form for $\varepsilon = 1$, using the thin-tailed exponential step length function of Equation (3.8).

Then, a Pareto distribution with a shift, i.e. Equation (3.9) for particle step length distribution is considered as well, so as to compare the case of heavy tail of the PDF of step length with the thin-tail exponential form. In the calculations for the entrainment rate with $\hat{E}_f = 2$, two cases are evaluated, (a) $\varepsilon = 0.015$ and (b) $\varepsilon = 1$. It is seen that the two profiles more or less agree for the case (a). A more substantial difference is seen for case (b), but the concavity is quite small for both the cases of thin-tailed and heavy-tailed PDF for step length. Assuming $L = 200$ m, with a thin-tailed PDF the value $\varepsilon = 0.015$ corresponds to a mean step length equal to 3 m, and the value $\varepsilon = 1$ corresponds to 200 m. We have set the shape parameter α in the Pareto PDF equal to 1.5, and the scale

parameter r_0 equal to 1.5 m for case (a), and 100 m for case (b). This yields values of \bar{r} from Equation (3.10), that are respectively equal to 3 m and 200 m, i.e. the same values as the thin-tailed case.

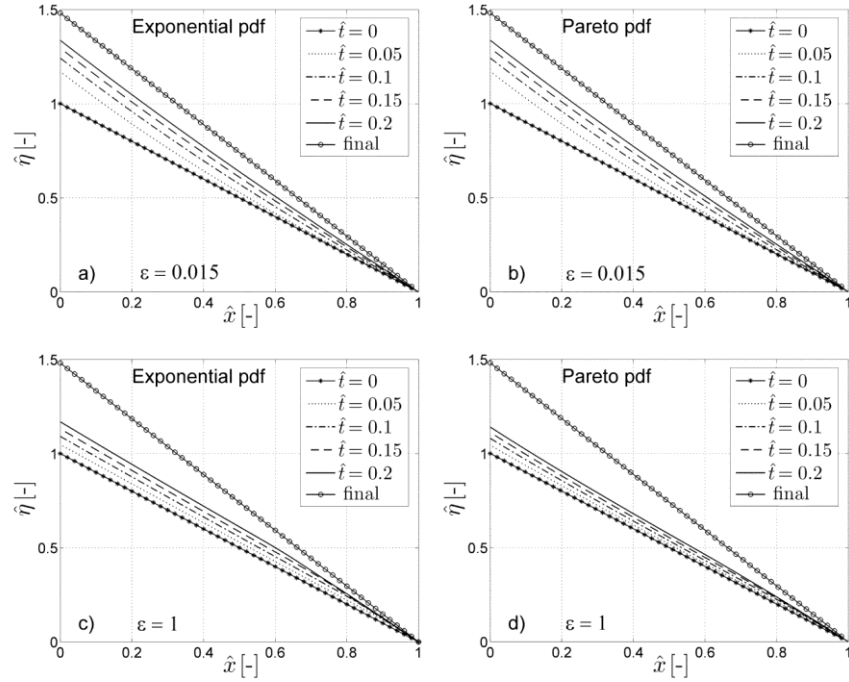


Figure 3.8 Bed profile evolution for the case $\hat{E}_f = 2$. i) $\varepsilon = 0.015$: a) Thin-tailed exponential step length PDF; b) heavy-tailed Pareto step length PDF ($\alpha = 1.5$, $r_0 = 1.5\text{m}$). ii) $\varepsilon = 1$ a) Thin-tailed exponential step length PDF; b) heavy-tailed Pareto step length PDF ($\alpha = 1.5$, $r_0 = 100\text{m}$).

The analysis shows that the shape of the tail of the step length PDF does not significantly change the results for $\varepsilon = 0.015$ but does result in some change compared to the thin-tailed case $\varepsilon = 1$. Figure 3.8 shows the long profiles resulting from both the thin-tailed and heavy-tailed case, and Figure 3.9 shows the corresponding evolution of concavity. As seen from Figure 3.9 (c) and (d) corresponding to the case of aggradation with $\varepsilon = 1$, the profiles are downward-concave for the thin-tailed PDF of step length, and upward-concave for the heavy-tailed case. The concavity in

both cases, however, is so small that the same rotational behavior for profile adjustment is seen, as documented in Figure 3.8(c) and (d).

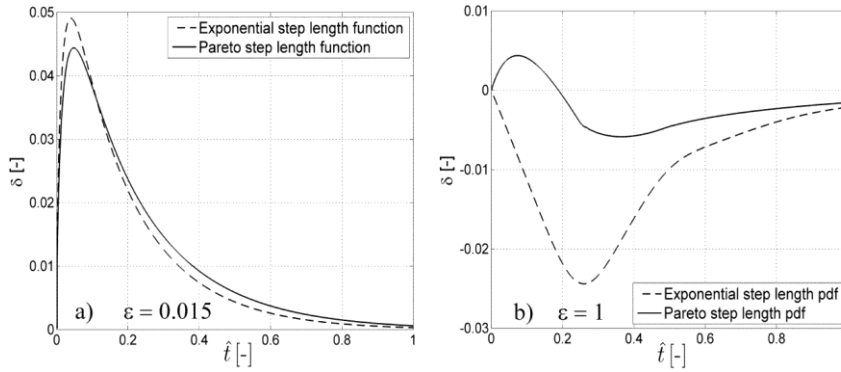


Figure 3.9 Variation in time of the concavity parameter δ for the case of the thin-tailed exponential distribution for step length, and the case of heavy-tailed Pareto distribution for step length. The parameter $\varepsilon = \bar{r}/L_d$ takes the value 0.015 in a) and 1.0 in b).

3.4 DISCUSSION AND CONCLUDING REMARKS

The main goal of the Chapter is to show how the entrainment form of the Exner equation of sediment continuity diverges from the flux form of the Exner equation when non-local behavior in particle motion arises: (i) as the mean particle step length \bar{r} increases from 0 to the order of magnitude of the domain length L_d for a thin-tailed step length PDF and (ii) as a heavy-tailed PDF for particle step length is used.

The dimensionless parameter ε is defined as the ratio between the mean step length \bar{r} and the length of the domain of interest L_d . We analyzed the effect of variation of ε on bed aggradational/degradational profiles by solving the entrainment form of the Exner equation, with the assumption of thin-tailed PDF for particle step length. As expected, the two forms collapse in the case $\varepsilon \ll 1$.

For high values of ε , however, the differences between the results from the two forms increase because of the non-locality of particle movement which is not captured by the classical flux form of the Exner equation: the transient aggradational (degradational) bed profiles tend to assume,

for ϵ greater than 0.5, a downward (upward) concave shape, rather than the upward (downward) concave shape of the flux form. When the value of ϵ is close to 0.5, an interesting behavior for both the cases of aggradation and degradation has been found: the transient profiles tend to rotate around the downstream point, keeping almost a straight shape. For value of ϵ in the range $[0,0.5)$, the concavity of the bed profiles is still upward for aggradation and downward, for degradation, but by increasing ϵ to 0.5, the concavity is nearly vanishing. . These results may serve as an explanation for relatively flat aggradational bed profiles which have been achieved in some short laboratory experiments (e.g. Muto, 2001 and Voller and Paola, 2010, Falcini et al., 2013), where the value of the ratio between mean particle step length and length of the domain of interest may not be negligible. At the laboratory scale, the mean step length becomes comparable to domain length so that the inclusion of non-local effects in the PDF of step length which this circumstance entails, should clearly be evaluated in order to properly model the bed evolution.

The analysis also investigates the effect of the heavy tailedness in the PDF of step length on bed profile. For the case studied, we show that the variation of the shape of the step length distribution from thin- to heavy-tailed does not significantly influence the results when step length is small. This is probably due to the “short” domain length compared to the tail of the power law distribution. There is a somewhat larger difference in the case when step length equals domain length, but the bed elevation profiles are nearly linear for both thin-tailed and heavy-tailed PDF. Voller and Paola (2010) introduced heavy-tailed behavior to explain profiles that evolve with concavity that is small compared to the standard flux case of Equation (3.1). Here we find that a heavy-tailed behavior is not necessary to obtain this result.

Long step lengths of bedload particles in the field may result from any bed pattern that induces preferential paths for transport, including grain size mixtures (Ganti et al, 2010), bedforms, scour and fill, and intermittent bedrock exposure (Stark et al, 2009). Thus our results may be applicable to these cases. The case of sediment suspension can also be represented in entrainment form (e.g. Parker, 2004). This case is generally associated with much longer mean path lengths than the case of bedload. As a result, the suspension-dominated case may show much more non-local behavior than the bedload case. This case deserves further investigation.

4 ON ADVECTION AND DIFFUSION OF RIVER PEBBLE TRACERS

The erosion, transport and deposition of pebbles in rivers have often been studied by considering the motion of tracer particles. Such studies have been staple components of field research (e.g. Ferguson and Hoey, 2002; Hassan et al., 2013) as well as experimental investigations (e.g. Wong et al., 2007; Martin et al., 2012). The existing knowledge and research intuition suggest that tracer particles motion could be considered as an advective-diffusive phenomenon (Nikora et al., 2002). While migrating downstream the particles tend to slowdown because of several circumstances (e.g. reallocation in more stable locations, such as deeper layers in the bed) and to diffuse with different regimes, depending on the observed spatial and temporal scale.

4.1 STREAMWISE ADVECTION SLOWDOWN OF TRACERS

The short-term behavior of tracers seeded on the surface differs from the longer-term behavior of tracers that have undergone vertical mixing, local spatial redistribution, and larger-scale advection.

For instance, in rivers with bar-pool-riffle morphology there may be a tendency for tracers to be reallocated into more stable locations (e.g. riffles and bars), and in some cases into long-term storage in abandoned channels, inactive bars, or even the floodplain. This leads to a long-term reduction in mobility. Then, advection of tracers for substantial distances along a river whose character alters downstream can (i) alter the size of a tracer relative to the bed it is traveling over, or (ii) expose it to systematically different hydraulic conditions. In particular, tracers traveling along a river with strong downstream fining toward a local base level will become relatively coarser and less mobile. Finally, there may be vertical mixing, that results in progressive burial of tracers at a range of depths. Buried tracers move less often than those on the surface (the probability of entrainment decreases with depth, as shown in Section

2.1), so there is again a reduction in overall long-term mobility (Ferguson and Hoey, 2002).

The first quantitative evidence of the amount of tracer slowdown through the combined effects of these processes was presented by Ferguson et al. (2002) who compared the short- and long-term movement of 1220 magnetic tracer pebbles seeded in 1991 at six sites along a 2.5-km-long reach of Allt Dubhaig, a small gravel bed river in Scotland, UK.

Ferguson et al. (2002) compared movement to 1999, after more than 100 competent flow events, with results from the first two years of the experiment (1991–1993; ~ 30 floods). In Figure 4.1, the observed percentage of slowdown for the six different sites is shown with the simulated slowdown by two different models, suggested by Ferguson and Hoey (2002).

The models consider the tracer-pebble slowdown (i) through only advection of any given size D_i from a relatively coarse upstream site to a finer downstream site where tracers have higher relative grain size and so less mobility and (ii) through advection and vertical mixing, which entails reaching portion of the bed with less chance of entrainment in bedload.

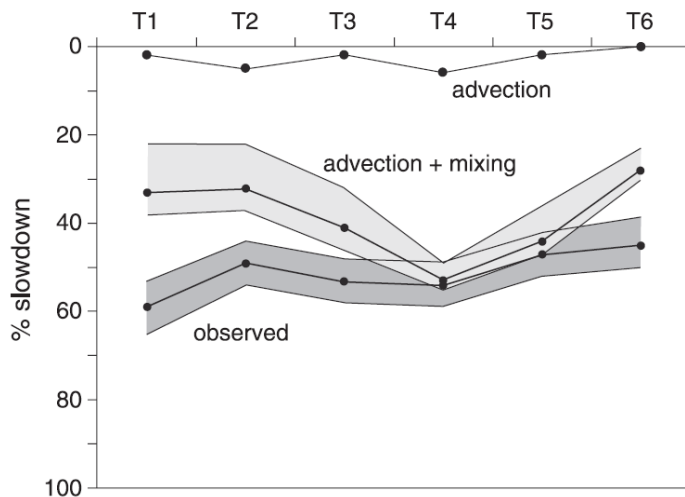


Figure 4.1 Observed and simulated slowdown of recovered tracers (with relative errors bands) – from Ferguson and Hoey (2002)

4.2 PARTICLES DIFFUSION

Mathematically, diffusion processes are described by the scaling growth in time, t [T], of the central moments of the coordinates of a patch of particles. More, specifically, to describe such processes, it is often considered the growth in time of the spatial standard deviation σ [L]:

$$\sigma \propto t^{\chi/2} \quad (4.1)$$

In case of normal (Fickian) diffusion, we have χ equal to unity, while diffusion with $\chi \neq 1$ is known as anomalous diffusion, which can be (i) ballistic diffusion, when $\chi = 2$, (ii) superdiffusion, when $\chi > 1$ and (iii) subdiffusion, when $\chi < 1$.

It is important to note that the diffusion exponents directly relate to parameters of probability distributions of particle motion characteristics such as step length and/or rest periods (as clarified in the following Chapter). For now, what we want to point out is that there may potentially be several diffusion regimes in bed particle motion (Nikora et al, 2002).

In particular, Nikora et al. (2002) provided an useful conceptual framework for understanding different scaling regimes in bed load particle diffusion, suggesting that the character of sediment diffusion may change with time scale (Figure 4.2). Considering saltating particles, they firstly identified three ranges of spatial and temporal scales: (i) local range, which corresponds to ballistic particle trajectories between two successive collisions with the bed; (ii) intermediate range, which corresponds to particle trajectories between two successive rests and it may consist of many local trajectories; (iii) global range, which corresponds to particle trajectories consisting of many intermediate trajectories. Then, in their conceptual model, they hypothesized ballistic diffusion at short time scales (local regime), caused by correlated particle motions arising from particle inertia, and subdiffusion at long time scales (global regime) resulted from periods of particle immobility. Over medium time scales (intermediate regime), they suggested that the character of diffusion may depend on system properties. For instance, at this scale the bed topography and near-bed turbulence may have opposite effects on bed particle diffusion. A “fractal” bed may slow down diffusion processes ($\chi < 1$), while turbulence may enhance them ($\chi > 1$) or they can mutually cancel their effects ($\chi = 1$).

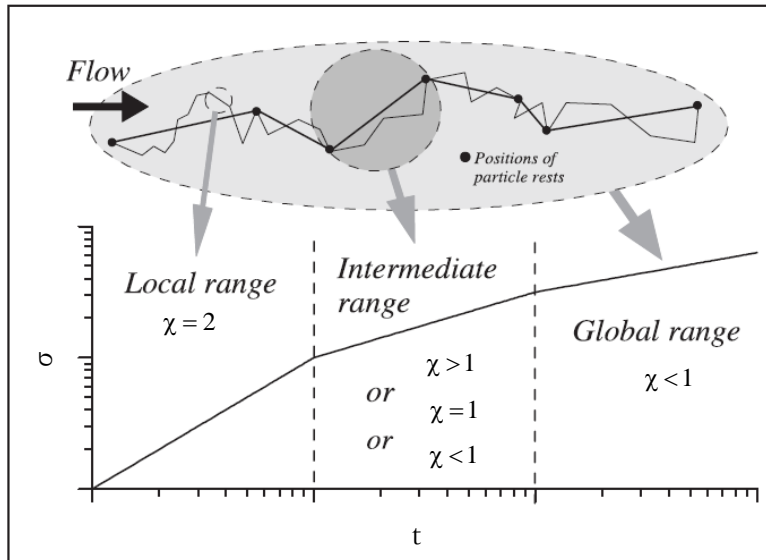


Figure 4.2 Conceptual representation of a particle trajectory consisting of three distinct ranges of scale: (i) local; (ii) intermediate; (iii) global. Nikora et al. hypothesized ballistic diffusion regime for the local range, normal or anomalous diffusion regime for the intermediate range and subdiffusion regime for the global range – from Nikora et al. (2002)

5 EXNER BASED MASTER EQUATION FOR TRANSPORT AND DISPERSION OF RIVER PEBBLE TRACERS. PART 1. DERIVATION, ASYMPTOTIC FORMS, AND QUANTIFICATION OF NONLOCAL VERTICAL DISPERSION

Ideas deriving from the standard formulation for Continuous Time Random Walk (CTRW) based on the Montroll-Weiss Master Equation (ME), have been recently applied to transport and diffusion of river tracer pebbles. CTRW, accompanied by appropriate probability distribution functions (PDFs) for walker step length and waiting time, yields asymptotically the standard advection-diffusion equation (ADE) for thin-tailed PDFs, and the fractional advection-diffusion equation (fADE) for heavy-tailed PDFs, the latter allowing the possibilities of subdiffusion or superdiffusion. Here we show that the CTRW Master Equation is inappropriate for river pebbles moving as bed material load: a deposited particle raises local bed elevation and an entrained particle lowers it, so that particles interact with the “lattice” of the sediment-water interface. Here we use the Parker-Paola-Leclair (PPL) framework, which captures the Exner equation of sediment conservation, to develop a new ME for tracer transport and dispersion for alluvial morphodynamics. The formulation is based on the existence of a mean bed elevation averaged over fluctuation, which precludes the possibility of streamwise subdiffusion mediated by a waiting time PDF with no mean. The new ME yields asymptotic forms for ADE and fADE that differ significantly from CTRW. It allows a) vertical dispersion, as well as streamwise advection-diffusion, and b) mean waiting time to vary in the vertical. Vertical dispersion is nonlocal, but cannot be expressed with fractional derivatives. In order to illustrate the new model, we apply it to the restricted case of vertical dispersion only, with both thin and heavy

tails for relevant PDFs. Vertical dispersion show subdiffusive behavior, as quantified by the time variation of the vertical variance of tracer distribution.

The current Chapter is a version of a manuscript that is ready to submit for publication in a refereed journal: “Exner Based Master Equation for transport and dispersion of river pebble tracers. Part 1. Derivation, asymptotic forms, and quantification of nonlocal vertical dispersion.”

5.1 INTRODUCTION

The theoretical basis for the study of the dispersal of sediment tracer particles was delineated by Einstein (1950), who formulated the problem in terms of a standard 1D random walk in which each particle moves in a series of steps punctuated by waiting times (see also Nakagawa and Tsujimoto, 1976; Tsujimoto, 1978). More specifically, each particle moves a step of length r [L] after waiting time τ [T], the statistics of which govern tracer particle dispersal.

Let $p_s(r)$ [L^{-1}] and $p_w(\tau)$ [T^{-1}] denote the probability distribution functions (PDFs) of step length and waiting time. When both these PDFs have thin tails, such that $p_s(r)$ decays exponentially as $r \rightarrow \infty$ and $p_w(\tau)$ decays exponentially as $\tau \rightarrow \infty$, the formulation can be reduced asymptotically to a standard advection-diffusion equation (ADE), according to which the streamwise spatial standard deviation σ [L] of a patch of tracer particles increases with the square root of time t [T], i.e. as $t^{1/2}$.

Subsequent to Einstein’s original work on tracers, the study of random walks has been extended to the case of continuous time random walks (CTRW; Montroll and Weiss, 1965). This more general formulation, which derives from a Master Equation (ME) governing the statistics of a walker, leads to a much richer range of behaviors. More specifically, the CTRW formulation allows exploration of the consequences of heavy-tailed PDFs for $p_s(r)$ or $p_w(\tau)$, i.e. PDFs that decay in r or τ according to a power law rather than exponentially. In such cases, moments above some value fail to exist. The asymptotic consequence of such a formulation is a fractional advection-diffusion equation (fADE) allowing for the possibility of anomalous diffusion, such that $\sigma \sim t^{\chi/2}$, where χ [1] can deviate from unity. The case encompassing anomalously long step length r corresponding to heavy-tailed $p_s(r)$ gives rise to superdiffusion,

for which $\chi > 1$, and the encompassing anomalously long waiting time τ corresponding to heavy-tailed $p_w(\tau)$ gives rise to subdiffusion, for which $\chi < 1$ (e.g. Schumer et al., 2009). Various combinations of heavy-tailed jump length and waiting time distributions can lead to non-intuitive ballistic, super-diffusive, or sub-diffusive behavior, particularly in the case of asymmetric random walks (Weeks et al, 1996).

In recent years, the concepts of CTRW and fADE have filtered into the study of tracer sediment transport in rivers, as well as the study of particle tracer transport in the more general context of Earth surface processes (e.g. Nikora et al., 2002; Schumer et al., 2009; Furbish et al., 2009; Bradley et al., 2010; Ganti et al., 2010; Furbish et al., 2012; Martin et al., 2012; Zhang et al., 2012). To provide context for these applications, we here summarize some results of Schumer et al. (2009) pertaining to Montroll-Weiss CTRW. The standard random walk model with thin-tailed functions for $p_s(r)$ and $p_w(\tau)$ applied in the context of CTRW gives rise to ADE, i.e.

$$\frac{\partial f_a}{\partial t} + c \frac{\partial f_a}{\partial x} = D_d \frac{\partial^2 f_a}{\partial x^2} \quad (5.1)$$

In the above equation x [L] denotes the streamwise coordinate, t [T] denotes time, $f_a(x,t)$ [1] denotes the fraction of particles within some reservoir layer near the bed surface (active layer; see Ganti et al., 2010) that are tracers at (x, t) , c [LT^{-1}] denotes a particle advection velocity and D_d [L^2T^{-1}] denotes a particle diffusivity (or more properly, dispersivity). When $p_s(r)$ is heavy-tailed such that it has a mean but no standard deviation, i.e.

$$p_s(r) \sim r^{-\alpha} \quad , \quad 1 < \alpha < 2 \quad (5.2a,b)$$

or $p_w(\tau)$ is heavy-tailed such that it has no mean, i.e.

$$p_w(\tau) \sim \tau^{-\gamma} \quad , \quad 0 < \gamma < 1 \quad (5.3a,b)$$

the relation governing tracer particle dispersal obtained from the ME of CTRW is no longer (5.1), but rather the more general fADE formulation;

$$\frac{\partial^\gamma f_a}{\partial t^\gamma} + c \frac{\partial f_a}{\partial x} = D_d \frac{\partial^\alpha f_a}{\partial x^\alpha} \quad (5.4)$$

Strictly speaking, in the above equations c is no longer an advection velocity and D_d is no longer a diffusivity, because the respective dimensions are $LT^{-\gamma}$ and $L^2T^{-\gamma}$, but they can be treated as such in a general sense. It can be found from (5.4) that the growth rate of the streamwise standard deviation σ of a patch of tracers now obeys the relation

$$\sigma \sim t^{\frac{\gamma}{\alpha}} \quad (5.5)$$

The case of standard ADE is captured by the choices $\gamma = 1$ and $\alpha = 2$. In the anomalous formulation, the derivatives are fractional; the choices $\gamma = 1$ and $\alpha < 2$ lead to superdiffusion, and the choices $\gamma < 1$ and $\alpha = 2$ lead to subdiffusion.

Superdiffusive behavior of particle tracer dispersion might be generated by mechanisms which allow for some particles to travel very long distances in a single step. One example of such a mechanism is that of preferential connected lanes of transport (Parker, 2008); Ganti et al. (2010) present another example associated with step length variation in grain size mixtures. Subdiffusion might be generated by burial of particles in zones where re-exhumation is unlikely (e.g. Voepel et al., 2013); Stark et al. (2009) have considered related problem in which long residence time of alluvium inhibits bedrock incision. Both these behaviors can be studied directly by analyzing data for dispersal patterns, without invoking either the framework of CTRW or a governing Master Equation (e.g. Nikora et al., 2002; Bradley et al., 2010; Martin et al., 2012).

The above notwithstanding, a deeper understanding of tracer particle dispersion in the context of CTRW requires the delineation of an ME suitable to the problem. To date, there have been two notable attempts to do so for the case of sediment transport in rivers, i.e. those of Ganti et al. (2010) and Furbish et al. (2012). Both of these expositions helped motivate the research presented here. This notwithstanding, neither include a) the concept of waiting time and b) the degree of freedom associated with particle deposition and entrainment from an arbitrary bed elevation. Here we tackle the problem of delineating a generalized ME for the case of bedload transport in rivers. Our model, the Exner-based Master Equation (EBME) encompasses both thin-and heavy-tailed step length and waiting time behavior. More importantly, it considers the

entrainment and deposition of particles on an elevation-specific basis, a key feature needed to describe the exchange of particles in the vertical direction as they disperse downstream. This feature is needed to describe the advective slowdown of tracer particles described by Ferguson and Hoey (2002) as particles are buried ever more deeply.

5.2 MASTER EQUATION FOR THE STANDARD CTRW MODEL

As noted above, fADE was originally derived in terms of a specific ME governing CTRW. This Master Equation, while of historical value in the development of CTRW, is inappropriate for the description of bedload tracer particle dispersion in rivers. In order to illustrate this, it is useful to briefly review the formulation. In the process of doing so, we introduce the tools necessary to develop our Exner-based Master Equation (EBME). The analysis presented here mostly follows that of Schumer et al. (2009); standard results from fractional calculus are used without specific citation.

In the standard 1D CTRW formulation (Montroll and Weiss, 1965; Klafter and Sibley, 1980; Klafter et al., 1987) the ME takes the following form: where $\rho(x,t)$ [L^{-1}] denotes the probability density that a particle is at x at time t ,

$$\rho(x,t) = \int_0^t \int_0^\infty \rho(r,\tau) p_s(x-r) p_w(t-\tau) dr d\tau + \left[1 - \int_0^t p_w(\tau) d\tau \right] \delta(x) \quad (5.6)$$

In fact (5.6) involves two simplifications of Klafter et al. (1987); a) step length and waiting time are taken to be uncoupled processes, and b) particles are assumed to move only downstream, so that $p_s(r)$ vanishes for $r < 0$. The above equation is nonlocal in so far as the kernel in the convolution integral is not concentrated at a single point (Du et al., 2012). Here we distinguish between two kinds of nonlocality; simple nonlocality associated with a thin-tailed form for p_s or p_w , and asymptotic nonlocality associated with the corresponding heavy-tailed form. At $t = 0$, (5.6) reduces to

$$\rho(x,0) = \delta(x) \quad (5.7)$$

so that a particle originates from the origin.

Laplace transforms in time and Fourier transforms in space are used to reduce (5.6) and (5.7). Where $A(t)$ is any function of time and $B(x)$ is any function of space, their Laplace and Fourier transforms are given respectively as

$$\tilde{A}(s) = \int_0^{\infty} A(t)e^{-st} dt \quad , \quad \hat{B}(k) = \int_{-\infty}^{\infty} B(x)e^{-ikx} dx \quad (5.8a,b)$$

Applying (5.8b) to (5.7) yields

$$\hat{\rho}(k, 0) = 1 \quad (5.9)$$

Applying (5.8a,b) to (5.6) yields,

$$\tilde{\hat{\rho}}(k, s) = \frac{1 - \tilde{p}_w}{s} \frac{1}{1 - \hat{p}_s \tilde{p}_w} \quad (5.10)$$

corresponding to (21) of Klafter et al. (1987) and (30) of Schumer et al. (2009).

The case of thin tails is considered first. Taylor expansions of $\hat{p}_s(k)$ to second order and $\tilde{p}_s(s)$ to first order give

$$\hat{p}_s(k) \cong 1 - ik\bar{r} + \frac{1}{2}(ik)^2\mu_2 + \dots \quad , \quad \tilde{p}_w(s) = 1 - \bar{\tau}s + \dots \quad (5.11a,b)$$

where \bar{r} [L] and $\bar{\tau}$ [T] denote mean step length and waiting time, and μ_2 [L²] is the second moment of p_s ;

$$\bar{r} = \int_0^{\infty} rp_s(r)dr \quad , \quad \mu_2 = \int_0^{\infty} r^2p_s(r)dr \quad (5.12a,b)$$

$$\bar{\tau} = \int_0^{\infty} \tau p_w(\tau)d\tau \quad (5.12c)$$

Substituting (5.11) into (5.10), using the following properties of Fourier and Laplace transforms,

$$\frac{dA}{dt} = s\tilde{A} - A(0) \quad , \quad \frac{d^n B}{dx^n} = (ik)^n \hat{B} \quad (5.13a,b)$$

reducing with (5.9) and truncating the expansions yields the formulation:

$$\frac{\partial \rho}{\partial t} + c \frac{\partial \rho}{\partial x} = D_d \frac{\partial^2 \rho}{\partial x^2} + \bar{r} \frac{\partial^2 \rho}{\partial x \partial t} \quad , \quad c = \frac{\bar{r}}{\bar{\tau}} \quad , \quad D_d = \frac{\mu_2}{2\bar{\tau}} \quad (5.14a,b,c)$$

Writing $\bar{r} = c\bar{\tau}$ and assuming that c and D_d remain finite in the limit as $\bar{\tau} \rightarrow 0$ allows the cross-derivative in x and t to be dropped. so resulting in the ADE formulation. In work below, the cross-derivatives are retained for consistency, and to allow for the case of large mean waiting time.

For the case of heavy tails, we now replace (5.11a,b) with the forms (resulting from fractional Taylor expansion)

$$\hat{p}_s(\mathbf{k}) \cong 1 - i\mathbf{k}\bar{r} + c_\alpha (i\mathbf{k})^\alpha \quad , \quad \tilde{p}_w(s) = 1 - c_\gamma s^\gamma + \dots \quad (5.15a,b)$$

where $0 < \gamma < 1$ (subdiffusive waiting time) and $1 < \alpha < 2$ (superdiffusive step length). Substituting (5.15) into (5.10), using the following properties of fractional Fourier and Laplace transforms,

$$\frac{dA^\gamma}{dt} = s^\gamma \tilde{A} - A(0) \quad , \quad \frac{d^\alpha B}{dx^\alpha} = (i\mathbf{k})^\alpha \hat{B} \quad (5.16a,b)$$

reducing with (5.9) and truncating the expansions yields the formulation:

$$\frac{\partial^\gamma \rho}{\partial t^\gamma} + c \frac{\partial \rho}{\partial x} = \bar{r} \frac{\partial}{\partial x} \frac{\partial^\gamma \rho}{\partial t^\gamma} + D_d \frac{\partial^\alpha \rho}{\partial x^\alpha} \quad , \quad c = \frac{\bar{r}}{c_\gamma} \quad , \quad D_d = \frac{c_\alpha}{c_\gamma} \quad (5.17a,b,c)$$

Dropping the cross-derivate in x and t yields the fADE formulation. Equations (5.14) and (5.17) might be applied to the case of bedload tracers by assuming that a) bedload particles exchange only with an “active layer” of bed material at the surface of thickness L_a [L] (Parker, 2008; Ganti et al., 2010), and b) the bed undergoes no aggradation or degradation, i.e. change in mean bed elevation η (averaged over an appropriate window). Let N_{tr} [1] denote the total number of tracer particles released, λ_p [1] denote the porosity of the bed, V_p [L³] denote particle volume and B [L] denote the width of the channel. The fraction of grains $f_a(x,t)$ [1] that are tracers at (x,t) is then given as

$$f_a = \frac{N_{tr} V_p}{L_a B (1 - \lambda_p)} \rho(x,t) \quad (5.18)$$

5.3 PROBLEMS ASSOCIATED WITH APPLICATION OF THE CRTW ME TO BEDLOAD TRACERS

CRTW was originally derived as the continuous limit for a random walker on a lattice. The lattice simply defines streamwise locations where the particle might come to rest or pass through. The particle does not interact with the lattice.

Bedload transport in a river functions differently. Sediment transport can be divided into two components. Bed material load interacts with the bed by changing its elevation as each grain deposits or erodes. Wash load or throughput load either a) passes through the reach of interest without changing bed elevation, or b) exchanges between the water column and the bed only via the pores of the bed material, again without changing bed elevation. Here we consider the case of bedload moving as bed material load.

In the case of bedload, the lattice has vertical as well as streamwise location, and its structure interacts strongly with the particles. A previously moving particle that comes to rest (deposits) raises the bed, and a previously resting particle that moves (is entrained) lowers the bed. Since bedload transport itself is a random process, the lattice structure through which particles move, and in particular bed elevation at a lattice point, also becomes a random variable. The ME of CTRW is incapable of handling this interaction.

The starting point for the Exner-based Master Equation (EBME) is the analysis of Parker et al. (2000), here referred to as the Parker-Paola-Leclair (PPL) framework. This framework provides a statistically-based equation of sediment conservation that captures the vertical structure of bed elevation variation as particles erode and deposit. Integral of this equation in the vertical yields the standard Exner equation of sediment mass conservation. As opposed to the formulation in Ganti et al. (2010), the formulation of Parker et al. (2000) does not invoke the simplification of an active layer.

5.4 PPL FRAMEWORK FOR EXNER EQUATION OF SEDIMENT CONTINUITY: SOME MORE COMMENTS

Here we apply (2.3) in the context of bedload transport of particles with uniform size D_p [L] and material density.

The formulation of (2.3) is predicated on the assumption that bed elevation, while fluctuating locally as particles are entrained or deposited, does indeed have a mean value η (averaged over an appropriate window). And in order for this mean value to exist, waiting time must also have a mean value, so precluding the possibility of subdiffusion. This can be illustrated as follows.

For simplicity, the particles are assumed to be arranged in a rectangular lattice, so that the removal or deposition of one particle of diameter D_p results in a precise change in vertical elevation of D_p . This corresponds to a bed porosity λ_p of $1 - \pi/4$. Other configurations can be considered by including an order-one multiplicative factor. The mean waiting time τ_{mean} [T] (averaged over all possible positions of a particle, as illustrated below) for a particle to be entrained can be used to define the frequency J [T⁻¹] of entrainment:

$$J(x, t) = \frac{1}{\tau_{\text{mean}}} \quad (5.19)$$

This mean waiting time may slowly vary of time, in so far as it correlates with mean flow parameters. The entrainment rate of sediment volume is then given as:

$$E(x, t) = (1 - \lambda_p) D_p J(x, t) \quad (5.20)$$

The deposition rate D can in turn be related to the entrainment rate, E as shown in equation (2.4) so

From equation (5.20) and (2.4), the deposition rate takes the form:

$$D(x, t) = (1 - \lambda_p) D_p \int_0^{\infty} J(x - r, t) p_s(r) dr \quad (5.21)$$

Combining (2.3), (5.20) and (5.21) yields the integral form of the Exner equation:

$$\frac{\partial \eta(x, t)}{\partial t} = -D_p J(x, t) + D_p \int_0^{\infty} J(x - r, t) p_s(r) dr \quad (5.22)$$

Pelosi and Parker (2013) have studied the behavior of (5.22) in the context of the ratio of mean step length \bar{r} to the length of the reach

under consideration. They considered both thin-tailed and heavy-tailed PDFs p_s for step length.

When extended to the case of tracer particles in uniform sediment or to mixtures of grain sizes, the equation (5.22) is usually implemented in the context of an active layer of thickness L_a , as described above (Parker, 2008; Ganti et al., 2010; Section 2.1). Thus, the erodible bed is ideally divided into layers: (i) an upper layer (active layer), which has no vertical structure and actively exchanges with the bedload and (ii) a deeper layer (substrate), that exchanges with the bedload only when aggradation or degradation, occurs (e.g. Viparelli et al., 2011).

Parker et al. (2000), however, specified a general probabilistic formulation of the Exner equation of sediment continuity with no discrete layers. It is able to capture vertical exchange of sediment particles, and specifically tracer particles, with no need of the relatively heavy-handed assumption of an active layer. Here we refer to this framework as PPL (Parker-Paola-Leclair) and as deeply shown in Section 2.1, we have the following formulation:

$$\frac{\partial P_e}{\partial t} + p_e \frac{\partial \eta}{\partial t} = -D_p J(x, t) p_I(y) + p_I(y) D_p \int_0^\infty J(x-r, t) p_s(r) dr \quad (5.23)$$

5.5 EXNER-BASED MASTER EQUATIONS FOR RIVERS CARRYING BEDLOAD

Equation (5.23) is, in and of itself, a fairly trivial extension of the Exner formulation. Its true value becomes apparent when applied to bedload tracers. The PPL framework is now applied to this case.

Let $f(x, y, t)$ [L^{-1}] denote the fraction density of tracers at elevation y , such that $f dy$ defines the fraction of bed particles that are tracers between elevations y and $y + dy$. The same formulation that yields (5.23) gives the following result for tracer conservation:

$$P_e \left(\frac{\partial f}{\partial t} - \frac{\partial f}{\partial y} \frac{\partial \eta}{\partial t} \right) + f \left(\frac{\partial P_e}{\partial t} + p_e \frac{\partial \eta}{\partial t} \right) = -p_I(y) D_p J(x, t) f(x, y, t) + p_I(y) D_p \int_{-\infty}^\infty \int_0^\infty J(x-r, t) f(x-r, y', t) p_I(y') p_s(r) dr dy' \quad (5.24)$$

Equation (5.24) defines the first of two Exner-based Master Equations (EBME) for the tracer problem obtained from the PPL framework.

Note that this formulation is nonlocal in x and y (Du et al., 2012). According to the above relation, a tracer particle may be entrained from any level y' and deposited at a different level y . The model thus incorporates vertical exchange of tracers, a feature that is captured neither in the ME of CTRW or the active layer formulation of the Exner equation. In addition, tracers are conserved as the bed aggrades and degrades, allowing burial and exhumation to be driven not only by random processes inherent in the density $p_j(y)$, but also through mean bed elevation variation.

Equation (5.24) contains the assumption that particle entrainment is determined as a local function of time, without considering the possibility of a waiting time. As a result, it is referred to below as EBME-N, i.e. Exner-based Master Equation with No waiting. The generalization to include waiting time is, however, straightforward. Let $p_w(\tau|y)$ [T^{-1}] denote the elevation-specific probability density of waiting time, i.e. the conditional PDF of waiting time at elevation y . The mean waiting time $\bar{\tau}(y)$ [T] at any elevation y is given as

$$\bar{\tau}(y) = \int_0^{\infty} \tau p_w(\tau|y) d\tau \quad (5.25)$$

The jump-weighted average waiting time τ_{mean} is given as

$$\tau_{\text{mean}} = \langle \bar{\tau} \rangle \quad (5.26)$$

where the brackets define “jump averaging” such that for any parameter $G(y)$,

$$\langle G \rangle = \int_{-\infty}^{\infty} G(y) p_j(y) dy \quad (5.27)$$

The parameter τ_{mean} specifically defines jump frequency in (5.19), again underlining the condition that the assumption of a mean bed elevation precludes the possibility of waiting time PDFs with no mean.

The direct extension of (5.24) to include waiting time is

$$\begin{aligned}
& P_e \left(\frac{\partial f}{\partial t} - \frac{\partial f}{\partial y} \frac{\partial \eta}{\partial t} \right) + f \left(\frac{\partial P_e}{\partial t} + P_e \frac{\partial \eta}{\partial t} \right) = \\
& -D_p p_J(y) \int_0^\infty J(x, t - \tau) f(x, y, t - \tau) p_w(\tau | y) d\tau + \\
& + D_p p_J(y) \int_{-\infty}^\infty \int_0^\infty J(x - r, t - \tau) f(x - r, y', t - \tau) p_J(y') p_w(\tau | y') p_s(r) dy' d\tau dr
\end{aligned} \tag{5.28}$$

The above formulation is referred to below as EBME-W, i.e. Exner-based Master Equation with Waiting based on the PPL framework.

For the sake of comparison, it is useful to delineate Master Equation associated with the active layer formulation used in Ganti et al. (2010). The general form is given in Parker et al. (2000): where f_1 [1] denotes the fraction of tracers in the bed material that is exchanged between the active layer and substrate as the bed aggrades or degrades,

$$\begin{aligned}
& f_1 \frac{\partial \eta(x, t)}{\partial t} + L_a \frac{\partial f_a(x, t)}{\partial t} = -D_p J(x, t) f_a(x, t) + \\
& + D_p \int_0^\infty J(x - r, t) f_a(x, t) p_s(r) dr
\end{aligned} \tag{5.29}$$

We refer to the above relation as EBME-A (Exner-based Master Equation, Active layer formulation) below.

5.6 VERTICAL AND STREAMWISE DISPERSAL OF TRACERS WITHIN AN EQUILIBRIUM BED

The physical contents of the above three formulations are best grasped in the context of macroscopic equilibrium conditions, for which the bed neither aggrades nor degrades. For this case,

$\partial P_e / \partial t = \partial \eta / \partial t = 0$, and the parameters J , $p_J(y)$, $p_s(r)$ and $p_w(\tau | y)$ are assumed to change neither in x nor in t . The respective forms for EBME-N, EBME-W and EBME-A are shown below in order of complexity. From (5.29), EBME-A becomes;

$$L_a \frac{\partial f_a(x, t)}{\partial t} = -D_p J f_a(x, t) + D_p J \int_0^\infty f_a(x - r, t) p_s(r) dr \tag{5.30}$$

From (5.24), EBME-N becomes;

$$\begin{aligned}
 P_c(y) \frac{\partial f(x, y, t)}{\partial t} &= -D_p J f(x, y, t) p_J(y) + \\
 &+ D_p J p_J(y) \int_{-\infty}^{\infty} \int_0^{\infty} f(x-r, y', t) p_J(y') p_S(r) dy' dr
 \end{aligned} \tag{5.31}$$

From (5.28), EBME-W becomes;

$$\begin{aligned}
 P_c(y) \frac{\partial f(x, y, t)}{\partial t} &= -D_p J p_J(y) \int_0^{\infty} f(x, y, t-\tau) p_W(\tau | y) d\tau + \\
 &+ D_p J p_J(y) \int_{-\infty}^{\infty} \int_0^{\infty} \int_0^{\infty} f(x-r, y', t-\tau) p_J(y') p_W(\tau | y') p_S(r) dy' d\tau dr
 \end{aligned} \tag{5.32}$$

The difference between the EBME-N and EBME-A formulations is best illustrated by writing (5.31) and (5.32) in forms that are as close as possible to (5.30), and then correcting with residual terms. In this way, (5.31) can be expressed as

$$\begin{aligned}
 P_c(y) \frac{\partial f(x, y, t)}{\partial t} &= -D_c J f(x, y, t) p_J(y) + D_c J p_J(y) \int_0^{\infty} f(x-r, y, t) p_S(r) dr \\
 &- D_c J p_J(y) \int_{-\infty}^{\infty} \int_0^{\infty} \varphi(x-r, y', t) p_J(y') p_S(r) dy' dr
 \end{aligned} \tag{5.33a}$$

where

$$\varphi(x, y, t) = f(x, y, t) - \langle f \rangle, \quad \langle f \rangle = \int_{-\infty}^{\infty} f(x, y, t) p_J(y) dy \tag{5.33b}$$

Here $\langle f \rangle$ denotes the jump-averaged value of f , and φ is a deviatoric tracer fraction density. A comparison of (5.30) and (5.33a) reveals that (5.33a) captures a nonlocal feature that (5.30) cannot, i.e. the vertical dispersal of tracers. That is, the term $\partial f / \partial t$ is driven by (among other things) the difference $\varphi = f - \langle f \rangle$ between local tracer fraction and jump-averaged fraction. The minus sign in front of the terms containing the deviatoric term φ in (5.32) ensure that particles disperse in the vertical from zones that are higher than the jump-averaged mean to those that are lower than it. This dispersion is nonlocal and therefore non-Fickian. The corresponding form for EBME-W (5.32) that isolates the vertical dispersion terms is given below;

$$\begin{aligned}
P_e(y) \frac{\partial f(x, y, t)}{\partial t} = & -D_p J p_J(y) \int_0^\infty f(x, y, t - \tau) p_w(\tau | y) d\tau + \\
& + D_p J p_J(y) \int_0^\infty \int_0^\infty f(x - r, y, t - \tau) p_w(\tau | y) p_s(r) d\tau dr \quad (5.34a) \\
& - D_p J p_J(y) \int_{-\infty}^\infty \int_0^\infty \int_0^\infty \varphi_w(x - r, y', t) p_J(y') p_w(\tau | y') p_s(r) dy' d\tau dr
\end{aligned}$$

where

$$\varphi_w = \overline{f p_w} - \langle \overline{f p_w} \rangle, \quad \langle \overline{f p_w} \rangle = \int_{-\infty}^\infty f(x, y, t) p_w(\tau | y) p_J(y) dy \quad (5.34b,c)$$

Here it is seen that the deviatoric term φ_w that drives vertical dispersion specifically involves the vertical variation of the PDF of waiting time. Equation (5.33a) is recovered from (5.34a) by assuming that $p_w = \delta(\tau)$.

5.7 ASYMPTOTIC FRACTIONAL FORMULATIONS

The convolution forms of EBME-A, EBME-N and EBME-W are all easy to solve numerically in a straightforward way. Their corresponding asymptotic fractional forms, however, are not easily solved numerically. This notwithstanding, the relevant forms are presented here for the purpose of illustration and comparison with the CTRW ME formulation. The results given below follow from the analysis given in Section 5.2 with one exception: the case $0 < \gamma < 1$, which is associated with waiting times with no mean, and which gives rise to subdiffusion, is omitted, in so far that EBME is predicated upon the existence of a finite value of τ_{mean} .

EBME-A yields the following asymptotic result for the thin- and heavy-tailed cases, respectively, based on the spatial Fourier transform (5.8b) and the expansions (5.11a) or (5.15a) for p_s . The thin-tailed, or ADE form is

$$\frac{\partial f}{\partial t} + c \frac{\partial f}{\partial x} = D_d \frac{\partial^2 f}{\partial x^2}, \quad c = \frac{D_p J \bar{\Gamma}}{L_a}, \quad D_d = \frac{1}{2} \frac{D_c J \mu_2}{L_a} \quad (5.35)$$

and the heavy-tailed, or fADE form is

$$\frac{\partial f}{\partial t} + c \frac{\partial f}{\partial x} = D_d \frac{\partial^\alpha f}{\partial x^\alpha}, \quad c = \frac{D_p J \bar{r}}{L_a}, \quad D_d = \frac{1}{2} \frac{D_c J c_\alpha}{L_a} \quad (5.36a,b,c)$$

The above relations correspond to the results of Ganti et al. (2010). Similarly reducing EBME-N yields the thin-tailed form

$$\begin{aligned} \frac{\partial f}{\partial t} &= -c(y) \frac{\partial f}{\partial x} + D_d(y) \frac{\partial^2 f}{\partial x^2} \\ &- K(f - \langle f \rangle) + c(y) \frac{\partial (f - \langle f \rangle)}{\partial x} - D_d(y) \frac{\partial^2 (f - \langle f \rangle)}{\partial x^2} \\ c(y) &= K(y) \bar{r}, \quad D_d(y) = \frac{1}{2} K(y) \mu_2, \end{aligned} \quad (5.37a-e)$$

$$K(y) = \frac{D_p J p_J(y)}{P_e(y)}, \quad \langle f \rangle = \int_{-\infty}^{\infty} f p_J dy$$

and the heavy-tailed form

$$\begin{aligned} \frac{\partial f}{\partial t} &= -c(y) \frac{\partial f}{\partial x} + D_d(y) \frac{\partial^\alpha f}{\partial x^\alpha} \\ &- K(f - \langle f \rangle) + c(y) \frac{\partial (f - \langle f \rangle)}{\partial x} - D_d(y) \frac{\partial^\alpha (f - \langle f \rangle)}{\partial x^\alpha} \end{aligned} \quad (5.38a)$$

where c and K are given in (5.37b,d) and

$$D_d(y) = K(y) c_\alpha \quad (5.38b)$$

Now (5.37a) does not define a standard ADE, and (5.38a) does not define a standard fADE. The advection speed and diffusivity are functions of the vertical coordinate y in this case. More importantly, vertical mixing is driven by the deviatoric term ϕ . This deviatoric term captures mixing in the vertical, driven by the difference between the local value f and its jump-averaged value $\langle f \rangle = \int_{-\infty}^{\infty} f(x, y, t) p_J(y) dy$. In addition, ϕ can be both advected and diffused downstream, and this diffusion can be either normal or anomalous.

In order to reduce, EBME-W, it is advantageous to use Fourier transforms in time rather than Laplace transforms. This can be done

because a) the lower limit of time in the integrals of (5.34a) can be changed from 0 to $-\infty$ by the simple artifice of specifying that $p_w = 0$ for $\tau < 0$, and b) as opposed to the Montroll-Weiss CTRW, i.e. (5.6) and (5.7), the initial condition is not built into EBME-W. With this in mind, we define the time Fourier transform of $A(t)$ as follows:

$$\tilde{A}(s) = \int_{-\infty}^{\infty} A(t)e^{ist} dt \quad (5.39)$$

and modify (11b) and (15b) to the respective form

$$\check{p}_w(s) = 1 - is\bar{\tau}(y) \quad (5.40)$$

Upon Fourier-transformation in both space and time, application of (5.11a) and (5.40), inverse transformation, and truncation so that the sum of the orders of derivatives in time and space does not exceed 2, the thin-tailed asymptotic form for EBME-W reduces to

$$\begin{aligned} \frac{\partial f}{\partial t} = & -c(y)\frac{\partial f}{\partial x} + K\bar{\Gamma}\bar{\tau}\frac{\partial^2 f}{\partial x\partial t} + D_d(y)\frac{\partial^2 f}{\partial x^2} \\ & - K(f - \langle f \rangle) + c(y)\frac{\partial(f - \langle f \rangle)}{\partial x} - K\bar{\Gamma}\bar{\tau}\frac{\partial^2(f - \langle f \rangle)}{\partial x\partial t} - \\ & - D_d(y)\frac{\partial^2(f - \langle f \rangle)}{\partial x^2} + K\frac{\partial}{\partial t} \left\{ [\bar{\tau}f - \langle \bar{\tau}f \rangle] - c(y)\frac{\partial[\bar{\tau}f - \langle \bar{\tau}f \rangle]}{\partial x} \right\} \end{aligned} \quad (5.41)$$

where c , D_d and K are specified in (5.37b,c,d). The corresponding heavy-tailed form is

$$\begin{aligned} \frac{\partial f}{\partial t} = & -c(y)\frac{\partial f}{\partial x} + K\bar{\Gamma}\bar{\tau}\frac{\partial^2 f}{\partial x\partial t} + D_d(y)\frac{\partial^\alpha f}{\partial x^\alpha} \\ & - K(f - \langle f \rangle) + c(y)\frac{\partial(f - \langle f \rangle)}{\partial x} - K\bar{\Gamma}\bar{\tau}\frac{\partial^2(f - \langle f \rangle)}{\partial x\partial t} - \\ & - D_d(y)\frac{\partial^\alpha(f - \langle f \rangle)}{\partial x^\alpha} + K\frac{\partial}{\partial t} \left\{ [\bar{\tau}f - \langle \bar{\tau}f \rangle] - c(y)\frac{\partial[\bar{\tau}f - \langle \bar{\tau}f \rangle]}{\partial x} \right\} \end{aligned} \quad (5.42)$$

where c , K and φ are specified in (5.37b,c,d) and D_d is specified in (5.38b). In the above equation, the vertical variation in mean waiting time is seen to contribute to vertical dispersion via the last two term on the right-hand side.

5.8 SIMPLIFIED MODEL FOR VERTICAL DISPERSION: THIN-VERSUS HEAVY-TAILED PROBABILITY DENSITIES FOR ELEVATION FROM WHICH A PARTICLE JUMPS

The EBME formulation based on PPL results in asymptotic fractional PDE's that show substantial differences from the CTRW ME formulation. The three most important of these are a) the absence of subdiffusion, b) the effect of vertical dispersal of particles, and c) the contribution of elevation-varying waiting time to this dispersal.

We do not implement the complete formulation herein. Instead, we show several simplified examples that illustrate the effect of nonlocal vertical dispersion in EBME-N. We do this by neglecting all the terms on the right-hand side of (5.37) except the term $K(f - \langle f \rangle)$:

$$\begin{aligned} P_e \frac{\partial f}{\partial t} &= -D_c J p_j(y) [f(y, t) - \langle f \rangle] \\ \langle f \rangle &= \int_{-\infty}^{\infty} f(y', t) p_j(y') dy \end{aligned} \quad (5.43a,b)$$

Note that the form of the equation is nonlocal, in that the values of f at all elevations y' contribute to the time rate of change of f at any given elevation y . In addition, $p_j(y)$ may be thin-tailed or heavy-tailed, but there is no obvious way to convert the governing equation into an asymptotic form involving fractional derivatives.

It is important to keep in mind that the conserved quantity in (5.43a) is not the density of fraction of tracers in the sediment $f(y, t)$, but rather the density of fraction of tracers

$$f_{sw} = P_e f \quad (5.44)$$

averaged along a line of constant y that includes portions that are instantaneously in sediment, and other portions that are instantaneous in the water column (Figure 2.5).

We first cast the problem in dimensionless form. Let γ^* denote an appropriate length scale (as specified below). Defining

$$f^* = \gamma^* f \quad , \quad y^* = \frac{y}{\gamma^*} \quad , \quad t^* = \frac{D_p}{\gamma^*} J t \quad , \quad p_J = \frac{1}{\gamma^*} p_J^* \quad (5.45a,b,c,d)$$

it is found that (5.43a,b) reduces to

$$\frac{\partial f}{\partial t^*} = \frac{p_J^*}{P_e} (f - \langle f \rangle) \quad , \quad \langle f \rangle = \int_{-\infty}^{\infty} f p_J^* dy^* \quad (5.46a,b)$$

We specify the length scale in terms of two alternatives. To study thin-tailed behavior, we consider a Gaussian distribution for p_J , in which case γ^* is the standard deviation σ_J of p_J and

$$p_J^*(y^*) = \frac{1}{\sqrt{2\pi}} \exp\left(-\frac{(y^*)^2}{2}\right) \quad (5.47)$$

To study heavy-tailed behavior, we let γ^* correspond to the scale parameter γ' of a Lévy α -stable distribution, which is defined by its Fourier transform as (Nolan, 1997):

$$p_J^*(k) = \left\{ -i\delta'k - |\gamma'k|^\alpha \left[1 + i\beta \operatorname{sgn}(k) \tan\left(\frac{\pi\alpha}{2}\right) \right] \right\} \quad (5.48)$$

where k is an integer value which defines the type of parameterization (here, equal to 1), α denotes the stability parameter (here chosen equal to 1.1) and β denotes the skewness parameter (here set equal to zero). In addition, the location and scale parameters δ' and γ' are respectively set equal to 0 and 1, so as to obtain correspondence with (5.47).

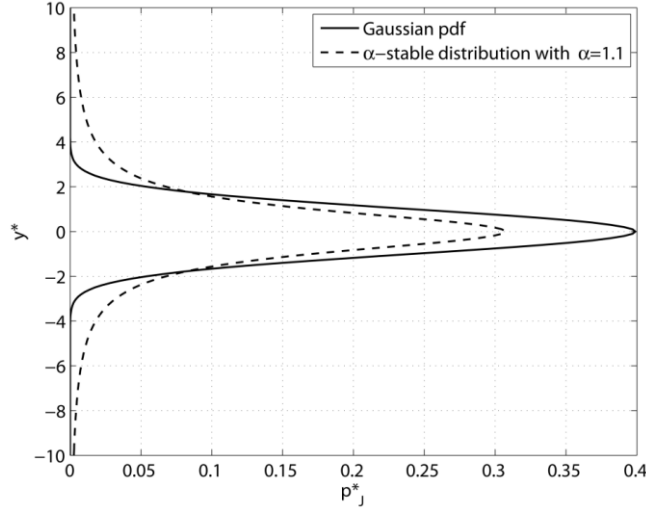


Figure 5.1 Thin-tailed (Gaussian) and heavy-tailed PDFs for p_j^* . The heavy-tailed distribution corresponds to a Lévy α -stable distribution with $\alpha = 1.1$.

Note that the Gaussian distribution is a limit case of a stable distribution obtained with $\alpha = 2$. Both these distributions are shown in Figure 5.1.

The first case we consider is one for which $P_c = 1$. In this case, there is no defined bed (interface between water and sediment); instead the lattice is filled with particles, and particle pairs at elevations y and y' exchange according to the PDF (y). In addition, $f_{sw} = f$ according to (5.44). The initial condition used in the calculations was arbitrarily set to the following top-hat distribution:

$$f^*(y^*, 0) = \begin{cases} 1 & , \quad -1 \leq y^* \leq 1 \\ 0 & , \quad |y^*| > 1 \end{cases} \quad (5.49)$$

Results of the calculations are shown in Figure 5.2 for the Gaussian distribution, and Figure 5.3 for the α -stable distribution.

Figures 5.2 and 5.3 both illustrate the tendency for tracer particles to be dispersed from high to low concentration in the vertical. The pattern of dispersion is non-Fickian, as evidenced by the tendency for the formation of a depression in tracer fraction at $y^* = 0$. The effect of heavy- versus thin-tailed PDFs for p_j is readily apparent; the heavy-tailed case of Figure 5.3 shows much more rapid, and much more far-reaching dispersal than the thin-tailed case of Figure 5.2.

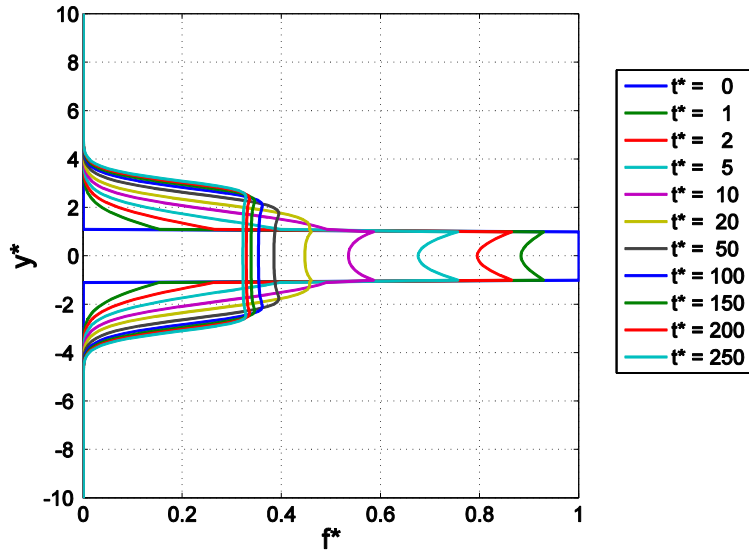


Figure 5.2 Evolution in time of distribution of tracer fraction f^* for the case of a thin-tailed (i.e. Gaussian) form for the PDF p_j^* describing the probability that an entrained particle jumps from elevation y^* . Here $P_e = 1$, resulting in a symmetric pattern.

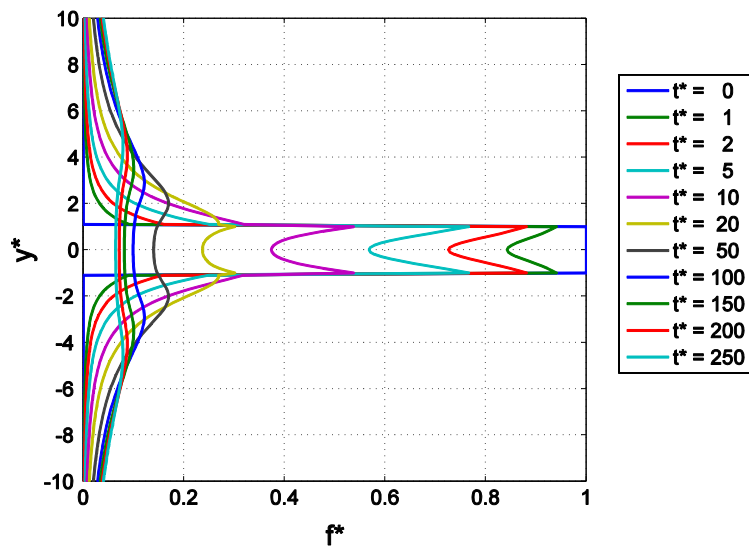


Figure 5.3 Evolution in time of distribution of tracer fraction f^* for the case of a heavy-tailed (i.e. α -stable) form for the PDF p_j^* describing the probability that an entrained particle jumps from elevation y^* . Here $P_e = 1$, resulting in a symmetric pattern.

The mean elevation \bar{y}^* and vertical standard deviation σ_y^* of the tracer particle distribution are given by the respective relations

$$\bar{y}^* = \frac{\int_{-\infty}^{\infty} y^* f_{sw}(y^*) dy^*}{\int_{-\infty}^{\infty} f_{sw}(y^*) dy^*}, \quad (\sigma_y^*)^2 = \frac{\int_{-\infty}^{\infty} (y^* - \bar{y}^*)^2 f_{sw}(y^*) dy^*}{\int_{-\infty}^{\infty} f_{sw}(y^*) dy^*} \quad (5.50a,b)$$

In the case $P_e = 1$ with the initial condition (5.49), the problem is symmetric so that $\bar{y}^* = 0$.

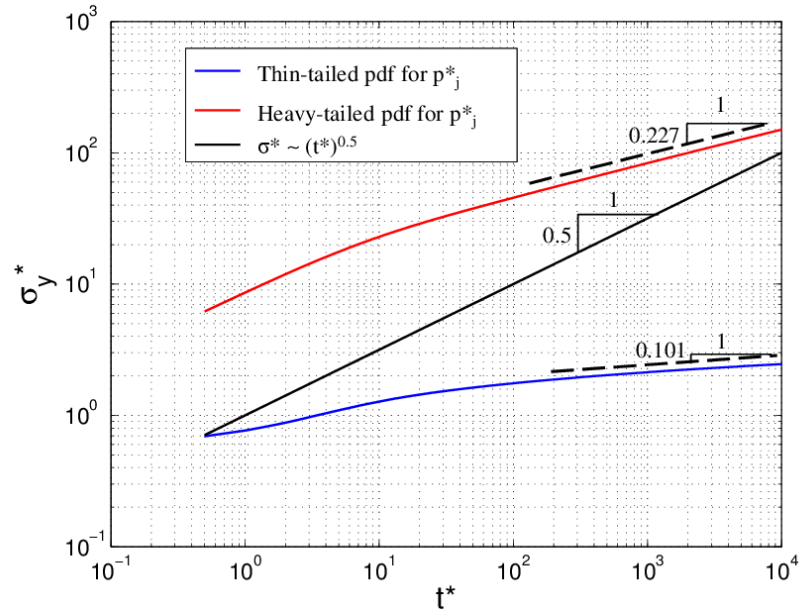


Figure 5.4 Evolution in time of the variance of the vertical standard deviation σ_y^* for the thin- and heavy- tailed case for p_j , with $P_e = 1$. Also plotted is the line $\sigma_y^* \sim (t^*)^{1/2}$ corresponding to normal diffusion.

Figure 5 shows plots of σ_y^* versus t^* for the thin- and heavy-tailed case.

Also plotted is the scale relation $\sigma_y^* \sim (t^*)^{1/2}$ corresponding to normal diffusion. In the thin-tailed case, the vertical dispersion is subdiffusive over the entire range of modeled times, while for the heavy-tailed case dispersion is first nearly normal, and then asymptotically becomes

subdiffusive. We now consider solutions to (5.46) for vertically varying $P_e(y)$ corresponding to the statistics of a fluctuating sediment-water interface (Figure 2.5). As a simple example, we approximate p_e with p_j , specified in (5.47) and (5.48), and evaluate P_e from (2.9). Otherwise, we solve the problem in the same way as the case $P_e = 1$.

In so far as the conserved quantity is f_{sw} , rather than f , plots of

$$f_{sw}^* = P_e f^* \quad (5.51)$$

versus y^* at various times are shown in Figures 5.5 for the thin-tailed case and 7 for the heavy-tailed case. The tendency for tracer particles to be dispersed from high to low concentration in the vertical is similar to the case $P_e = 1$ shown above, but is now modulated by the form of P_e which takes an ever smaller value for large positive values of y^* , and approaches unity for large negative value of y^* . This pattern results in preferentially downward migration of particles in the deposit. The effect of heavy- versus thin-tailed PDFs for p_j is still very evident: the heavy-tailed case of Figure 5.6 shows again much more rapid, and much more far-reaching dispersion than the thin-tailed case of Figure 5.5.

Figure 5.7 shows the variation in time of the mean elevation \bar{y}^* of tracer pebble distribution. Particles are transported downward at a much more rapid rate in the heavy-tailed case. The rate of downward migration of \bar{y}^* slows in time as pebbles are emplaced deep in the bed, where the probability of entrainment and deposition asymptotically approaches 0. This downward vertical transport is likely responsible for the long-term slowdown of the streamwise advection speed of river tracer pebbles observed by Ferguson and Hoey (2002). Verification of this requires a full implementation of (5.31) or (5.32).

Finally, Figure 5.8 shows plots of σ_y^* versus t^* for the thin- and heavy-tailed case with varying P_e . Strongly subdiffusive behavior is seen in both cases at large t^* . This behavior is stronger than the case of constant P_e . The heavy-tailed case is less subdiffusive than the thin-tailed case. This reflects the higher probability of a particle migrating to a deep elevation in the heavy-tailed case.

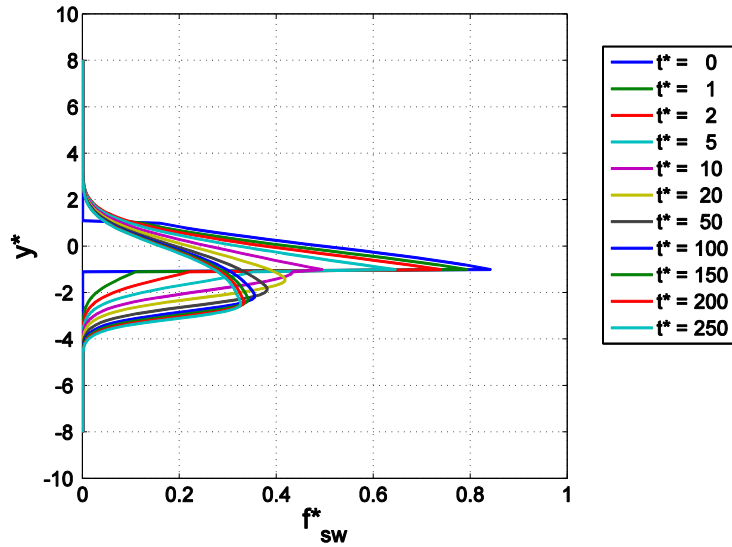


Figure 5.5 Evolution in time of the distribution of tracer fraction f_{sw}^* , for the case of vertically varying P_e corresponding to a fluctuating water-sediment interface (river bed). Here a thin-tailed (i.e. Gaussian) form for the PDF p_j^* describing the probability that an entrained particle jumps from elevation y^* is used.

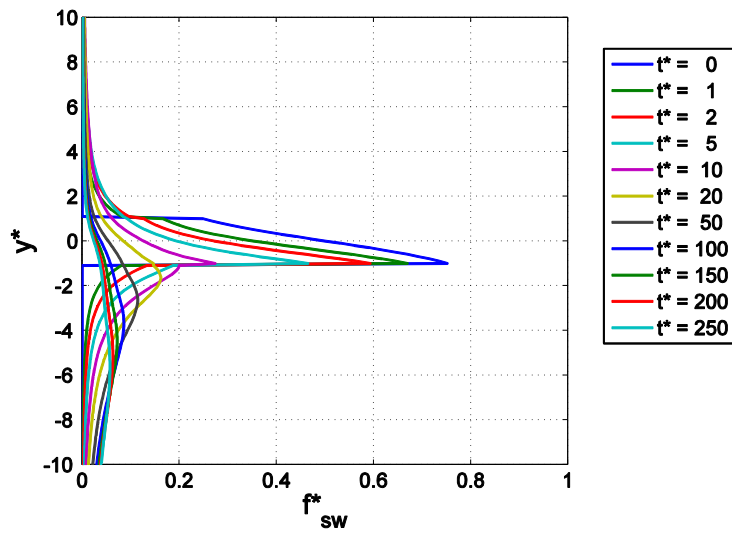


Figure 5.6 Evolution in time of the distribution of tracer fraction f_{sw}^* , for the case of vertically varying P_e corresponding to a fluctuating water-sediment interface (river bed). Here a heavy-tailed form for the PDF p_j^* describing the probability that an entrained particle jumps from elevation y^* is used.

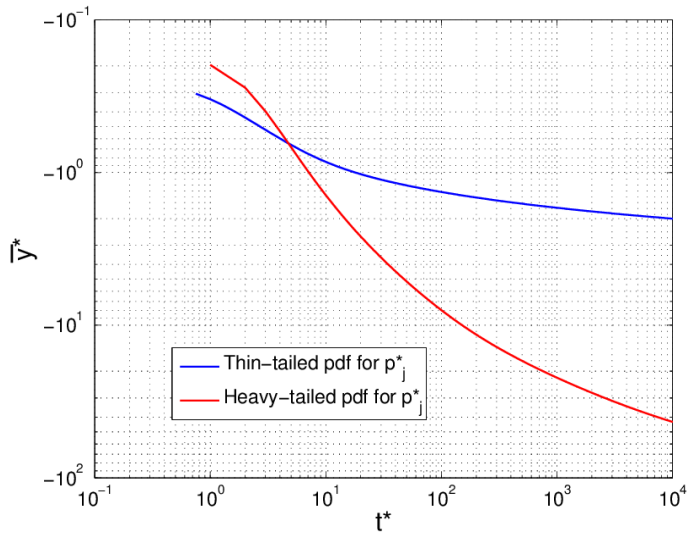


Figure 5.7 Evolution in time of the mean elevation \bar{y}^* of tracer particle distribution for the thin- and heavy- tailed cases. Here a vertically varying form P_e corresponding to a fluctuating water-sediment interface (river bed) is used.

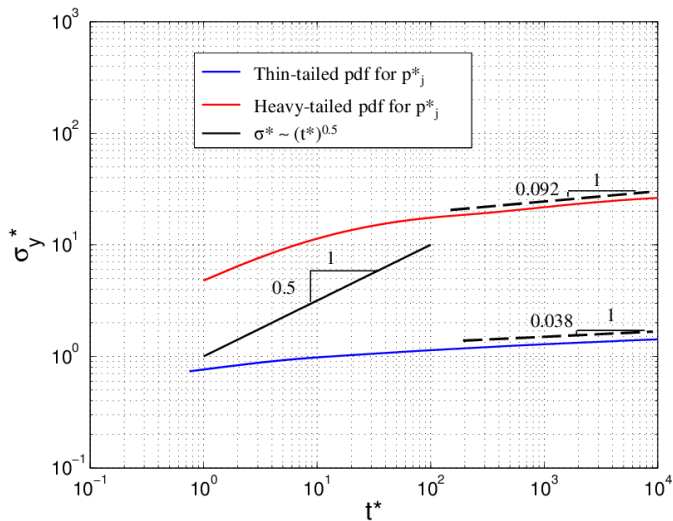


Figure 5.8 Evolution in time of the variance of the vertical standard deviation σ_y^* of the tracer distribution for the thin- and heavy- tailed cases. Also plotted is the line $\sigma_y^* \sim (t^*)^{1/2}$ corresponding to normal diffusion. Here a vertically varying form P_e corresponding to a fluctuating water-sediment interface (river bed) is used.

5.9 DISCUSSION AND CONCLUDING REMARKS

The principal objective of the Chapter is to define a generalized Master Equation for the case of bedload transport (moving as bed material load) in rivers, so as to include PDFs of particle step length and particle waiting time, as well as vertical exchange of particles. It is shown here that the Montroll-Weiss (1965) Master Equation for the Continuous Time Random Walk (CTRW) model does not apply to the case where the walker (sediment particle) interacts with the lattice by causing the sediment-water interface to change in elevation. The Master Equation forms proposed here are derived from the probabilistic Exner equation of sediment mass conservation of Parker et al. (2000); they are substantially different from the Master Equation of CTRW. Our formulation characterizes vertical dispersion, as well as streamwise advection-diffusion of tracer particles.

Two forms for the Exner-based Master Equation are presented. The most general form EBME-W (Exner-Based Master Equation with Waiting time), encompasses probability distributions for both step length and waiting time. The form EMBE-N (Exner-Based Master Equation with No waiting time) is recovered from EBME-W by assuming a Dirac function for waiting time. The Exner-based formulation precludes subdiffusion associated with a PDF for waiting time with no mean, because such a PDF is incompatible with the existence of an Exner equation describing the evolution of a bed with a finite mean elevation.

Asymptotic forms of the Master Equations are derived so as to allow comparison with the standard ADE (normal advection-diffusion equation) and fADE (fractional advection-diffusion equation). Although they include streamwise advection and diffusion, the Exner-based Master Equations take forms that differ substantially from standard ADE and fADE. The key differences are as follows: a) advection and diffusion coefficients vary in the vertical, b) a nonlocal, asymptotically non-fractional dispersion term mixes tracers in the vertical, and c) the vertical variation of mean waiting time explicitly enters into the governing equation.

In order to illustrate the key aspect of vertical dispersion, a simplified version of EBME-N, in which streamwise variation is neglected, is solved numerically. The key statistical parameter in this model is $p_j(y)$ corresponding to the probability that when a particle jumps, it jumps from elevation y relative to the mean bed. Both thin-tailed and heavy-

tailed PDFs for p_j are considered. We consider two cases, one modeling a vertical lattice that is invariant in the vertical direction,, and one modeling a lattice characterizing a sediment bed, such that the probability of the bed being at elevation y decreases upward and increases downward. Asymptotically, both the thin- and the heavy-tailed cases show subdiffusive vertical dispersion of pebbles. This subdiffusive behavior is enhanced for the thin-tailed case: when p_j is heavy-tailed, particles can be dispersed more rapidly in the vertical direction.

For the case of a sediment bed, i.e. when the probability of the bed being at a given elevation increases downward, tracer particles migrate downward as they disperse. The rate of downward migration decreases in time, as particles reach locations so deep that their probability of entrainment is asymptotically low. This downward migration is the likely reason for the slowdown of streamwise advection of tracer pebbles observed in the field.

The Master Equations given here provide a basis for future studies in which a) streamwise advection and diffusion are included, and b) specific PDFs for bed elevation $p_e(y)$, jump elevation $p_j(y)$, step length $p_s(r)$ and waiting time $p_w(\tau)$ based on laboratory and field data are used. The work of Wong et al. (2007), Hassan et al. (2013) and Voepel et al. (2013) provide information concerning these structure functions. One exciting goal for the next Chapter is a further clarification of the phenomenon of streamwise advective slowdown of tracer particles.

6 EXNER BASED MASTER EQUATION FOR TRANSPORT AND DISPERSION OF RIVER PEBBLE TRACERS. PART 2. IMPLEMENTATION FOR COEVOLVING VERTICAL AND STREAMWISE DISPERSION

Patches of tracer pebbles are often emplaced in gravel-bed rivers in order to study bedload transport processes. As time passes, the patch of tracer particles is advected downstream, and shows downstream diffusion as the patch spreads. These processes have been captured in earlier models. Tracer particles can also be advected and diffused in the vertical direction. Here we use the EBME-N (Exner Based Master Equation with No waiting) derived in Chapter 5 to characterize for the first time the coevolution of streamwise and vertical advection-diffusion. The structure functions for our model are obtained from experimental measurements, which indicate thin-tailed PDFs describing bed elevation, and bed elevation from which a particle jumps into transport. Coevolution gives rise to behavior that can differ markedly from that associated with purely streamwise processes. One example is streamwise advective slowdown. Particles that are advected downward into zones where the probability of re-entrainment becomes asymptotically small are essentially trapped, and can no longer participate in streamwise advection. As a result, the mean streamwise velocity of the patch declines in time.

This Chapter 6 is an early-short version of a manuscript that is going to be submitted to a refereed journal as: “Exner Based Master Equation for transport and dispersion of river pebble tracers. Part 2. Implementation for coevolving vertical and streamwise dispersion.”

6.1 INTRODUCTION

This chapter contains a summary of salient results obtained from a computation of the transport, horizontal dispersion, and vertical dispersion of tracers, using one of the Master Equations derived in Chapter 5. The chapter will shortly be expanded into a manuscript ready to submit to a refereed journal.

Three Master Equations for tracer pebble transport and dispersion are derived in Chapter 5. The first of these, EBME-A (Exner Based Master Equation, Active Layer formulation), which is based on the concept of a surface active layer, has been presented previously (Parker et al., 2000; Ganti et al., 2010). The second and third of these, EBME-N (Exner Based Master Equation with No waiting) and EBME-W (Exner Based Master Equation with Waiting) represent innovations in that for the first time, they characterize vertical advection and dispersion of tracer particles, as well as streamwise advection and dispersion. These equations allow explanation of phenomena regarding tracer transport that heretofore have been difficult to characterize mathematically due to the inability to establish the governing equation. One of these phenomena is the tendency for the mean streamwise virtual velocity of a patch of tracers to slow down over time (Ferguson et al., 2002). Here we explain this phenomenon in terms of the coevolution of vertical and streamwise dispersion, using EBME-N.

We begin by introducing relevant results from Chapter 5. The governing Master Equation is

$$P_c(y) \frac{\partial f(x, y, t)}{\partial t} = -D_p J f(x, y, t) p_j(y) + D_p J p_j(y) \int_{-\infty}^{\infty} \int_0^{\infty} f(x-r, y', t) p_j(y') p_s(r) dy' dr \quad (6.1)$$

Here, f denotes the density of fraction of tracer particles per unit volume at streamwise point x , vertical point y and time t , D_p denotes particle size, J denotes the probability per unit time that a bed particle jumps into bedload transport per unit, defined in term of the inverse of a mean waiting time, $p_j(y)$ is the PDF that when a particle jumps, it jumps from vertical point y and $p_s(r)$ is the PDF of jump step length y . Here y is defined in terms of mean bed elevation; y is positive for elevation above the mean elevation, and negative for elevation below the mean elevation. The parameter $P_c(y)$ is the cumulative PDF that the instantaneous bed

elevation is below or at level y ; thus $P_e \rightarrow 0$ as $y \rightarrow \infty$ (high in the water column) and $P_e \rightarrow 1$ as $y \rightarrow -\infty$. This cumulative PDF can be obtained from the integral of the PDF $p_e(y)$ that the instantaneous bed is at elevation y :

$$P_e(y) = 1 - \int_{-\infty}^y p_e(y) dy \quad (6.2)$$

The parameter that is conserved in (6.1) is not f , but rather f_{sw} , which describes the density per unit volume sediment of tracer particles, where

$$f_{sw} = P_e(y)f \quad (6.3)$$

The difference between f and f_{sw} is as follows. In a sediment bed with fluctuating bed elevation, a horizontal line at elevation y intersects zones of sediment (within the bed) and zones of water (above the instantaneous bed). The parameter f denotes a density of particles at elevation y averaged over the zones below the bed and those above it. The parameter f_{sw} , on the other hand, is normalized to give a density based only on the zones that are in the bed. Thus (6.1) can be rewritten as

$$\begin{aligned} \frac{\partial f_{sw}(x, y, t)}{\partial t} = & -D_p J f(x, y, t) p_J(y) + \\ & + D_p J p_J(y) \int_{-\infty}^{\infty} \int_0^{\infty} f(x-r, y', t) p_J(y') p_S(r) dy' dr \end{aligned} \quad (6.4)$$

It is easily demonstrated from (6.4) that

$$\frac{d}{dt} \int_0^{\infty} \left(\int_{-\infty}^{\infty} f_{sw} dy \right) dx = 0 \quad (6.5)$$

so that f_{sw} rather than f is the conserved tracer density.

In order to characterize the problem for any given case, pebble size D_p , frequency of jump J and the PDFs $p_J(y)$ of jump elevation and $p_S(r)$ of step length must be specified. In order to do this, we use the experiments on tracers of Wong et al. (2007).

6.2 FLUME EXPERIMENTS BY WONG ET AL. (2007)

In Chapter 5, EBME-N was applied to a hypothetical problem for vertical dispersion alone, using plausible forms for the necessary structure functions. Here we apply EBME-N using structure functions determined from experiments on pebble transport and tracer pebble advection-diffusion by Wong et al. (2007) in a flume located at St. Anthony Falls Laboratory (SAFL), University of Minnesota.

Here some experimental information are reported for the sake of completeness. For more details about experimental conditions and devices, refer to the paper by Wong et al., 2007.

As indicated by the authors, the general arrangement of the experimental facility included: (i) a 0.5-m-wide, 0.9-m-deep, 27.5-m-long, straight flume of rectangular cross section and smooth metallic walls; (ii) a regulated water supply with maximum flow rate of $0.120 \text{ m}^3\text{s}^{-1}$ calibrated with a rectangular sharp-crested weir located at the downstream end of the head tank; (iii) pressure tubes (piezometers) used to measure water surface levels, which were placed every 0.5 m in the streamwise direction, between 2.0 and 20.0 m downstream from the entrance weir; (iv) controlled gravel supply at the upstream end of the test reach, via an auger-type sediment feeder, for a maximum feed rate of 0.150 kg s^{-1} ; and (v) automated recirculation of the gravel collected in a sediment trap at the downstream end of the flume, from where it was jet-pumped back to a buffer containment box installed above the sediment feeder. Because of the presence of the sediment feeder, the system operated as a sediment-fed flume rather than a sediment-recirculating flume. The test reach had a length of 22.5 m, as measured from the upstream weir to the downstream sediment trap.

Two point gauges were used to measure longitudinal bed profiles. In addition, a sonar-transducer system was used to record bed elevation fluctuations simultaneously at five fixed streamwise positions, with a measurement interval of 3 s. Independent measurements with the same sonar system in standing water and a fixed gravel bottom surface resulted in a standard deviation of signal fluctuations (i.e. the measurement error) in the range of 0.16 and 0.04 mm.

The sediment used in all experiments was well-sorted gravel, with geometric mean particle size $D_g = 7.2 \text{ mm}$, geometric standard deviation

$\sigma_g = 1.2$, median particle size $D_{50} = 7.1$ mm, particle size for which 90% of the sediment is finer $D_{90} = 9.6$ mm, and density $\rho_s = 2550$ kg m⁻³. The flume was let run long enough to achieve lower-regime plane-bed normal (uniform and steady) flow equilibrium transport conditions, for constant values of water discharge Q_w [L³T⁻¹] and sediment feed rate Q_f [MT⁻¹]. Ten different runs were performed.

Table 6.1 Water discharge Q_w , sediment feed rate Q_f and Shields number τ^* for each run

Run	Q_w m ³ s ⁻¹	Q_f kgs ⁻¹	τ^*
1	0.081	0.117	0.1046
2	0.067	0.124	0.1052
3	0.044	0.058	0.0892
4	0.038	0.034	0.0758
5	0.039	0.076	0.0915
7	0.069	0.060	0.0908
8	0.102	0.096	0.1044
9	0.034	0.026	0.0760
10	0.074	0.051	0.0843
11	0.093	0.150	0.1193

Table 6.1 shows some parameters of the experiments: Q_w is the flow discharge, Q_f is the volume transport rate of sediment and τ^* is the dimensionless Shields number. for each run, once lower-regime plane-bed equilibrium conditions were achieved.

Once mobile-bed equilibrium was achieved, simultaneous measurements of bed elevation were recorded with the sonar-transducer system at five streamwise positions (6.75, 7.75, 8.75, 12.75, and 16.75 m).

The absence of bedforms was verified during all the surveys.

In Figure 6.1, times series of bed fluctuations, in five streamwise locations, obtained with the ultrasonic probes are shown for two different runs. In Figure 6.1a, corresponding to a run with a low τ^* , the magnitude of the bed fluctuations is clearly less than in Figure 6.1b, corresponding to a run with a high τ^* . So the magnitude of the fluctuations depends, in a way that will be shown later, from the “strength” of the flow.

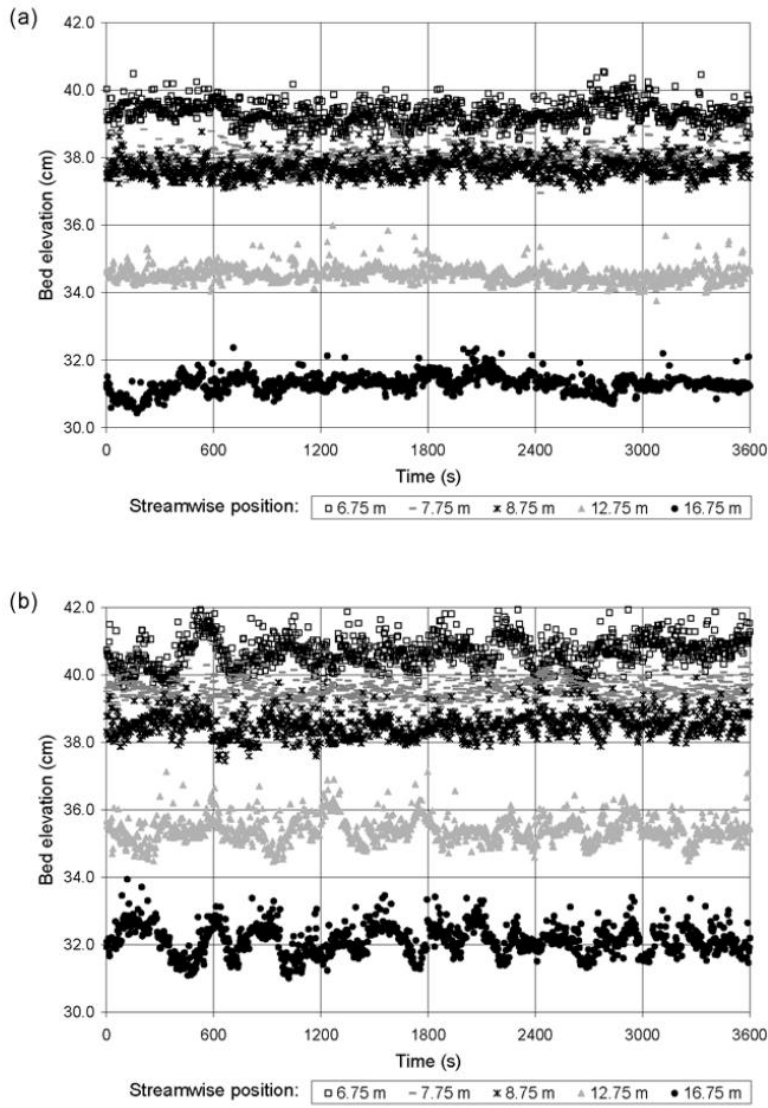


Figure 6.1 Examples of time series of bed elevation fluctuations obtained with ultrasonic transducer probes. Simultaneous recording at five indicated streamwise positions along the flume. (a) Run 10. (b) Run 8. (Wong et al., 2007)

6.3 STRUCTURE FUNCTIONS OF PDFs FOR PARTICLE STEP LENGTH, BED FLUCTUATION AND JUMP ELEVATION

6.3.1 Particle step length

Hassan et al. (2013) analyzed 64 sets of field data on pebble tracer dispersion in mountain rivers. They found that only 5 of those sets show heavy-tailed step-length distributions while the majority clearly display thin-tailed step-length distributions.

The standard thin-tailed form for particle step length probability density function is the exponential distribution (e.g. Nakagawa and Tsujimoto, 1980; Hill et al., 2010; Pelosi and Parker, 2013):

$$p_s(r) = \frac{1}{\bar{r}} \exp\left(-\frac{r}{\bar{r}}\right) \quad (6.6)$$

where \bar{r} denotes mean step length. The corresponding dimensionless mean step length \hat{r} is defined as

$$\hat{r} = \frac{\bar{r}}{D_p} \quad (6.7)$$

Wong et al. (2007) provided a predictor function for the dimensionless mean step length \hat{r} in terms of the (sidewall-corrected) Shields number τ^* :

$$\hat{r} = 53.2(\tau^* - 0.0549)^{-0.35} \quad (6.8)$$

In Figure 6.2, we show an example of an exponential distribution for p_s . The dimensionless mean step length \hat{r} is computed with $\tau^* = 0.1044$, which is the Shields number for Run 8 of Table 6.1; the value is 152.

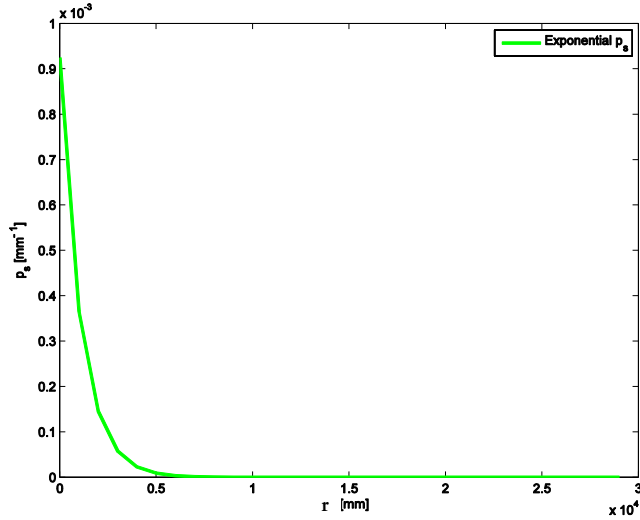


Figure 6.2 Exponential PDF for particle step length p_s based on Run 8.

6.3.2 Bed fluctuations

Wong et al. (2007) analyzed the time series of bed fluctuations (Figure 6.1) and fitted them to a Gaussian PDF for p_e :

$$p_e(y) = \frac{1}{s_y \sqrt{2\pi}} \exp\left(-\frac{(y - m_y)^2}{2s_y^2}\right) \quad (6.9)$$

with mean, m_y [L], equal to zero (tautologically, because of the definition of y) and standard deviation s_y [L], which is a function of the (sidewall-corrected) Shields number τ^* . In particular, they found that the dimensionless standard deviation

$$\hat{s}_y = \frac{s_y}{D_{50}} \quad (6.10)$$

is related to τ^* as follows:

$$\hat{s}_y = 3.09(\tau^* - 0.0549)^{0.56} \quad (6.11)$$

The values for s_y for each run are given in Table 6.2.

Table 6.2 Parameters of the Gaussian distribution for bed fluctuations by Wong et al. (2007).

Run	1	2	3	4	5
m_y	0.00	0.00	0.00	0.00	0.00
s_y	4.09	4.11	3.32	2.52	3.44

Run	7	8	9	10	11
m_y	0.00	0.00	0.00	0.00	0.00
s_y	3.41	4.08	2.53	3.04	4.72

We reanalyzed the data in order to whether or not the PDF for p_e based on the data show a heavy tail, using the Gaussian PDF suggested by Wong et al. (2007) as benchmark. In order to study the implications of a heavy-tailed distribution for comparison purposes, we fit an α -stable distribution to the measured bed fluctuations. The α -stable distribution is defined by its Fourier transform as (Nolan, 1997):

$$p_e(k) = \left\{ -i\delta k - |\gamma k|^\alpha \left[1 + i\beta \operatorname{sgn}(k) \tan\left(\frac{\pi\alpha}{2}\right) \right] \right\} \quad (6.12)$$

where k is an integer value which defines the type of parameterization (here, equal to 1), α denotes the stability parameter, β denotes the skewness parameter, and δ and γ are respectively the location and the scale parameter. When $\alpha = 2$, the α -stable distribution coincides with the Gaussian distribution.

Table 6.3 Parameters of the α -stable distribution fitted to the measured bed fluctuations of Wong et al. (2007).

Run	1	2	3	4	5
α-stable fit for p_e					
α	1.91	1.93	1.84	1.85	1.78
β	1.00	1.00	0.77	0.69	0.77
γ	2.79	2.29	1.87	1.60	2.03
δ	0.08	0.05	0.10	0.05	0.14

Run	7	8	9	10	11
α-stable fit for p_e					
α	1.87	1.91	1.79	1.82	2.00
β	1.00	0.78	0.06	0.80	-
γ	1.78	2.72	1.77	1.74	4.27
δ	0.12	0.06	0.00	0.07	0.04

In Table 6.3, we give the values of the parameters of the fitted α -stable distributions to p_e for each run. The data show a weak heavy-tailedness (values of α below but very close to 2) which progressively weakens as τ^* increases, until the PDF becomes Gaussian ($\alpha = 2$) for Run 11.

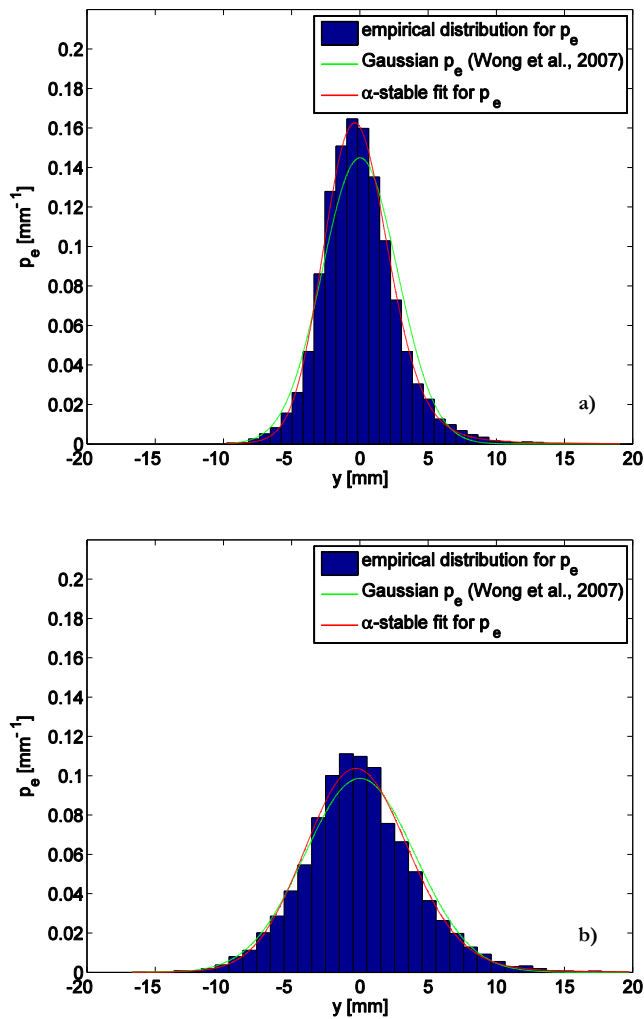


Figure 6.3 Empirical probability density function for bed elevation p_e , as well as with the Gaussian fit given in Wong et al. (2007) and the α -stable distribution fit. a) Run 10 and b) Run 8

In Figure 6.3, the empirical probability density distribution for p_e is shown in comparison with both the Gaussian PDF suggested by Wong et al. (2007) and the α -stable PDF fits for Runs 8 and 10.

In Figure 6.4, we plot only the tails of the distributions for negative values of y (deep in the sediment).

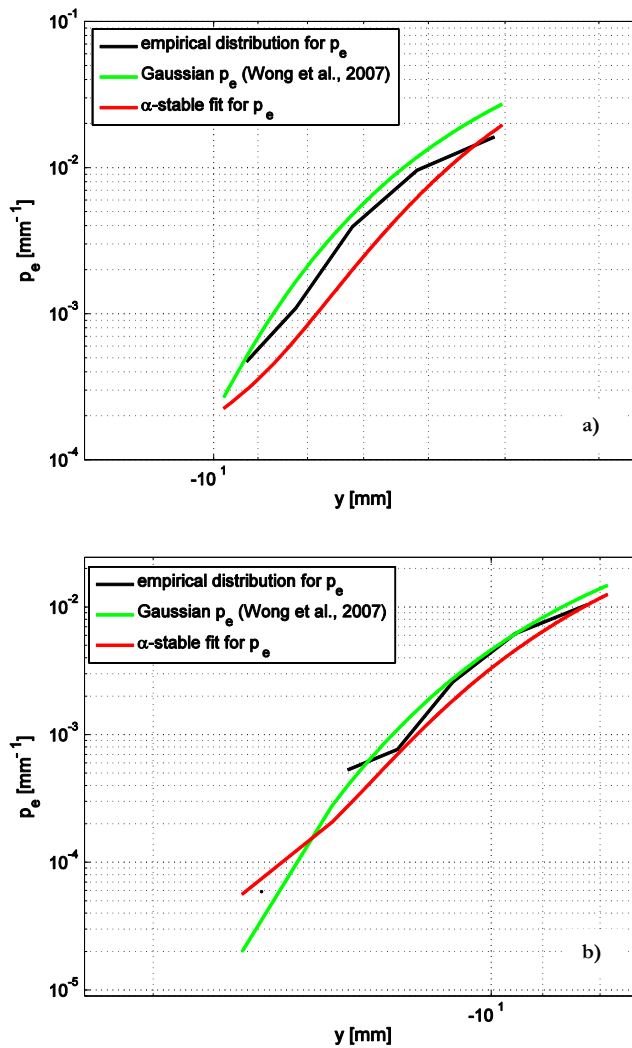


Figure 6.4 Tails of the empirical distributions for p_e , as well as the Gaussian fit and the α -stable fit. a) Run 10 and b) Run 8

The plots illustrate the better agreement of the thin-tail (Gaussian PDF), as opposed to the α -stable distribution with the empirical data. This brings us to the conclusion that we can keep, for the following analysis, the structure function (6.9) from Wong et al. (2007).

6.3.3 Jump elevation

The probability density p_j (PDF for elevation from which a particle jumps) can be determined from a time record of bed elevation fluctuations, by analyzing the mean number of downward crossings per unit time at any level (Figure 6.5) and normalizing over all levels.

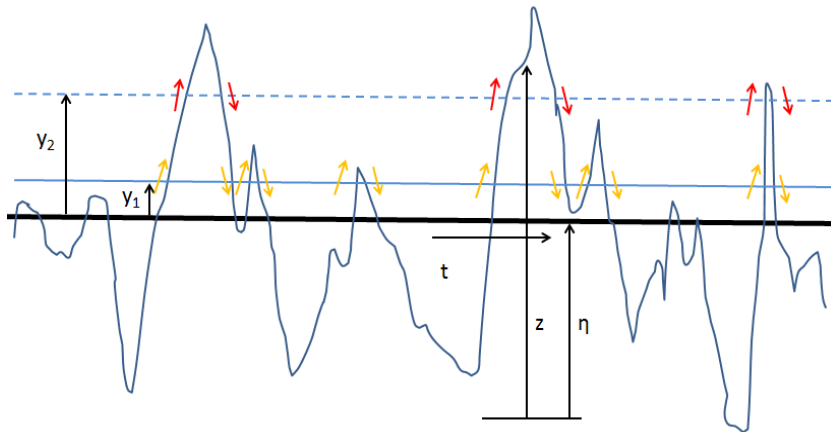


Figure 6.5 Schematic time series of bed fluctuations. The yellow (red) arrows indicates the crossing of bed at levels y_1 (y_2).

Table 6.4a Fitted values of the parameters of the PDFs for p_j

Run	1	2	3	4	5
Gaussian fit for p_j					
m_y	0.40	0.33	0.16	0.15	0.29
s_y	4.07	3.27	2.96	2.50	3.33
α-stable fit for p_j					
α	1.79	1.84	1.58	1.71	1.64
β	0.98	0.85	2.10	0.79	0.81
γ	2.86	2.21	0.81	1.76	2.33
δ	1.21	0.76	0.30	0.72	1.32

Table 6.4b Fitted values of the parameters of the PDFs for p_j

Run	7	8	9	10	11
Gaussian fit for p_j					
m_y	0.21	0.46	0.22	0.13	0.87
s_y	2.80	3.94	2.92	2.74	6.13
α-stable fit for p_j					
α	1.70	1.72	1.53	1.62	2.00
β	1.00	2.77	0.30	0.84	-
γ	1.96	1.18	2.05	1.92	4.34
δ	1.07	0.39	0.29	1.07	0.61

In Table 6.4, we show the parameters found by fitting the empirical data for p_j to both a Gaussian PDF (thin-tailed) and an α -stable PDF (heavy-tailed).

At first glance of Figure 6.6, which plots the empirical distributions for p_j against the Gaussian and α -stable PDFs, the α -stable distribution appears to give a somewhat better fit for p_j . This is due mainly to the fact that the α -stable distribution has more fitting parameters than the Gaussian PDF. In Figure 6.7, however, we show that for highly negative values of y the Gaussian PDF instead gives a better description of the tail of p_j . This is because the data better fit the thin-tailed Gaussian PDF than the power law form of the heavy-tailed α -stable PDF.

In Figures 6.6 and 6.7, we have also plotted the Gaussian PDF for p_e with the values of the parameters proposed by Wong et al. (2007) and reiterated in Table 6.3. It is quite clear that there are no significant differences between the Gaussian fits to the data for p_j and p_e . This behavior characterizes all the runs, as can also be deduced from Table 3: slight differences in the parameters values appear for the mean, but they are between the 7% and 1% of D_p . So here we assume, as a first approximation, that the two functions, p_j and p_e are identical.

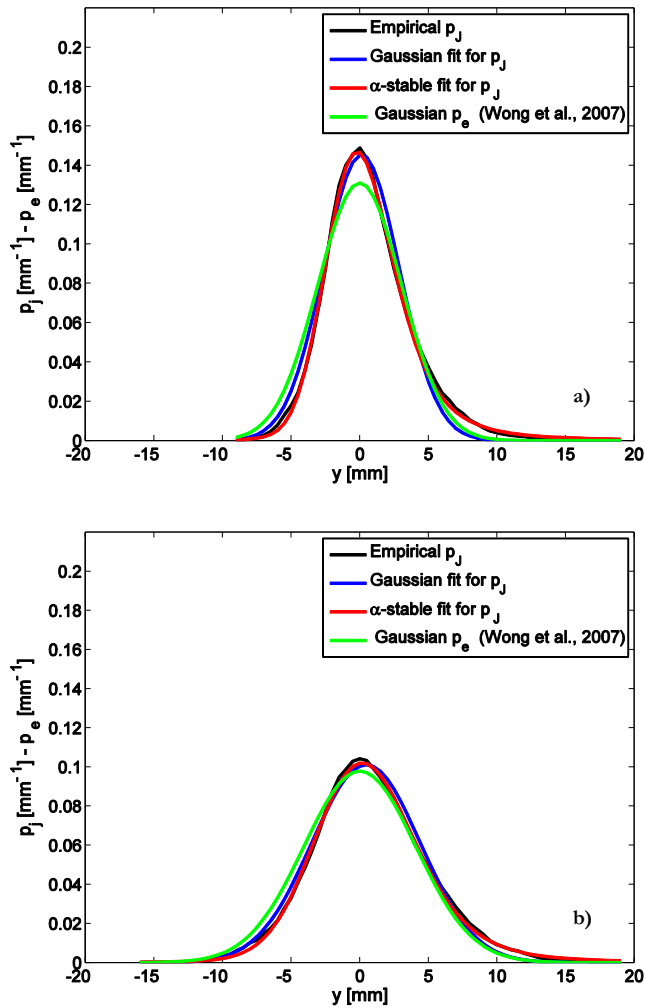


Figure 6.6 Empirical distribution for p_J , along with a Gaussian fit for p_J , a fit using the α -stable PDF for p_J and Gaussian distribution for p_e given by Wong et al. (2007). a) Run 10 and b) Run 8.

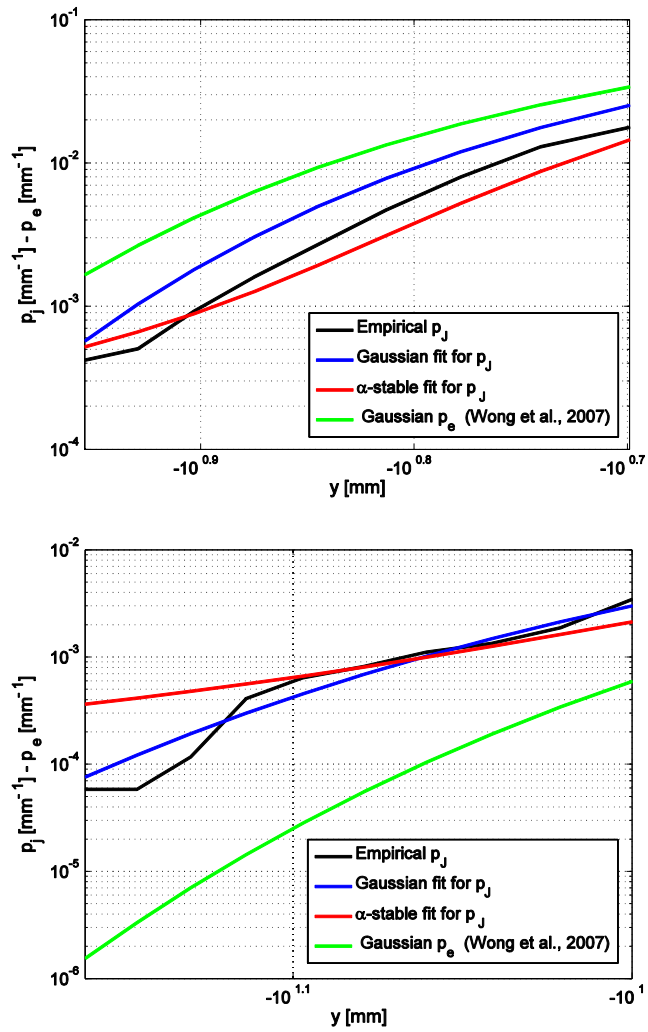


Figure 6.7 Tails of the distributions of Figure 6.6 plotted in a log-log graph. a) Run 10 and b) Run 8.

6.4 NUMERICAL RESULTS FOR EBME-N: VERTICAL AND STREAMWISE DISPERSION OF RIVER PEBBLE TRACERS

Here we numerically solve (6.1), i.e. the Master Equation EBME-N, using the above structure functions, to illustrate vertical and streamwise transport and dispersal of pebble tracers. All of our results are dimensional, so as to correspond to one of the runs of Wong et al. (2007).

As pointed out above conserved quantity in the EBME-N is not the density of fraction of tracers in the sediment $f(x,y,t)$ along a line of elevation y which includes sediment and water, but rather the density of fraction of tracers $f_{sw} = P_e f$ corresponding only to the sediment. We consider the case of transport and dispersion of a patch of pebble tracers with an initial condition consisting of a top hat function, i.e. constant f_{sw} centered at mean bed elevation and having a thickness of 8 mm in the vertical and a length of and 50 m in the streamwise direction, with $f_{sw} = 0$ otherwise:

$$f_{sw}(x,y,0) = \begin{cases} 1 & , \quad -4\text{mm} \leq y \leq 4\text{mm} \quad 0\text{m} \leq x \leq 50\text{m} \\ 0 & , \quad \text{elsewhere} \end{cases} \quad (6.13)$$

We choose Shields number τ^* of 0.1044 (Run 8), and we hypothesize a uniform grain size $D_p = 7.1$ mm for the sediment and the tracer pebbles within it. The entrainment rate $E = D_p J$ is computed as suggested by Wong et al. (2007) as follows:

$$E = \sqrt{RgD_p} 0.05(\tau^* - 0.0549)^{1.85} \quad (6.14)$$

The mean particle step length, according to (6.7) and (6.8), is equal to 1.08 m.

The exponential PDF for particle step length of (6.6), is used in the calculations. We further set $p_j = p_e$, and represent them with a Gaussian PDF having mean m_y , equal to 0 and standard deviation, s_y equal to 4.08, as obtained from (6.10) and (6.11).

Figures 6.8 to Figure 6.16 show the evolution of $f_{sw} = P_e f$ in time t and space (x, y) , within a domain such that x varies from 0 to 7500 m and y varies from -24 mm to 12 mm. along the domain at different time steps. Figures (8, 9, 10, 11, 12, 13, 14, 15 and 16) are views of f_{sw} in the x - y plane for the corresponding times (0hr, 6hr, 30hr, 60hr, 120hr, 180hr, 240hr, 300hr and 360 hr).

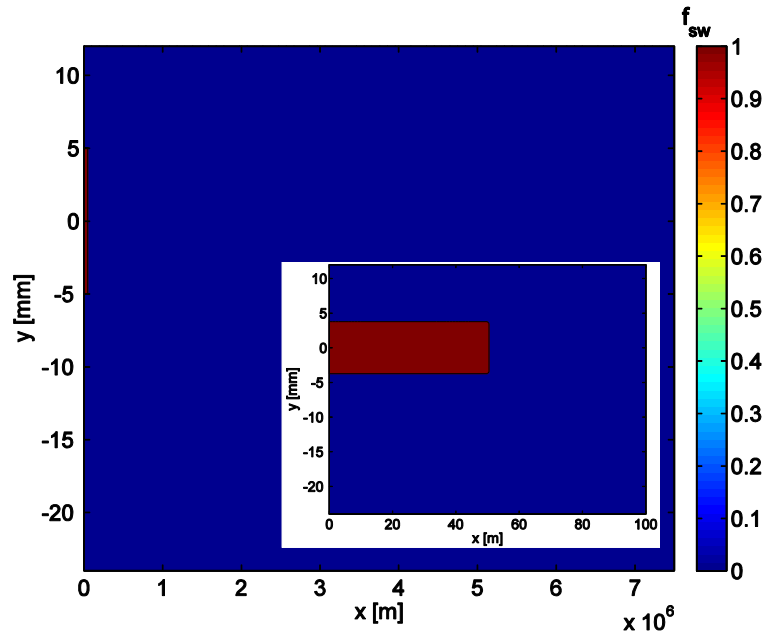


Figure 6.8 Contour map of f_{sw} at $t=0$ hr. The inset provides an expanded view of the initial condition.

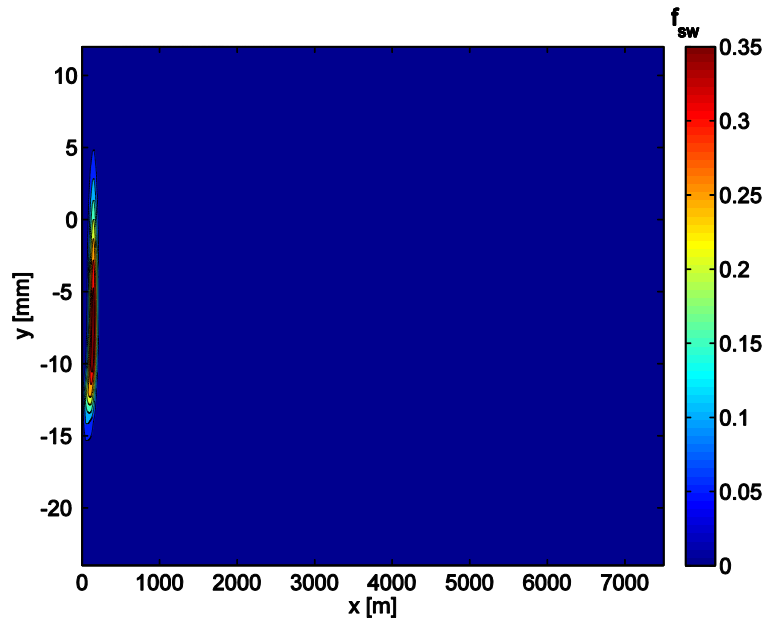


Figure 6.9 Contour map of f_{sw} at $t = 6$ hr

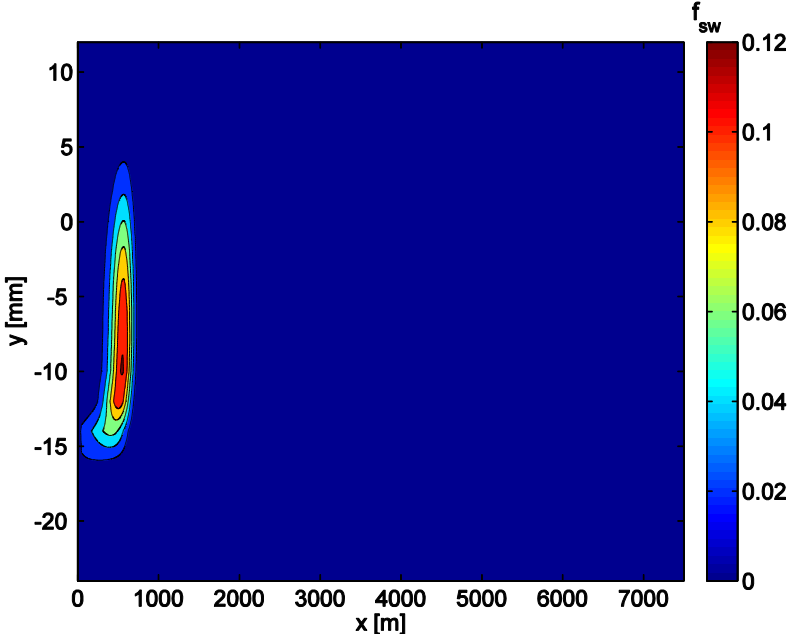


Figure 6.10 Contour map of f_{sw} at $t = 30$ hr

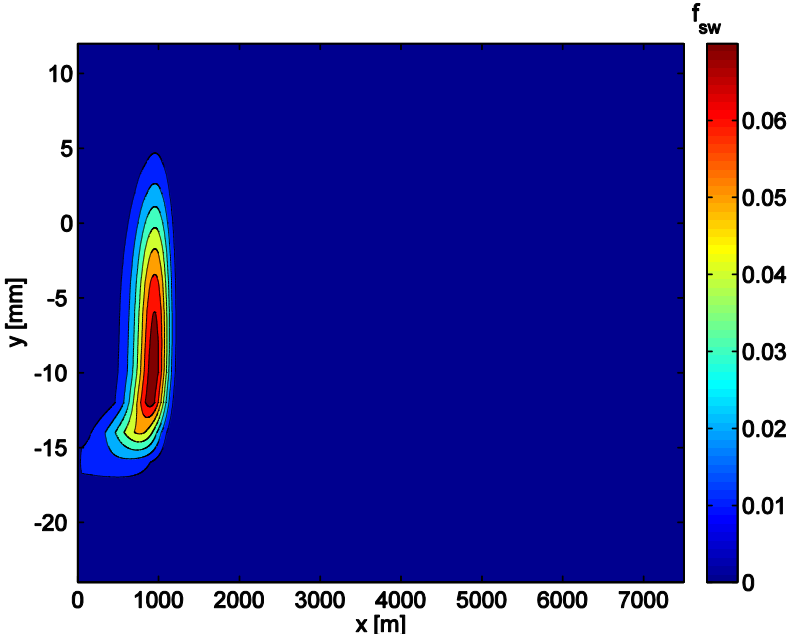


Figure 6.11 Contour map of f_{sw} at $t = 60$ hr

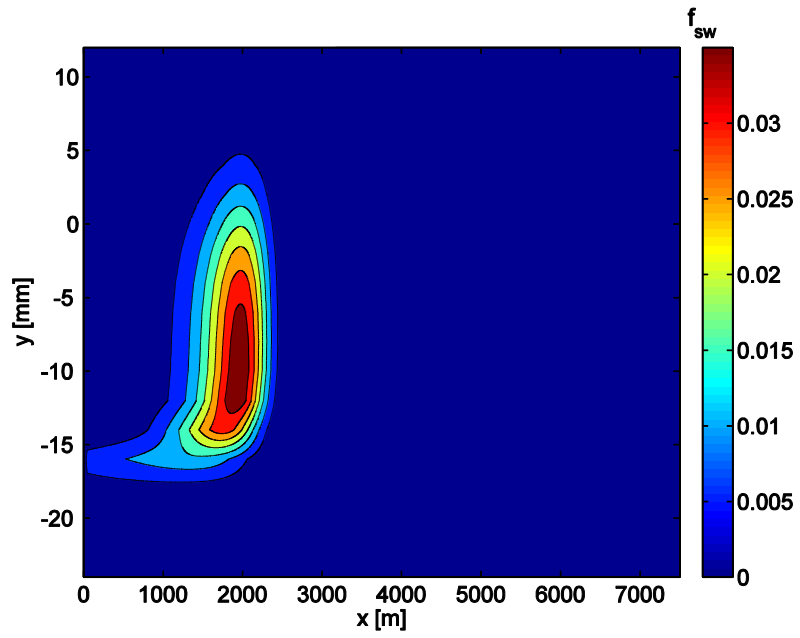


Figure 6.12 Contour map of f_{sw} at $t = 120$ hr

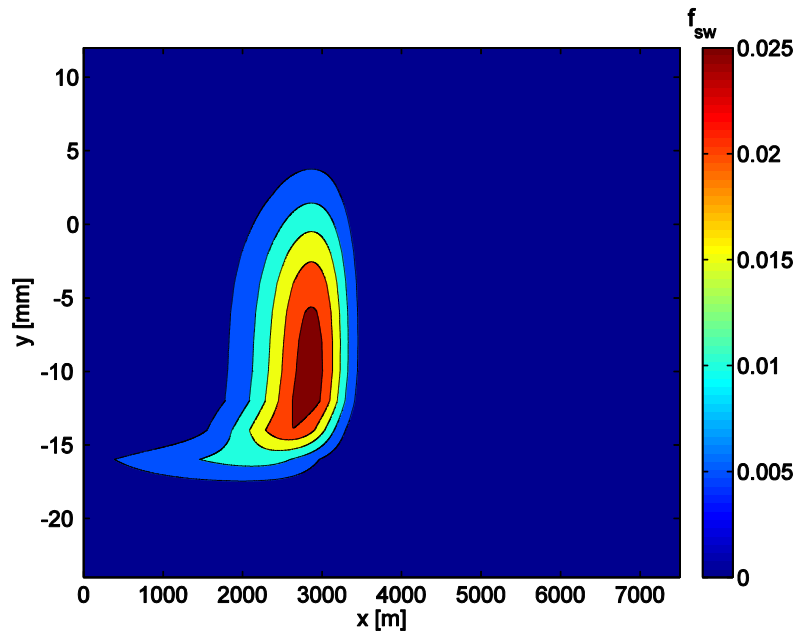


Figure 6.13 Contour map of f_{sw} at $t = 180$ hr

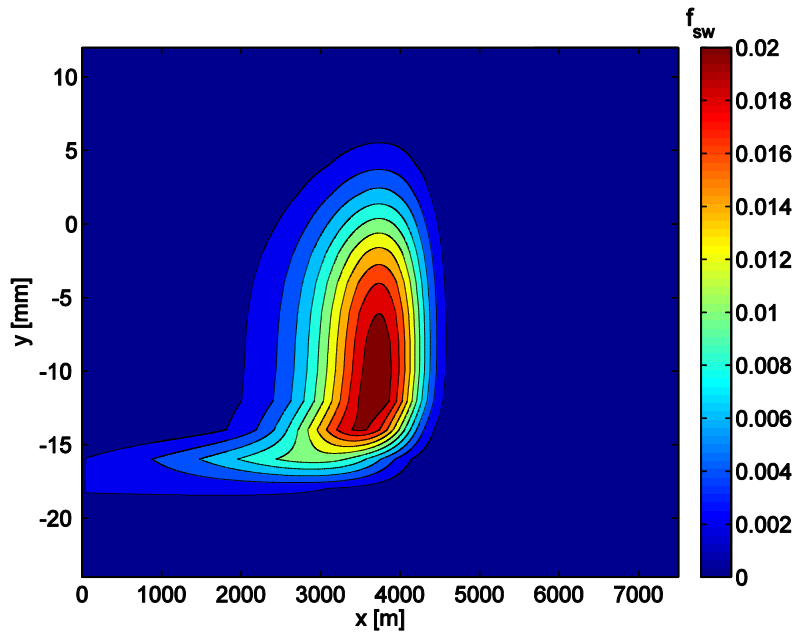


Figure 6.14 Contour map of f_{sw} at $t = 240$ hr

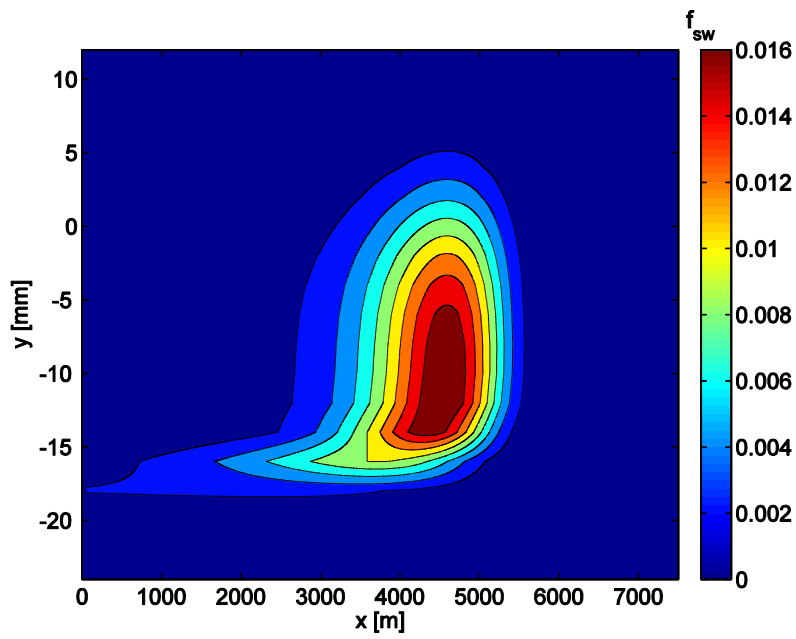


Figure 6.15 Contour map of f_{sw} at $t = 300$ hr

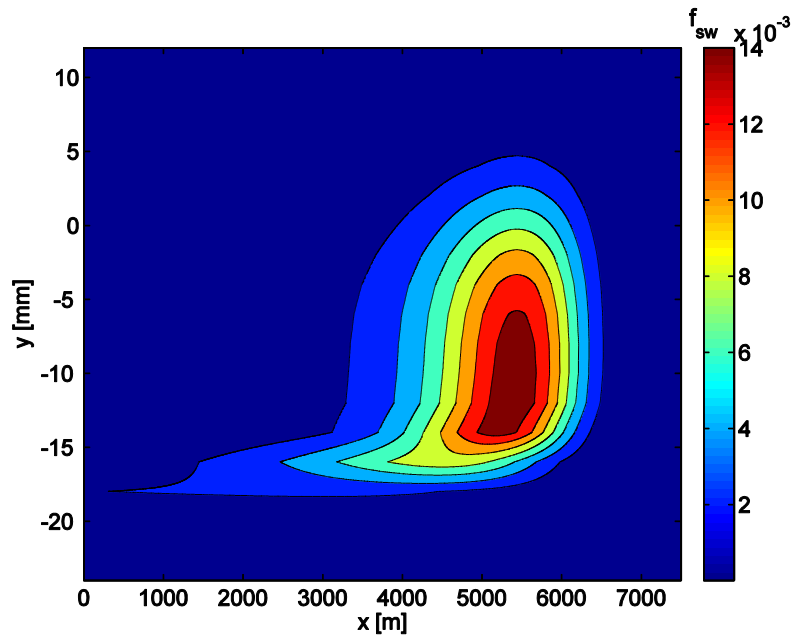


Figure 6.16 Contour map of f_{sw} at $t = 360$ hr

It can be clearly seen from the figures (Figure 6.8 to Figure 6.16) that tracer pebbles are advected and diffused in both the streamwise direction (x) and the vertical direction (y).

Of particular interests are the tails in the x direction that appear deep in the flow. It is evident that once a particle is subject to the unlikely event of being buried deep in the deposit, its re-entrainment is also unlikely. Thus a low fraction density of tracers become more or less trapped deep in the deposit. Our model is the first of its kind to capture the formation of deep tails in the distribution of tracer particles.

One aspect of Figures 6.8 to 6.16 deserved clarification. In Figure 6.13 corresponding to $t = 180$ hr, the deep tail does not extend upstream to the origin, whereas it does so for Figure 6.14 corresponding to the later time $t = 240$ hr. This does not mean that tracers have migrated upstream. Instead, it reflects the fact that the maximum value of f_{sw} in the vertical color bar is different for each one, a condition that changes the threshold for each color range. This has been done for the sake of clarity in viewing the evolution of f_{sw} ; were the maximum value in the vertical

color bar of Figure 6.16 be the same as that Figure 6.1, no contours of the spatial variation of f_{sw} would be visible in Figure 6.16.

The results of the calculation allow the computation of the time variation of several statistical parameters. The mean streamwise travel distance \bar{x}_{travel} and streamwise standard deviation $\sigma_{x-travel}$ of the tracer particle distribution are given respectively by the relations

$$\bar{x}_{travel} = \frac{\int_0^{\infty} \int_{-\infty}^{\infty} x f_{sw}(x, y, t) dy}{\int_0^{\infty} \int_{-\infty}^{\infty} f_{sw}(x, y, t) dy} \quad (6.15a,b)$$

$$\sigma_{x-travel}^2 = \frac{\int_0^{\infty} \int_{-\infty}^{\infty} (x - \bar{x}_{travel})^2 f_{sw}(x, y, t) dy}{\int_0^{\infty} \int_{-\infty}^{\infty} f_{sw}(x, y, t) dy}$$

The mean streamwise speed of the pebble patch is $c_{x-travel}$, where

$$\bar{c}_{x-travel} = \frac{d\bar{x}_{travel}}{dt} \quad (6.16)$$

Here (6.16) characterizes the streamwise advection of the pebble patch, and (6.15b) characterizes the streamwise dispersion. The corresponding relations for mean vertical travel distance \bar{y}_{travel} and vertical standard deviation $\sigma_{y-travel}$ are

$$\bar{y}_{travel} = \frac{\int_0^{\infty} \int_{-\infty}^{\infty} y f_{sw}(x, y, t) dy}{\int_0^{\infty} \int_{-\infty}^{\infty} f_{sw}(x, y, t) dy} \quad (6.17a,b)$$

$$\sigma_{y-travel}^2 = \frac{\int_0^{\infty} \int_{-\infty}^{\infty} (y - \bar{y}_{travel})^2 f_{sw}(x, y, t) dy}{\int_0^{\infty} \int_{-\infty}^{\infty} f_{sw}(x, y, t) dy}$$

and the corresponding relation for mean vertical speed $c_{y-travel}$ is

$$\bar{c}_{y-travel} = \frac{d\bar{y}_{travel}}{dt} \quad (6.18)$$

We computed these parameters using the results of the calculation only up to 240 hrs, because beyond that time a non-negligible fraction of the tracer pebbles migrate out of the domain.

Figure 6.17 shows the variation in time of the mean streamwise travel distance \bar{x}_{travel} ; the corresponding plot for $\bar{c}_{x\text{-travel}}$ is shown in Figure 6.18.

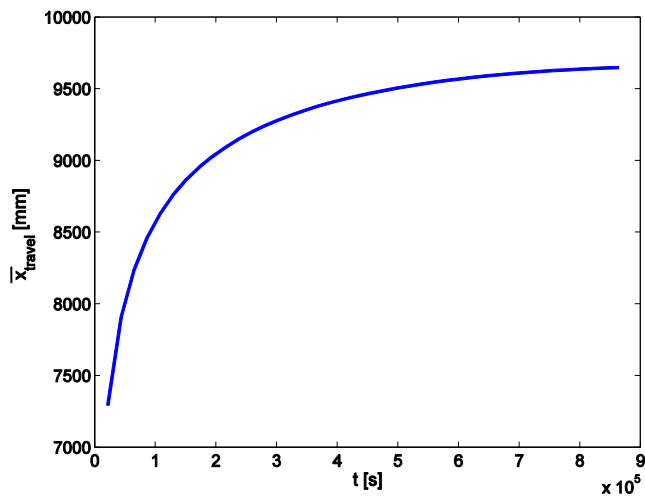


Figure 6.17 Mean streamwise travel distance versus time.

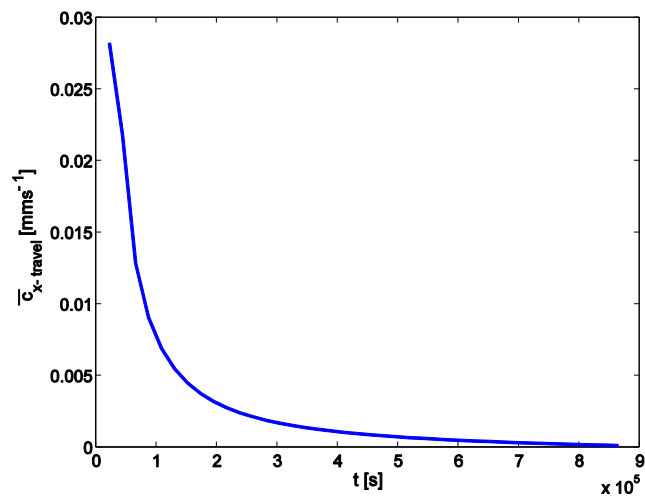


Figure 6.18 Mean streamwise speed of advection versus time.

The streamwise speed of advection $\bar{c}_{x\text{-travel}}$ of the patch continuously declines in time. The reason for this can be seen from Figure 6.9 – 6.16; trapping of particles deep in the deposit, where they are not easily re-entrained, results in the precisely the advective slowdown observed by Ferguson et al. (2002).

Figure 6.19 shows the variation in time of the standard deviation $\sigma_{x\text{-travel}}$ of the streamwise travel distance of the pebble patch. For the case of normal diffusion in the streamwise direction, $\sigma_{x\text{-travel}}$ should asymptotically increase in time as $t^{1/2}$; an exponent larger than $1/2$ corresponds to superdiffusion, and an exponent smaller than $1/2$ corresponds to subdiffusion. Figure 6.19 shows subdiffusive behavior, but only slightly so. At least part of the reason for this is the use of a thin-tailed Gaussian distribution for step length PDF p_s . Using a Master Equation that does not account for the vertical dispersion included here, Ganti et al. (2010) have demonstrated that a heavy-tailed form for p_s can give rise to anomalous streamwise diffusion.

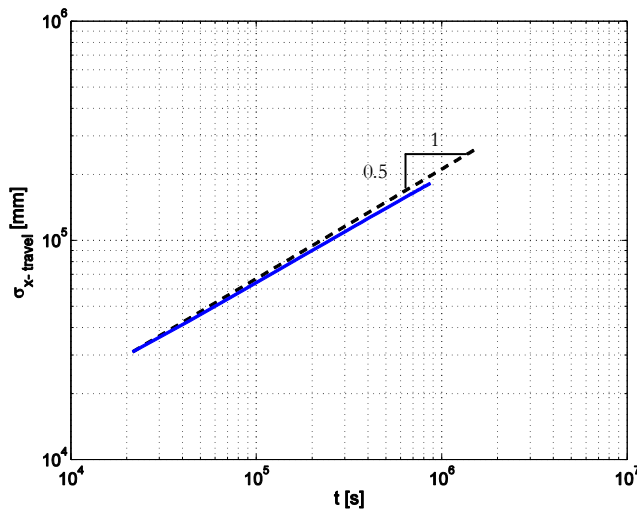


Figure 6.19 Standard deviation of streamwise travel distance versus time. The solid blue line denotes the calculational results, and the dashed black line corresponds to normal diffusion.

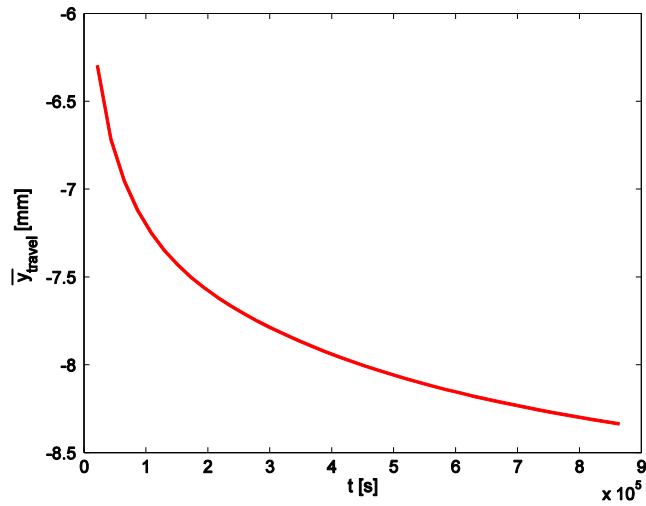


Figure 6.20 Mean vertical travel distance versus time.

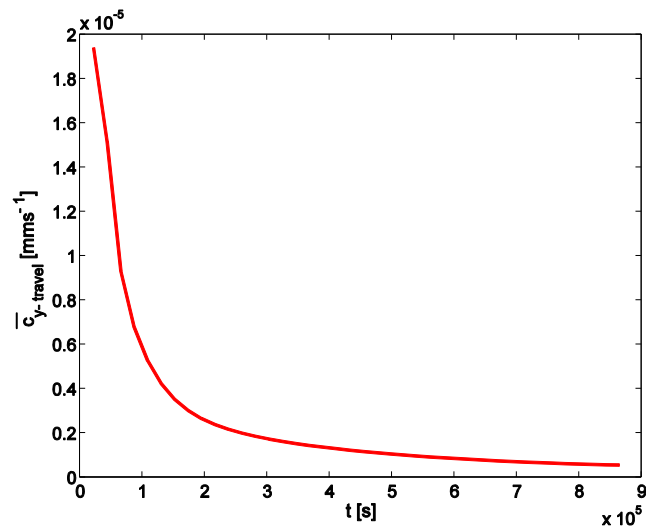


Figure 6.21 Mean vertical speed of advection versus time.

Figure 20 shows the variation in time of the mean vertical travel distance \bar{y}_{travel} ; the corresponding plot for $\bar{c}_{y\text{-travel}}$ is shown in Figure 6.21. The plots document a tendency for tracer pebbles to be advected downward, but the magnitude of the advection velocity declines in time. This

behavior is in part dependent on initial conditions. Figure 6.9 shows an initial distribution of tracers that is symmetrical about $y = 0$ (mean bed elevation), and with no tracers below $y = -4$ mm. Downward advection occurs as particles gradually find positions below $y = -4$ mm. The temporal decline in downward advection speed is caused by the decrease in $p_j(y)$ as $y \rightarrow -\infty$; particles at depth are trapped and cannot jump out. Were the entire patch initially placed at depth, however, a tendency for upward advection would result.

Figure 6.22 shows the variation in time of the standard deviation $\sigma_{y\text{-travel}}$ of the vertical travel distance of the pebble patch. The pattern is seen to be highly subdiffusive. This is again due to the decline in $p_j(y)$ as $y \rightarrow \infty$; particle trapping at depth strongly limits diffusion to even deeper layers. A comparison of Figures 6.17, 6.18 and 6.19 characterizing streamwise advection-diffusion and Figures 6.20, 6.21 and 6.22 characterizing vertical advection-diffusion reveals that streamwise and vertical processes interact and co-evolve. Vertical advection is the cause of the streamwise advective slowdown. On the other hand, the streamwise tails of trapped tracer particle density at depth is driven by streamwise advection. Downward advection thus increases the streamwise standard deviation of the pebble patch.

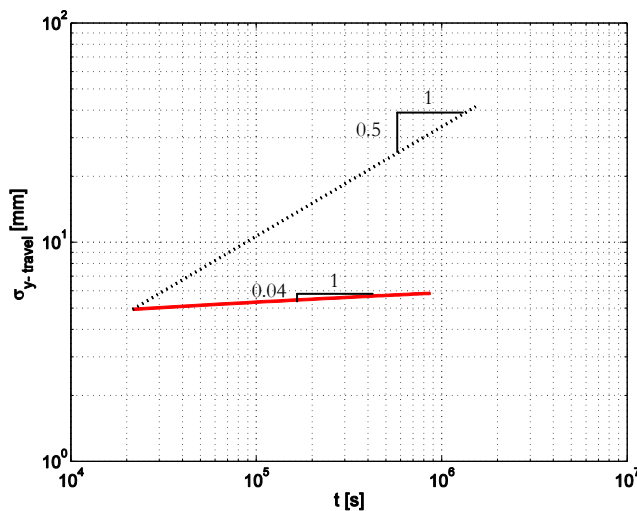


Figure 6.22 Standard deviation of vertical travel distance versus time. The solid red line denotes the calculational results, and the dashed black line corresponds to normal diffusion.

6.5 DISCUSSION

The case considered here is that of lower-regime plane-bed transport. Bedforms such as dunes, antidunes and bars were absent in the experiments of Wong et al. (2007). It can be expected that increasing complexity due to bedforms, as well as planform variation associated with e.g. meandering would increase both streamwise and vertical diffusion. In principle, these cases can be incorporated into the model framework given here, but a) structure functions would have to be determined based on the state of the bedforms, b) the model would have to be extended to the two-dimensional case, and c) advection and diffusion may exhibit multiscale behavior (e.g. Sapozhnikov et al., 1998) as different scales of bed elevation variation driven by different phenomena (e.g. dunes versus channel bends) are accessed by the dispersing tracer patch.

Blom and Parker (2004), Blom et al. (2006) and Blom et al. (2008) have developed a model for vertical sorting of grain sizes in fields of dunes. Their model framework is based on the same one used as the basis for the Master Equation used here, i.e. that of Parker et al. (2000). Their sorting model could easily be adapted to tracer particle advection-diffusion in rivers with dunes.

We show the streamwise and vertical dispersion of river pebble tracers by using recent formulation of EBME. In particular, here the EBME with no waiting time is numerically solved. It requires the definition of structure functions of PDFs for bed elevation $p_b(y)$, jump elevation $p_j(y)$ and step length $p_s(r)$. For particle step length, it is assumed a standard exponential (thin-tailed) distribution as suggested by recent findings on field data from gravel-bed rivers (Hassan et al., 2013). A systematic analysis is performed to verify from existing experimental data (Wong et al., 2007) the hypothesis of thin-tailedness of PDFs for bed elevation and jump elevation. Both PDF for bed elevation and PDF for jump elevation show indeed a thin-tail and we can further approximate the two PDFs with the same Gaussian distribution. Here we consider the Gaussian fit proposed by Wong et al. (2007) with mean, tautologically, equal to zero and standard deviation function of the flow properties by means of the Shields number.

Considering the evolution in time of a patch of tracers, numerical results of the EBME-N show the advection and dispersion along streamwise coordinate and the vertical. The model allows to detect the streamwise

advective slowdown, firstly pointed out by Ferguson and et al. (2002) and the subdiffusive behavior in the vertical. We notice normal diffusion condition in streamwise dispersion.

6.6 CONCLUDING REMARKS

The main objective of the work shown here is the characterization of co-evolving streamwise and vertical advection and dispersion of river pebble tracers. We use the EBME-N (Exner Based Master Equation with No waiting) derived in Chapter 5 as the basis for our calculations. In order to apply the model, it is necessary to define structure functions for the PDFs of bed elevation $p_e(y)$, elevation $p_j(y)$ from which a particle jumps and step length $p_s(r)$. Here we develop these functions using experimental data from Wong et al. (2007). These experiments characterize lower-regime plane-bed conditions, for which bedforms are absent. The data justify the use of thin-tailed PDFs for all these functions. Thin-tailed behavior is also supported by field observations presented in Hassan et al. (2013). Heavy-tailed distributions may be more likely in more complex cases, e.g. when dunes, bars and channel meandering coexist.

The key result of our modeling is the successful characterization of the phenomenon of streamwise advection slowdown, which has been observed in the field. The inclusion of vertical processes in our model allows tracer particles to be advected downward to a level from which they are not easily re-entrained. These particles are essentially trapped, and thus have near-vanishing streamwise advection velocity. As a result, when averaged over the whole patch, the streamwise advection velocity of tracer particles declines.

The model shows other features of interest related to the coevolution of streamwise and vertical advection-diffusion. The streamwise standard deviation of the patch is increased by vertical advection-diffusion, as particle trapped at depth form tails lagging behind the main body of tracers. Streamwise diffusion is nearly normal, so that the streamwise standard deviation of the patch increases as the square root of time. Vertical diffusion is strongly subdiffusive.

The formulation of EBME-N does not incorporate the statistics of particle waiting time as a function of vertical position. The EBME-W

(Exner Based Master Equation with Waiting) is specified in Chapter 5 of this thesis. The relevant structure function for the statistics of waiting time can be easily extracted from e.g. the data of Wong et al. (2007): at any level y , the waiting time τ is time from an upward-directed arrow, i.e. particle deposits, to the next downward-directed arrow, i.e. particle is eroded (Figure 6.5).

7 CONCLUSIONS

Patches of tracer pebbles are often emplaced in gravel-bed rivers in order to study bedload transport processes. As time passes, the patch of tracer particles is advected downstream, and shows downstream diffusion as the patch spreads. These processes have been captured in earlier models (e.g. Ganti et al, 2010) by applying the ideas deriving from the standard formulation for Continuous Time Random Walk (CTRW) accompanied by appropriate probability distribution functions (PDFs) for walker step length and waiting time. CTRW yields asymptotically the standard advection-diffusion equation (ADE) for thin-tailed PDFs, and the fractional advection-diffusion equation (fADE) for heavy-tailed PDFs, the latter allowing the possibilities of subdiffusion or superdiffusion of particles, which is often referred as non-local behavior or anomalous diffusion (e.g. Schumer et al., 2009). However, tracer particles can also be advected and diffused in the vertical direction. The principal objective of the Thesis is to define a generalized Master Equation for the case of bedload transport (moving as bed material load) in rivers, so as to include PDFs of particle step length and particle waiting time, as well as vertical exchange of particles.

A complementary objective is to analyze the morphodynamics of river bed variation when non-local behaviors in particle motion occur (heavy-tailed PDFs or thin-tailed PDFs with mean particle step length comparable to the domain of interest). The outcomes for the latter analysis show arising differences between the results of the flux form of the Exner equation of sediment continuity and the entrainment form of the same equation on the transient aggradational-degradational bed profiles when the non-local effects are not negligible.

Then, with reference to pebble tracers, it is shown here that the Montroll-Weiss (1965) Master Equation for the Continuous Time Random Walk (CTRW) model does not apply to the case where the walker (sediment particle) interacts with the lattice by causing the sediment-water interface to change in elevation. So, we provide Exner Based Master Equation forms for transport and dispersion of river pebble tracers. The MEs proposed here are derived from the probabilistic (entrainment form) Exner equation of sediment mass

conservation of Parker et al. (2000); they are substantially different from the Master Equation of CTRW. Our formulation characterizes vertical dispersion, as well as streamwise advection-diffusion of tracer particles.

In particular, two forms for the Exner-based Master Equation are presented. The most general form EBME-W (Exner-Based Master Equation with Waiting time), encompasses probability distributions for both step length and waiting time. The form EMBE-N (Exner-Based Master Equation with No waiting time) is recovered from EBME-W by assuming a Dirac function for waiting time. Asymptotic forms of the Master Equations are derived so as to allow comparison with the standard ADE (normal advection-diffusion equation) and fADE (fractional advection-diffusion equation). Although they include streamwise advection and diffusion, the Exner-based Master Equations take forms that differ substantially from standard ADE and fADE. The key differences are as follows: a) advection and diffusion coefficients vary in the vertical, b) a nonlocal, asymptotically non-fractional dispersion term mixes tracers in the vertical, and c) the vertical variation of mean waiting time explicitly enters into the governing equation.

In order to illustrate the key aspect of vertical dispersion, a simplified version of EBME-N, in which streamwise variation is neglected, is solved numerically. The key statistical parameter in this model is $p_j(y)$ corresponding to the probability that when a particle jumps, it jumps from elevation y relative to the mean bed. Both thin-tailed and heavy-tailed PDFs for p_j are considered. Asymptotically, both the thin- and the heavy-tailed cases show subdiffusive vertical dispersion of pebbles. This subdiffusive behavior is enhanced for the thin-tailed case: when p_j is heavy-tailed, particles can be dispersed more rapidly in the vertical direction.

For the case of a sediment bed, i.e. when the probability of the bed being at a given elevation increases downward, tracer particles migrate downward as they disperse. The rate of downward migration decreases in time, as particles reach locations so deep that their probability of entrainment is asymptotically low. This downward migration is the likely reason for the slowdown of streamwise advection of tracer pebbles observed in the field. In order to verify this concept, we also characterize the co-evolving streamwise and vertical advection and dispersion of river pebble tracers. We use the EBME-N (Exner Based Master Equation with No waiting) as the basis for our numerical calculations. In order to apply the model, it is necessary to define structure functions for the

PDFs of bed elevation $p_e(y)$, elevation $p_j(y)$ from which a particle jumps and step length $p_s(r)$. Here we develop these functions using experimental data from Wong et al. (2007). These experiments characterize lower-regime plane-bed conditions, for which bedforms are absent. The data justify the use of thin-tailed PDFs for all these functions. Thin-tailed behavior is also supported by field observations presented in Hassan et al. (2013). Heavy-tailed distributions may be more likely in more complex cases, e.g. when dunes, bars and channel meandering coexist.

The key result of our modeling is the successful characterization of the phenomenon of streamwise advection slowdown, which has been observed in the field. The inclusion of vertical processes in our model allows tracer particles to be advected downward to a level from which they are not easily re-entrained. These particles are essentially trapped, and thus have near-vanishing streamwise advection velocity. As a result, when averaged over the whole patch, the streamwise advection velocity of tracer particles declines.

The model shows other features of interest related to the coevolution of streamwise and vertical advection-diffusion. The streamwise standard deviation of the patch is increased by vertical advection-diffusion, as particle trapped at depth form tails lagging behind the main body of tracers. Streamwise diffusion is nearly normal, so that the streamwise standard deviation of the patch increases as the square root of time. Vertical diffusion is strongly subdiffusive.

It can be expected that increasing complexity due to bedforms, as well as planform variation associated with e.g. meandering would increase both streamwise and vertical diffusion. In principle, these cases can be incorporated into the model framework given here, but a) structure functions would have to be determined based on the state of the bedforms, b) the model would have to be extended to the two-dimensional case, and c) advection and diffusion may exhibit multiscale behavior (e.g. Sapozhnikov et al., 1998) as different scales of bed elevation variation driven by different phenomena (e.g. dunes versus channel bends) are accessed by the dispersing tracer patch.

Blom and Parker (2004), Blom et al. (2006) and Blom et al. (2008) have developed a model for vertical sorting of grain sizes in fields of dunes. Their model framework is based on the same one used as the basis for the Master Equation used here, i.e. that of Parker et al. (2000). Their

sorting model could easily be adapted to tracer particle advection-diffusion in rivers with dunes.

Finally, the formulation of EBME-N does not incorporate the statistics of particle waiting time as a function of vertical position. The relevant structure function for the statistics of waiting time can be easily extracted from e.g. the data of Wong et al. (2007).

The implementation of EBME-W and the extension of the model framework given here to more complex cases (presence of bedforms and multiple grain sizes, meander rivers) represent exciting challenges for the future.

REFERENCES

- Ashida, K. and Michiue, M. (1972). Study on hydraulic resistance and bedload transport rate in alluvial streams. *Transactions, Japan Society of Civil Engineering*, No. 206: 59-64.
- Blom, A and Parker, G. (2004). Vertical sorting and the morphodynamics of bed form-dominated rivers: A modeling framework. *Journal of Geophysical Research*, 109, F02007, doi:10.1029/2003JF000069
- Blom, A., Parker, G., Ribberink, J.S, and de Vriend, H.J. (2006). Vertical sorting and the morphodynamics of bed-form-dominated rivers: An equilibrium sorting model. *Journal Of Geophysical Research*, 111, F01006, doi:10.1029/2004JF000175
- Blom, A., Ribberink, J.S. and Parker, G (2008). Vertical sorting and the morphodynamics of bed form-dominated rivers: A sorting evolution model. *Journal Of Geophysical Research*, 113, F01019, doi:10.1029/2006JF000618
- Bradley, D. N., Tucker, G. E. and Benson, D. A. (2010). Fractional dispersion in a sand bed river. *J. Geophys. Res.*, 115, F00A09, doi:10.1029/2009JF001268.
- Chaudhry, M. H. (1993). *Open-Channel Flow*. Prentice-Hall, Englewood Cliffs, 483 p.
- Du, Q., Gunzburger, M., Lehoucq, R.B. and Zhou, K. (2012). Analysis and approximation of nonlocal diffusion problems with volume constraints. *SIAM Review*, 54(4).
- DeVries, P. (2000). Scour in low gradient gravel bed streams: patterns, processes and implications for the survival of salmonid embryos. *PhD thesis*, University of Washington, Seattle, 365 pp.
- Einstein, H. A. (1937). Bed load transport as a probability problem. *PhD thesis*, Res. Inst. of Hydraul. Eng., Eidgenossische Tech. Hochschule, Zurich, Switzerland.
- Einstein, H. A. (1950). The Bed-load Function for Sediment Transportation in Open Channel Flows. *Technical Bulletin 1026*, U.S. Dept. of the Army, Soil Conservation Service, Washington, D.C.

- Exner, F. M. (1920). Zur physik der dunen, Akad. Wiss. Wien Math. Naturwiss. *Klasse*, 129(2a): 929– 952.
- Exner, F. M. (1925). U ber die wechselwirkung zwischen wasser und geschiebe in flussen. *Akad. Wiss. Wien Math. Naturwiss. Klasse*, 134(2a): 165– 204.
- Falcini, F., Foufoula-Georgiou, E., Ganti, V., Paola, C. and Voller, V. R. (2013). A combined nonlinear and nonlocal model for topographic evolution in channelized depositional systems. *J. Geophys. Res. Earth Surf.*, 118, doi:10.1002/jgrf.20108.
- Ferguson, R. I., Bloomer, D. J., Hoey, T. B. and Werritty, A. (2002). Mobility of river tracer pebbles over different timescales. *Water Resources Res.* 38(5), 10.1029/2001WR000254.
- Ferguson, R.I. and Hoey, T.B. (2002). Long-term slowdown of river tracer pebbles: Generic models and implications for interpreting short-term tracer studies. *Water Resources Res.* 38(8), doi: 10.1029/2001WR000637.
- Foufoula-Georgiou, E., Ganti, V. and Dietrich, W. (2010). A nonlocal theory of sediment transport on hillslopes. *J. Geophys. Res.*, 115, F00A16, doi:10.1029/2009JF001280.
- Furbish, D.J., Haff, P.K., Dietrich, W.E. and Heimsath, A.M. (2009). Statistical description of slope-dependent soil transport and the diffusion-like coefficient. *J. Geophys. Res.*, 114(F3), DOI: 10.1029/2009JF001267
- Furbish, D.J., Haff, P.K., Roseberry, J.C. and Schmeckle, M.W. (2012). A probabilistic description of the bed load sediment flux: 1. Theory. *J. Geophys. Res. Earth Surface*, 117, F03031, doi:10.1029/2012JF002352.
- Ganti, V., M. M. Meerschaert, E. Foufoula-Georgiou, E. Viparelli, and G. Parker (2010). Normal and anomalous diffusion of gravel tracer particles in rivers. *J. Geophys. Res.*, 115, F00A12, doi:10.1029/2008JF001222.
- Hassan, M. A. and Ergenzinger, P. (2005). Use of Tracers in Fluvial Geomorphology. *Tools in Fluvial Geomorphology* (eds G. M. Kondolf and H. Piégay), John Wiley & Sons, Ltd, Chichester, UK. doi: 10.1002/0470868333.ch14
- Hassan, M., Voepel, H., Schumer, R., Parker, G. and Fraccarollo, L. (2013). Displacement characteristics of coarse fluvial bed sediment. *J. of Geophys. Res. Earth Surface*, 118(1), 155–165, doi: 10.1029/2012JF002374.

- Hill, K. M., DellAngelo, L. and Meerschaert, M. M. (2010). Heavy-tailed travel distance in gravel bed transport: An exploratory enquiry. *J. Geophys. Res.*, 115, F00A14, doi:10.1029/2009JF001276.
- Klafter, J. and Silbey, R. (1980). Derivation of continuous-time random walk equation. *Phys. Rev. Lett.*, 44(2): 55– 58.
- Klafter, J., Blumen, A. and Shlesinger, M. F. (1987). Stochastic pathways to anomalous diffusion. *Phys Rev. A*, (35)7: 3081-3085.
- Leliavsky, S. (1955). *An Introduction to Fluvial Hydraulics*. 245 pp., Constable, London.
- Leopold, L.B., Emmet W.W. and Myrick, R.M. (1966). Channel and hillslope Processes in a Semi-arid Area, New Mexico. *US Geological Survey Professional Paper*, 352G: 193-253.
- Martin, R. L., Jerolmack, D. J. and Schumer, R. (2012). The physical basis for anomalous diffusion in bed load transport. *J. Geophys. Res.*, 117, F01018, doi:10.1029/2011JF002075.
- Meyer-Peter, E. and Müller, R. (1948). Formulas for Bed-Load Transport, Proceedings. 2nd Congress, *International Association of Hydraulic Research*, Stockholm: 39-64
- Montroll, E.W. and Weiss, G.H. (1965). Random walks on lattices. II. *J. Math. Phys.*, 6:167.
- Muto, T (2001). Shoreline autoretreat substantiated in flume experiment. *J. Sed. Res.*, 71: 246–254.
- Nakagawa, H., and Tsujimoto, T. (1976). On probabilistic characteristics of motion of individual sediment particles on stream beds. *Proceedings of the 2nd IAHR International Symposium on Stochastic Hydraulics*, 293–316, Int. Assoc. of Hydraul. Eng. and Res., Madrid.
- Nakagawa, H. and Tsujimoto, T. (1980). A Stochastic Model for Bed Load Transport and its Applications to Alluvial Phenomena. *Application of Stochastic Processes in Sediment Transport, Water Resources Publications*, edited by H. W. Shen and H. Kikkawa, Colorado, USA.
- Nikora, V., Habersack, H., Huber, T. and MacEwan, I. (2002). On bed particle diffusion in gravel bed flows under weak bed load transport. *Water Resour. Res.*, 38(6): 1081, doi:10.1029/2001WR000513.
- Nolan, J. P. (1997). Numerical calculation of stable densities and distribution functions. *Commun. Statist. - Stochastic Models*, 13(4): 759-774.
- Paola, C., Heller, P. L. and Angevine, C. L. (1992). The largescale dynamics of grain-size variation in alluvial basins, 1: Theory. *Basin Res.*, 4: 73–90.

- Paola, C., and Voller, V. R. (2005). A generalized Exner equation for sediment mass balance. *J. Geophys. Res.*, 110, F04014, doi:10.1029/2004JF000274.
- Parker, G. (1991). Selective sorting and abrasion of river gravel. II: Applications. *J. of Hydraul. Eng.*, 117(2): 150-171.
- Parker, G. (2004). *1D Sediment Transport Morphodynamics with Applications to Rivers and Turbidity Currents*. Copyrighted e-book, available at: http://hydrolab.illinois.edu/people/parkerg//morphodynamics_e-book.htm.
- Parker, G. (2008). Transport of gravel and sediment mixtures, Sedimentation engineering processes, measurements, modeling and practice. *ASCE Manual and Reports on Engineering Practice, 110*, M. Garcia, ed., chap. 3, 165–252, Am. Soc. of Civ. Eng., New York..
- Parker, G., Paola, C. and Leclair, S. (2000). Probabilistic Exner sediment continuity equation for mixtures with no active layer. *J. Hydraul. Eng.*, 126(11): 818–826.
- Parker, G., Paola, C., Whipple, K. and Mohrig, D. (1998). Alluvial fans formed by channelized fluvial and sheet flow. I: Theory. *J. Hydraul. Eng.*, 124: 985–995, doi:10.1061/(ASCE)0733-9429(1998)124:10(985).
- Pelosi, A. and Parker, G. (2013). Morphodynamics of river bed variation with variable bedload step length. *Earth Surf. Dynam. Discuss.*, 1: 1097-1126, doi:10.5194/esurfd-1-1097-2013.
- Postma, G., Kleinhans, M. G., Meijer, P. T. and Eggenhuisen, J. T. (2008). Sediment transport in analogue flume models compared with real world sedimentary systems: A new look at scaling sedimentary systems evolution in a flume. *Sedimentology*, 55, 1541–1557, doi:10.1111/j.1365-3091.2008.00956.x.
- Sapozhnikov, V.B., Brad Murray, A., Paola, C. and Fofoula-Georgiou, E. (1998). Validation of Braided-Stream Models: Spatial state-space plots, self-affine scaling, and island shapes. *Water Resources Research*, 34 (9): 2353–2364.A
- Sayre, W., and Hubbell, D. (1965). Transport and dispersion of labeled bed material. North Loup River, Nebraska, *U.S. Geol. Surv. Prof. Pap.*, 433-C, 48 pp.
- Schumer, R., Benson, D.A., Meerschaert, M. M. and Baeumer B. (2003). Fractal mobile/immobile solute transport. *Water Resour. Res.*, 39(10): 1296, doi:10.1029/2003WR002141.

- Schumer, R., M. M. Meerschaert, and B. Baeumer (2009). Fractional advection-dispersion equations for modeling transport at the Earth surface. *J. Geophys. Res.*, 114, F00A07, doi:10.1029/2008JF001246.
- Stark, C.P., Fofoula-Georgiou, E. and Ganti, V. (2009). A nonlocal theory of sediment buffering and bedrock channel evolution. *J. Geophys. Res.*, 114, F01029, doi:10.1029/2008JF000981.
- Takayama, S., (1965). Bedload movement in torrential mountain streams, *Tokyo Geographical Paper* 9: 169-188 (in Japanese).
- Tsujimoto, T. (1978). Probabilistic model of the process of bed load transport and its application to mobile-bed problems. *Ph.D. thesis*, 174 pp., Kyoto Univ., Kyoto, Japan.
- Viparelli E., Lauer W. J., Belmont P. and Parker G. (2011). A numerical model to develop long-term sediment budgets using isotopic sediment fingerprints. *Computer and Geoscience*, CSDMS special issue on Modeling For Environmental Change, doi:10.1016/j.cageo.2011.10.003.
- Voepel, H., Schumer, R. and Hassan, M. (2013). Sediment residence time distributions: Theory and application from bed elevation measurements. *J. Geophys. Res. Earth Surf.*, 118, doi:10.1002/jgrf.20151.
- Voller, V. R., and Paola, C. (2010). Can anomalous diffusion describe depositional fluvial profiles?. *J. Geophys. Res.*, 115, F00A13, doi:10.1029/2009JF001278.
- Voller, V. R., Ganti, V., Paola, C. and Fofoula-Georgiou, E. (2012). Does the flow of information in a landscape have direction?. *Geophys. Res. Lett.*, 39, L01403, doi:10.1029/2011GL050265.
- Weeks, E. R., J. S. Urbach, and H. L. Swinney (1996). Anomalous diffusion in asymmetric random walks with a quasi-geostrophic flow example, *Physica D*, 97, 291--310.
- Whipple, K. X., Parker, G., Paola, C. and Mohrig, D. (1998). Channel Dynamics, Sediment Transport, and the Slope of Alluvial Fans: Experimental Study. *J. Geol.*, 106: 677–693.
- Wilcock, P. R. (1997). Entrainment, displacement and transport of tracer gravels. *Earth Surf. Processes Landforms*, 22: 1125–1138.
- Wong, M. and Parker, G. (2006). Reanalysis and Correction of Bed-Load Relation of Meyer-Peter and Müller Using Their Own Database. *J. Hydraul. Eng.*, 132(11): 1159–1168.
- Wong, M., Parker, G. , DeVries, P. , Brown, T. M. and Burges, S. J. (2007). Experiments on dispersion of tracer stones under lower-

References

- regime plane-bed equilibrium bed load transport. *Water Resour. Res.*, 43, W03440, doi:10.1029/2006WR005172.
- Zhang, Y., Meerschaert, M.M. and Packman, A.I. (2012). Linking fluvial bed sediment transport across scales. *Geophys. Res. Letters*, 39, L20404, doi:10.1029/2012GL053476.
- Blom, A and Parker, G. (2004). Vertical sorting and the morphodynamics of bed form-dominated rivers: A modeling framework. *Journal Of Geophysical Research*, 109, F02007, doi:10.1029/2003JF000069